(12) INTERNATIONAL APPLICATION PUBLISHED UNDER THE PATENT COOPERATION TREATY (PCT)

(51) International Patent Classification[7]: H04Q

(21) International Application Number: PCT/US00/26106

(22) International Filing Date:
22 September 2000 (22.09.2000)

(25) Filing Language: English

(26) Publication Language: English

(30) Priority Data:
60/155,487   23 September 1999 (23.09.1999)   US
60/209,529   5 June 2000 (05.06.2000)   US

(71) Applicants and
(72) Inventors: NADEAU, Richard, G. [US/US]; 364 Walnut Lane, North East, MD 21901 (US). WINKELMAN, James, W. [US/US]; 62 Rangeley Road, Chestnut Hill, MA 02167 (US).

(74) Agents: KESSLER, Edward, J. et al.; Sterne, Kessler, Goldstein & Fox P.L.L.C., Suite 600, 1100 New York Avenue, N.W., Washington, DC 20005-3934 (US).

(81) Designated States (national): AE, AG, AL, AM, AT, AU, AZ, BA, BB, BG, BR, BY, BZ, CA, CH, CN, CR, CU, CZ, DE, DK, DM, DZ, EE, ES, FI, GB, GD, GE, GH, GM, HR, HU, ID, IL, IN, IS, JP, KE, KG, KP, KR, KZ, LC, LK, LR, LS, LT, LU, LV, MA, MD, MG, MK, MN, MW, MX, MZ, NO, NZ, PL, PT, RO, RU, SD, SE, SG, SI, SK, SL, TJ, TM, TR, TT, TZ, UA, UG, US, UZ, VN, YU, ZA, ZW.

(84) Designated States (regional): ARIPO patent (GH, GM, KE, LS, MW, MZ, SD, SL, SZ, TZ, UG, ZW), Eurasian patent (AM, AZ, BY, KG, KZ, MD, RU, TJ, TM), European patent (AT, BE, CH, CY, DE, DK, ES, FI, FR, GB, GR, IE, IT, LU, MC, NL, PT, SE), OAPI patent (BF, BJ, CF, CG, CI, CM, GA, GN, GW, ML, MR, NE, SN, TD, TG).

Published:
— Without international search report and to be republished upon receipt of that report.

For two-letter codes and other abbreviations, refer to the "Guidance Notes on Codes and Abbreviations" appearing at the beginning of each regular issue of the PCT Gazette.

WO 01/22741 A2

(54) Title: MEDICAL APPLICATIONS OF ORTHOGONAL POLARIZATION SPECTRAL IMAGING

(57) Abstract: Medical applications of orthogonal polarization spectral (OPS) imaging technology are provided. This technology provides for a high contrast image of sub-surface phenomena such as blood vessel structure, blood flow within vessels, gland structure, etc., as well as a high resolution image of the surface of solid organs. Numerous clinical (diagnostic and therapeutic), as well as research applications of this technology, in the medical and pharmaceutical fields, are discussed.

Medical Applications of Orthogonal Polarization Spectral Imaging

Background of the Invention

1.   Field of the Invention

5   The present invention relates to orthogonal polarization spectral (OPS) imaging analysis. More particularly, the present invention relates to *in vivo* medical and clinical uses of OPS imaging to directly, and in many cases non-invasively, visualize, characterize, evaluate, monitor, and/or analyze a subject's microvascular and/or vascular system. The present invention also relates to *in* 10 *vitro* and *in vivo* applications of reflected spectral imaging analysis for basic research, clinical research, and as a teaching tool.

2.   Related Art

    Different disease states, including, *e.g.*, diabetes, hypertension, numerous opthalmological conditions, and coronary heart disease, produce distinctive 15 microvascular pathologies. To date, imaging of the human microcirculation for diagnosis and/or treatment has been limited to vascular beds, where the vessels are visible and close to the surface (*e.g.*, nailfold; conjunctiva).

    For example, nailfold capillaroscopy has been used in the diagnosis and treatment of peripheral vascular diseases, Raynaud's phenomenon, diabetes, and 20 hematological disorders (Forst, T., *et al.*, *Clinical Science 94*:255-261 (1998); Fagrell, B. & Bollinger, A., *Clinical Capillaroscopy: A Guide to Its Use in Clinical Research and Practice*, Hogrefe & Huber, Seattle (1990); Fagrell, B. & Intaglietta, M., *J. Int. Med. 241*:349-362 (1997)). These studies were done to obtain experimental data regarding capillary density, capillary shape, and blood 25 flow velocity, and were limited to gross physical measurements on capillaries. No spectral measurements, or individual cellular measurements, were made, and Doppler techniques were used to assess velocity.

- 2 -

The use of the bulbar conjunctiva vessels for clinical applications in ophthalmology has been restricted due to problems with movement (Davis, E. & Landau, J., in *Clinical Capillary Microscopy*, Thomas, Springfield (1966); Fenton, B.M., *et al., Microvasc. Res. 18*:153-166 (1979); Wolf, S., *et al, Hypertension 23*:464-467 (1994)).

Other locations observed by intravital microscopy include the microcirculation of the skin, lip, gingival tissue, and tongue (Davis, E. & Landau, J., *supra*).

Laser scanning confocal imaging is one new technique that does allow reflected light imaging of the microcirculation *in vivo* (Bussau, L.J., *et al., J. Anat 192* (Pt 2):187-194 (1998); Rajadhyaksha, M., *et al., J. Invest. Dermatol. 104*:946-952 (1995)). This method can distinguish between layers of skin and can image microcirculation in the skin. However, images obtained using laser scanning confocal microscopy can only be collected at a fraction of normal video rate (up to 16 versus 30 frames/second) and the best microvascular images using this technique require fluorescent labels for contrast enhancement (Bussau, L.J., *et al., supra*).

Direct observation, using conventional methods, of vascular beds of other organs in humans has been prevented by the need for transillumination, fluorescent dyes for contrast enhancement, or by the size of instrumentation required to acquire images, especially during surgery.

Several devices for *in vivo* analysis based on reflectance spectrophotometry have been developed recently. However, these conventional reflectance-based devices are less than optimal for several reasons.

One non-invasive device for *in vivo* analysis is disclosed in U.S. Patent 4,998,533 to James W. Winkelman (1991). This device uses image analysis and reflectance spectrophotometry to measure individual cell parameters such as cell size. Measurements are taken only within small vessels, such as capillaries where individual cells can be visualized. Because this device takes measurements only in capillaries, measurements made will not accurately reflect measurements for larger vessels. Consequently, the Winkelman device is not capable of measuring

the central or true hematocrit, or the total hemoglobin concentration, which depend upon the ratio of the volume of red blood cells to that of the whole blood in a large vessel such as a vein.

The Winkelman device measures the number of white blood cells relative to the number of red blood cells by counting individual cells as they flow through a micro-capillary. The Winkelman device depends upon accumulating a statistically reliable number of white blood cells in order to estimate the concentration. The Winkelman device does not provide any means by which platelets can be visualized and counted or a means by which the capillary plasma can be visualized, or the constituents of the capillary plasma quantified. Also, this device does not provide a means by which abnormal constituents of blood, such as tumor cells, can be detected.

Other devices utilize light application means that focus an illumination source directly onto a blood vessel in a detection region. As a result, these devices are extremely sensitive to movements of the device with respect to the patient. This increased sensitivity to device or patient movement can lead to inconsistent results. To counteract this motion sensitivity, these devices require stabilizing and fixing means.

Other conventional devices have been developed based on a traditional dark field illumination technique. As understood in traditional microscopy, dark field illumination is a method of illumination which illuminates a specimen but does not admit light directly to the objective. For example, a traditional dark field imaging approach is to illuminate an image plane such that the angular distribution of illumination and the angular distribution of light collected by an objective for imaging are mutually exclusive. The illumination is incident on the field of view of the detector, however, so in these devices scattering off optically active tissue in the image path can create an orientation dependent backscatter or image glare that reduces image contrast. Moreover, rotation of these devices causes a change in contrast.

To date, there is no non-invasive method to visualize and characterize the microcirculation of the interior of the eye. Of major interest is the

- 4 -

microcirculation of the retina and optic disc. Also of interest is the microcirculation of the external ocular structures and changes that occur related to disease processes such as benign and malignant tumors and circulatory problems that occur, for example, the sludging and clumping of red blood cells that occurs in various forms of sickle cell disease.

The retinal circulation is affected by many systemic diseases, such as diabetes mellitus, sickle cell anemia, and macroglobulinemia. The various types of macular degenerations are also affected by circulatory changes. There are, in fact, many other ocular and systemic conditions which also affect the retinal microcirculation. Medications also affect circulation. Glaucoma is a condition of the eye usually associated with a high eye pressure. There are, however, forms of glaucoma, often called low tension glaucoma, where the intraocular pressure is not found to be elevated when tested. In glaucoma, visual loss is associated with loss of function and death of the nerve fibers in the optic nerve which transmits impulses to the brain where they are eventually interpreted as vision. There are changes in the microcirculation of the optic disc which contribute to the loss of function of some of the nerve fibers and death of some, thus affecting vision. The optic disc is easily visualized in the normal eye with the use of instruments such as various types of ophthalmoscopes or fundus cameras. Very little is now known about the microcirculation of the optic disc, the surrounding structures and the effects of medications on the micro-circulation in this area, as well as the rest of the intraocular structures.

With present techniques, microcirculation of various intraocular structures are visualized only after various dyes are injected into the patient's circulatory system. Photographs are then taken. If treatment is necessary, such as laser ablation of a leaking retinal vessel or capillary, this is done by comparing the photograph, which is usually placed on a screen next to the laser, with what is seen in the eye by the treating physician. Clearly, new methods are needed to visualize and characterize the ocular microcirculation, as well as the microcirculation of other human tissues and organs.

- 5 -

Orthogonal Polarization Spectral (OPS) Imaging

OPS imaging is a new method for visualizing and characterizing the microcirculation using reflected light that allows imaging of the microcirculation noninvasively through mucus membranes, as well as on the surface of solid organs.

OPS imaging has been described in Groner and Nadeau's U.S. Patent 5,983,120 (issued November 9, 1999), U.S. Patent 6,104,939 (issued August 15, 2000), and PCT publication WO 97/15229; all of which are incorporated by reference in their entirety. In both the 5,983,120 and 6,104,939 patents and the WO 97/15229 publication, Groner and Nadeau used high resolution images of the microcirculation to directly measure and compute key elements of the complete blood count (CBC), including the white blood cell differential (CBC + Diff). The CBC + Diff is one of the most frequently requested diagnostic tests with about two billion done in the United States per year. The combination of OPS imaging, image processing, reflectance spectroscopy, and algorithmic calculation was used to compute a rapid determination of hemoglobin concentration, hematocrit, red and white blood cell count, and platelet count without drawing blood samples from the body.

In addition, OPS imaging technology was used to non-invasively measure other types of blood components, such as non-cellular constituents (*e.g.*, blood gases and bilirubin) present in the plasma component of blood. Rapidly and non-invasively quantitatively measuring a variety of blood and vascular characteristics clearly eliminates the need to draw a venous blood sample to ascertain blood characteristics, which may pose particular problems for newborns, elderly patients, burn patients, and patients in special care units. A device of this type also eliminates the delay in waiting for the laboratory results in the evaluation of the patient. Such a device also has the advantage of added patient comfort, as well as obviating the risk of exposure to AIDS, viral hepatitis, and other blood-borne diseases. Noninvasive blood testing will have substantial utility in current medical practice.

- 6 -

An enhanced OPS imaging system for high contrast *in vivo* imaging of the vascular system is described in copending U.S. Patent Application No. 09/401,859, filed September 22,1999, and is incorporated by reference in its entirety.

Thus, OPS imaging provides an apparatus for complete non-invasive, *in vivo* analysis of the vascular system with high-image quality. The apparatus provides high resolution visualization and characterization of: blood cell components (red blood cells, white blood cells, and platelets); blood rheology; the vessels in which blood travels; and vascularization throughout the vascular system. The apparatus further minimizes the glare and other deleterious artifacts arising in conventional reflectance spectrophotometric systems.

Although the above-referenced documents sufficiently describe OPS imaging, a brief review of this technology follows.

In OPS imaging, the tissue is illuminated with linearly polarized light and imaged through a polarizer oriented orthogonal to the plane of the illuminating light. Only depolarized photons scattered in the tissue contribute to the image. The optical response of OPS imaging is linear and can be used to perform reflection spectrophotometry over the wide range of optical density typically achieved by transmission spectrophotometry.

In OPS imaging, the subject medium is illuminated with light which has been linearly polarized in one plane, while imaging the remitted light through a second polarizer (analyzer) oriented in a plane precisely orthogonal to that of the illumination. To form the image, the light is collected, passed through a spectral filter to isolate the wavelength region, and linearly polarized. The polarized light is then reflected toward the target by a beam splitter. An objective lens focuses the light onto a region of approximately 1 mm in diameter. The length of the objective lens can vary; two exemplary OPS imaging probes have a 3 inch and an 8 inch objective lens. Light that is remitted from the target is collected by the same objective lens, which then forms an image of the illuminated region within the target upon an imaging detector such as a charge coupled device (CCD) video camera or a complementary metal oxide semiconductor (CMOS) video camera.

The polarization analyzer is placed directly in front of the camera. A polarizing beam splitter can be chosen for maximum efficiency. That is, one orthogonal polarization state is reflected while the other is transmitted.

In polarized light, the state of polarization of light is preserved in ordinary
5   reflections as well as single scattering events. Typically, more than 10 scattering events are required to effectively depolarize light (MacKintosh, F.C., *et al., Phys. Rev. B 40*:9342 (1989); Schmitt, J.M., *et al., Applied Optics 31*:6535 (1992)). Thus, the only remitted light from the subject that can pass through the analyzer results from multiple scattering occurring relatively deep (>10 times the single
10 scattering length) within the medium. This depolarized scattered light effectively back-illuminates any absorbing material in the foreground. If a wavelength within the hemoglobin absorption spectrum is chosen, the blood vessels of the peripheral microcirculation can be visualized using OPS imaging as in transilluminated intravital microscopy. A wavelength region centered at an isobestic point of oxy-
15 and deoxy-hemoglobin (548 nm) was chosen for optimal imaging of the microcirculation. This wavelength region represented a compromise between using an isobestic point in the Soret region (about 420 nm), where hemoglobin absorption is maximum, but the scattering length is shorter, or one in the near infrared region (810 nm), where multiple scattering occurs deep in the tissue, but
20 absorption for hemoglobin is insufficient to provide good contrast in smaller vessels.

It is noted that the scattered light can be used to view subsurface cellular structure irrespective of the absorption characteristics that allow visualization and characterization of blood cells.

25   Conventional reflectance spectrophotometry is carried out on an extended diffuse reflecting surface to which the analyte has been applied. Typically, reflectance spectrophotometry has a much more limited range of measurement of optical density (OD) than does transmission spectrophotometry, which can easily measure changes from 0 to 3 OD. In reflected light spectrophotometry, the
30 apparent OD of the analyte is reduced by specular reflections and light scattering. The reflection and light scatter are due to physical characteristics rather than the

- 8 -

chemical concentration of the analyte (Kortüm, G., *Reflectance Spectroscopy*, Springer-Verlag, New York (1969)).

OPS imaging was developed in part to eliminate some of the confounding error inherent to reflectance spectroscopy that was due to reflection and light scatter. Studies have shown that OPS imaging techniques can be used to accurately measure in reflection the wide range of OD typically achieved only in standard transmission spectrophotometry.

A theoretical explanation of OPS imaging begins by recalling that forming an image in reflected light requires both scattering for illumination and absorption for contrast. In continuous media, these are typically considered the result of a pair of material constants (coefficients) (Star, W.M., *et al., Phys Med Biol* *33*:437-454 (1988)). Both scattering and absorption depend linearly upon penetration, and the remitted light intensity is given by the ratio of the coefficients (Kortüm, G., *Reflectance Spectroscopy*, Springer-Verlag, New York (1969)). High quality imaging is therefore generally not possible in turbid media due to the scattering which degrades the image resolution. However, in OPS imaging, the remitted illumination is provided only by multiple scattering. This is a distinctly non-linear function of the penetration depth and thus is decoupled from the absorption. Consequently, absorbing substances at shallow depth can be visualized and characterized with both high contrast and good resolution.

Comparison of OPS Imaging With Intravital Microscopy

A comparison of fluorescence intravital microscopy (Harris, A.G., *et al., Int. J. Microcirc.-Clin. Exp 17*:322-327 (1997)) with OPS imaging in the hamster demonstrated equivalence in measured physiological parameters under controlled conditions and after ischemic injury (Harris, A. G., *et al.*, The study of the microcirculation using orthogonal polarization spectral imaging, in Yearbook of Intensive Care and Emergency Medicine 2000, Ed. J.-L. Vincent, Springer-Verlag, Berlin, pp 705-14 (2000); Harris, A. G., *et al.*, Validation of OPS imaging, 21st

- 9 -

European Conference on Microcirculation, Ed. B. Fagrell, Bologna, Monduzzi Editore, pp. 43-48 (2000)).

The ability of OPS imaging to provide quantitative measurements of relevant physiological parameters and pathophysiological changes in the microcirculation was shown by measurement of functional capillary density (FCD) in the dorsal skinfold chamber of the awake Syrian golden hamster. FCD is defined as the length of red blood cell perfused capillaries per observation area and is given in cm/cm^2. As the capillaries must contain flowing red cells to be counted in the measurement, FCD is a direct measure of nutritional tissue perfusion and an indirect measurement of oxygen delivery to tissue (Harris, A.G., *et al., Am. J. Physiol. 271*:H2388-2398 (1996)). The hamster dorsal skinfold model is standardized and has been used extensively to study ischemia/reperfusion injury (*Id.*; Nolte, D., *et al., Int. J. Microcirc.-Clin. Exp. 15*:244-249 (1995)).

FCD was measured on the same capillary networks using standard intravital fluorescence videomicroscopy (IVM) (Harris, A.G., *et al., Int. J. Microcirc.-Clin. Exp 17*:322-327 (1997)) and OPS imaging at baseline, 0.5 hour, and 2 hours after 4 hours of pressure ischemia (Nolte, D., *et al., Int J.Microcirc-Clin Exp 15*:9-16 (1995)). A total of six capillary networks per animal (n=10) were imaged and recorded on videotape by both methods. The images from both systems were analyzed during repetitive playback using a computer assisted microcirculation analysis system (CapImage™) (Klyscz, T., *et al., Biomed Tech (Berl) 42*:168-175 (1997)) and FCD was determined using the images from both methods. FCD was measured equally well by the two imaging methods. Furthermore, Bland-Altman analysis (Bland, J.M. & Altman, D.G., *Lancet 1*:307-310 (1986)) showed very good agreement between methods as well as no systematic bias over the entire range of FCD measurements.

A direct comparison was made of the contrast between OPS imaging and fluorescence on paired images of the hamster dorsal skinfold microcirculation. There was no significant difference between the two methods in absolute contrast (p=0.43, paired t-test). Thus, contrast obtained by OPS imaging without the use of dyes was equivalent to that obtained with contrast enhancement by IVM.

- 10 -

In the following study, validation of the CYTOSCAN™ A/R (a high contrast OPS imaging device owned by Cytometrics, Inc.) under both physiological and pathophysiological conditions was performed using standard IVM.

5   *Methods*: In the dorsal skin-fold chamber model in the awake Syrian golden hamster measurements of vessel diameter, RBC velocity and functional capillary density (FCD) were made before and after a 4 hour ischemia. In a tumor growing in the chamber, measurements were made 3, 6, and 9 days after implantation of amelanomic melanoma tumor cells. In the rat liver, venular

10   diameter, RBC velocity and the number of perfused sinusoids were measured before and after a 60 minute ischemia. The data were analyzed using Bland-Altman plots to test the agreement between the two methods (IVM vs. CYTOSCAN™ A/R).

Results: There was excellent agreement between the two methods for the

15   measurement of venular RBC velocity in all three models. There was no bias, the variance was constant over the entire range, the 95% confidence interval was of an acceptable range and 95% of all data points were within this range. For the measurement of perfusion (FCD in the chamber, functional vessel density in the tumor, and the number of perfused sinusoids in the liver) there was also good

20   agreement between the two methods. In the hamster chamber (muscle and tumor), measurements of vessel diameter showed good agreement, although the IFM demonstrated a bias of approximately 4 microns. This is actually to be expected since the two methods measure two different diameters (from endothelial cell to endothelial cell (IFM) vs. RBC column (OPS imaging)) and since the

25   fluorescence scattering causes the vessels to appear larger. In the liver, there was good agreement between the two methods for the measurement of vessel diameter. Similar results were obtained in the pancreas, intestine, brain, skin-flap and during wound healing.

Conclusions: The CYTOSCAN™ A/R can be used to make accurate

30   microvascular measurements of vessel diameter, RBC velocity, and perfusion in

- 11 -

a variety of organs in animal models. Similar measurements are therefore possible in humans.

Quantitative Determination of Optical Density In Vitro

Quantitative data regarding local hematocrit, which can be obtained with transillumination using the absorbance of blood hemoglobin, is not possible using epi-illumination methods without fluorescent labeling of the red cells. Previous studies to determine local hematocrit using intravital microscopy were carried out in thin tissue sections (such as the rat mesentery or cremaster muscle) (Pittman, R.N. & Duling, B.R., *J. Appl. Physiol.* *38*:321-327 (1975)). The optical systems used for those studies were evaluated and calibrated using glass capillaries filled with solutions of hemoglobin and/or whole blood (Pittman, R.N. & Duling, B.R., *J. Appl. Physiol.* *38*:315-320 (1975); Lipowsky, H.H., *et al.*, *Microvasc Res* *24*:42-55 (1982)).

It has been demonstrated that the OPS imaging system produces images of blood filled capillary tubes similar to those obtained by transillumination (Groner, W., *et al.*, *Nat. Med.* *5*:1209-1213 (1999)). The optical densities obtained from transillumination and OPS imaging were compared for a series of measurements made on glass capillaries filled with diluted whole blood or solutions of hemoglobin. The receiving optics were identical. The optical densities were essentially identical ($r^2 = 0.984$). Thus, OPS imaging can be useful in the quantitative determination of local hematocrit using the optical density approach in epi-illumination.

OPS imaging relies on the absorbance of hemoglobin to create contrast. Thus, the vessel must contain RBCs to be visualized. For measurement, the vessel needs to be greater in diameter than the minimum resolution of the camera and optics. For these particular images, the magnification at the camera was one micrometer per pixel. Therefore, the resolving power of the system was sufficient to resolve a single RBC and individual capillaries of approximately 5 μm in

- 12 -

diameter. Finally, there must be sufficient contrast between RBCs and the surrounding tissue.

Although OPS imaging technology has been described in U.S. Patents 5,983,120 and 6,104,939 to Groner and Nadeau, and an enhanced OPS imaging system for high contrast *in vivo* imaging of the vascular system described in copending U.S. Patent Application No. 09/401,859, filed September 22, 1999, the medical, clinical, and research applications of this exciting technology have not yet been fully realized.

Summary of the Invention

The present invention relates to medical applications of OPS imaging technology for visualizing and characterizing the microcirculation. These new medical applications may result in the development of new diagnostic tests for human and/or veterinary microvascular pathologies.

Accordingly, the present invention provides a method of detecting a circulation disturbance comprising: (a) obtaining a single captured image or a sequence of images of the microcirculation of an individual afflicted with, or suspected of being afflicted with a circulation disturbance, using an orthogonal polarization spectral ("OPS") imaging probe, comprising the steps of: (i) illuminating a tissue in the microcirculatory system of said individual with light polarized in a first plane of polarization, and (ii) capturing at least one image or a sequence of images reflected from said tissue, wherein said reflected image(s) are passed through an analyzer having a plane of polarization substantially orthogonal to said first plane of polarization to produce a raw reflected image(s), thereby obtaining the captured image(s); and (b) analyzing said captured image(s) to identify characteristics of the microcirculation, thereby detecting said circulation disturbance.

In addition, the invention provides a method of monitoring the microcirculation of an individual before, during, or after a medical procedure comprising:(a) obtaining a single captured image or a sequence of images of the

- 13 -

microcirculation of an individual before, during, or after a medical procedure, using an OPS imaging probe, comprising the steps of: (i) illuminating a tissue in the microcirculatory system of said individual with light polarized in a first plane of polarization, and (ii) capturing at least one image or a sequence of images

5   reflected from said tissue, wherein said reflected image(s) are passed through an analyzer having a plane of polarization substantially orthogonal to said first plane of polarization to produce a raw reflected image(s), thereby obtaining the captured image(s); and (b) analyzing said captured image(s) to monitor the microcirculation of said individual before, during, or after a medical procedure.

10   The small size of the optical probe will facilitate its use as a non-invasive diagnostic tool in both experimental and clinical settings to evaluate and monitor the microvascular sequelae of conditions known to impact the microcirculation, such as shock (hemorrhagic, septic), hypertension, high altitude sickness, diabetes, sickle cell anemia, and numerous other red blood cell or white blood cell

15   abnormalities. In addition to non-invasive applications, imaging and quantitative analysis of the microcirculation during surgery (transplant, cardiac, vascular, orthopedic, neurological, plastic, etc.), wound healing, tumor diagnosis and therapy and intensive care medicine are also applications of OPS imaging technology. The ability to obtain high contrast images of the human

20   microcirculation using reflected light will allow quantitative determination of parameters such as, capillary density, vessel (and microvessel) morphology, vessel density, vasospasm, red blood cell (RBC) velocity, cell morphology, vessel diameter, leukocyte-endothelial cell interactions, vascular dynamics, such as vasomotion, functional vessel density, functional capillary density, blood flow,

25   area-to-perimeter ratio, hemoglobin concentration, and hematocrit, at many previously inaccessible sites. Preferably, two or more parameters will be determined using OPS imaging technology. These measurements will be instrumental in developing precise tools to evaluate perfusion during clinical treatment of those diseases that impact tissue viability and microvascular function.

30   Using this methodology, physicians may now be able to follow the progression

- 14 -

and development of microvascular disease and directly monitor the effects of treatment on the microcirculation.

The OPS image of the microcirculation may be a single captured OPS image or a sequence of images, depending on the parameter to be determined.

Parameters which can be measured from a single captured OPS image include: vessel diameter (vessel can include arteriole, capillary, and venule); vessel morphology; cell morphology; capillary density; vessel density; area-to-perimeter ratio; and vasospasm.

Parameters which are dynamic and can only be measured from a sequence of images include: red blood cell velocity; functional capillary density; functional vessel density; blood flow; leukocyte-endothelial interactions (includes rolling leukocytes and sticking (or adherent) leukocytes); and vascular dynamics, such as vasomotion.

Thus, the present invention is directed to new medical applications of the OPS imaging probe apparatus described in U.S. Patents 5,983,120 and 6,104,939 (also called herein, the "standard" probe), as well as the OPS imaging probe described in copending U.S. Patent Application No. 09/401,859, filed September 22,1999 (also called herein, the "high contrast" probe). It is believed that the medical applications described herein will be applicable to both the standard and high contrast versions of the OPS imaging system. In many instances, however, the high contrast OPS image will be preferred.

The OPS imaging technology described herein is useful for imaging human subjects and animal subjects, as well as *in vitro* applications in research and teaching.

The apparatus used includes a light source, an illumination system, and an imaging system. The light source provides an illumination beam that propagates along an illumination path between the light source and the plane in which the object is located (the object plane). The illumination system transforms the illumination beam into a high contrast illumination pattern and projects that illumination pattern onto the sub-surface object. The illumination pattern has a high intensity portion and a low intensity portion. The imaging system includes

an image capturing device that detects an image of the sub-surface object, such as blood or tissue under the skin of a patient, as well as internal organs (heart, brain, colon) exposed during surgery.

Intravital imaging by transmission microscopy is not possible in humans or animals for inaccessible sites or solid organs. The OPS imaging method employs a small sized optical probe and produces clear images of the microcirculation by reflectance from the surface of solid organs and from sites such as the sublingual area in the awake human. OPS imaging could thus reveal differences between normal and pathological microvascular structure and function non-invasively. The diagnosis and progression of disease, and the effectiveness of treatment could be monitored for disorders in which altered microvascular function has been noted.

In one embodiment of the present invention, a standard or high contrast OPS imaging probe is used for *in vivo* cancer diagnosis, prognosis, or as an aid in cancer surgery.

In one aspect of this embodiment, a standard or high contrast OPS imaging probe is used for the direct diagnosis of epithelial or intraepithelial neoplasms or pre-cancerous conditions. Examples of epithelial or intraepithelial neoplasms that could be diagnosed by OPS imaging include cervical, dermal, esophageal, bronchial, intestinal, or conjunctival neoplasms.

In another aspect of this embodiment, a standard or high contrast OPS imaging probe is used to assess tumor boundaries or tumor margins, prior to, during, or following cancer therapy.

In another aspect of this embodiment, a standard or high contrast OPS imaging probe is used to diagnosis different types of tumors based on their vascular structure.

In another aspect of this embodiment, a standard or high contrast OPS imaging probe is used to monitor the effects of cancer radiation therapy, such as the occurrence of telangiectasia or other microvascular or vascular effects on irradiated tissue.

In another embodiment of the present invention, a standard or high contrast OPS imaging probe is used for *in vivo* wound care and wound healing

- 16 -

management. In this embodiment, the OPS imaging probe would be used in the visualization, characterization, assessment and management of different types of wounds--venous ulcers, decubitis ulcers, traumatic wounds, non-healing surgical wounds, and burn wounds. Since venous ulcers are formed as a result of an underlying circulatory problem, knowledge about the microcirculation would be essential to effective treatment.

In one aspect of this embodiment, a standard or high contrast OPS imaging probe is used to visualize and characterize microvessels in and around wounds.

In another aspect of this embodiment, a standard or high contrast OPS imaging probe is used to visualize, characterize, and quantify the perfused microvessel density in venous stasis ulcers or diabetic ulcers.

In another aspect of this embodiment, a standard or high contrast OPS imaging probe is used to observe necrotic tissue and determine the degree of debridement a wound would require.

In another aspect of this embodiment, a standard or high contrast OPS imaging probe is used to assess the margins of a wound to determine the likelihood it is going to heal.

In another aspect of this embodiment, a standard or high contrast OPS imaging probe is used to assess the viability of wound tissue to successfully support a skin graft.

In another aspect of this embodiment, a standard or high contrast OPS imaging probe is used to more accurately and objectively determine the line of amputation.   In another aspect of this embodiment, a standard or high contrast OPS imaging probe is used to measure and compare the revascularization and healing of a wound using different wound healing therapies.

In another aspect of this embodiment, a standard or high contrast OPS imaging probe is used to monitor capillary budding during wound healing.

In another embodiment of the present invention, a standard or high contrast OPS imaging probe is used *in vivo* during plastic surgery.

- 17 -

In one aspect of this embodiment, a standard or high contrast OPS imaging probe is used to monitor blood flow (perfusion) during and following plastic, reconstructive, reattachment, or microsurgery.

In another aspect of this embodiment, a standard or high contrast OPS imaging probe is used to determine healthy versus necrotic or dead tissue around a skin flap.

In another aspect of this embodiment, a standard or high contrast OPS imaging probe is used after surgery to continuously monitor the microcirculation and identify any potential problems with reperfusion. Early indication of reperfusion problems may help avoid the need for repeat surgery.

In another embodiment of the present invention, a standard or high contrast OPS imaging probe is used *in vivo* in the field of cardiology and cardiac surgery.

In one aspect of this embodiment, a standard or high contrast OPS imaging probe is used to increase visualization and characterization of the cardiac microcirculation, to confirm reperfusion during minimally invasive cardiac surgical procedures that avoid the heart/lung bypass machine, such as "keyhole" surgeries (*i.e.*, Heartport) and thoracotomies.

In another aspect of this embodiment, a standard or high contrast OPS imaging probe is used for monitoring and detecting changes in patient blood flow (the microcirculation) during open heart surgery while the patient is on the heart-lung machine. Thus, the OPS imaging probe could be used to monitor the progress of the patient on the heart-lung machine.

In another aspect of this embodiment, the OPS imaging probe also can be used during coronary artery bypass graft (CABG) surgery to determine if the graft is getting good blood flow and providing the downstream vessels with good blood flow. That is, a cardiac surgeon could use the OPS imaging probe, directly contacting the heart, to monitor the blood flow to the capillaries after bypass surgery.

In another aspect of this embodiment, the OPS imaging probe is used for cardiac risk monitoring. The use of the OPS imaging probe to visualize and

- 18 -

characterize the microcirculation may assist in non-invasively determining a high risk cardiac profile. The microvascular sequalae of hypertension could be studied and also be used in determining cardiac risk.

In another embodiment of the present invention, the OPS imaging probe is used in the visualization, characterization, and assessment of lung tissue.

In another embodiment of the present invention, a standard or high contrast OPS imaging probe is used *in vivo* prior to or during neurosurgery.

In one aspect of this embodiment, a standard or high contrast OPS imaging probe is applied directly to the brain during diagnostic or therapeutic neurosurgery to visualize and characterize the microcirculation, and measure parameters, such as, *e.g.*, diameter, flow velocity, and functional capillary density.

In another aspect of this embodiment, a standard or high contrast OPS imaging probe is used to detect vasospasm following an aneurism or subarachnoid hemorrhage.

In another aspect of this embodiment, a standard or high contrast OPS imaging probe is used to detect boundaries of tumors in the brain.

In another aspect of this embodiment, a standard or high contrast OPS imaging probe is used for the determination and typing of brain tumors based on the vascular structure and differences in the microcirculation of different brain tumors.

In another aspect of this embodiment, a standard or high contrast OPS imaging probe is used to directly visualize and characterize the vascular consequences of neural trauma. The OPS imaging probe may also be used to determine the extent of neural trauma.

In another embodiment of the present invention, a standard or high contrast OPS imaging probe is used *in vivo* during organ transplantation.

In one aspect of this embodiment, a standard or high contrast OPS imaging probe is used during transplant surgery to determine the amount of perfusion after the transplanted tissue/organ is connected.

In another embodiment of the present invention, a standard or high contrast OPS imaging probe is used *in vivo* during vascular grafting surgery, such as in Peripheral Arterial Occlusive Disease (PAOD).

In one aspect of this embodiment, a standard or high contrast OPS imaging probe is used during vascular graft surgery to determine the amount of perfusion after the graft is connected.

In another embodiment of the present invention, a standard or high contrast OPS imaging probe is used *in vivo* during orthopedic surgery, as well as in the field of orthopedic medicine.

In one aspect of this embodiment, a standard or high contrast OPS imaging probe is used during orthopedic surgery to identify and observe necrotic tissue, for surgical removal. The site of the probe would be on the area that has undergone trauma.

The probe can also be used to visualize bones, tendons, and ligaments.

In another aspect of this embodiment, a standard or high contrast OPS imaging probe is used to visualize and characterize the microcirculation around periosteum (bone). Differences in microcirculation were observed when the image was taken before or after a fracture.

In another embodiment of the present invention, a standard or high contrast OPS imaging probe is used *in vivo* in the fields of gastroenterology and gastrointestinal (GI) or gastroesophageal surgery.

In one aspect of this embodiment, a standard or high contrast OPS imaging probe is used to visualize and characterize the large intestine and diagnose and treat inflammatory bowel disease, ulcerative colitis, Crohn's disease, or other gastrointestinal disorders affecting the microcirculation. The probe can be inserted into the rectum to directly contact the wall of the large intestine.

In another aspect of this embodiment, the OPS imaging probe can be used during gastrointestinal (GI) surgery to visualize and characterize the colon during bowel resection. Other GI organs may be visualized as well.

In another aspect of this embodiment, the OPS imaging probe can be used to determine the boundaries of a cancerous GI tumor and to visualize and

- 20 -

characterize necrotic tissue. Removal of the affected tissue from the stomach and/or esophagus area can thus be more easily accomplished during surgery.

In another aspect of this embodiment, the OPS imaging probe can also be used to visualize and characterize the rectal mucosal microcirculation, such as, for example, in patients with inflammatory bowel disease.

In another embodiment of the present invention, a standard or high contrast OPS imaging probe is used *in vivo* in the field of opthamology.

In one aspect of this embodiment, a standard or high contrast OPS imaging probe is used to visualize and characterize the ocular microcirculation. Such a visualization tool can be used for diagnostic purposes and treatment as well as providing information regarding the effectiveness of various types of medications on the circulatory system in the area examined.

In another aspect of this embodiment, OPS imaging technology can be used to diagnose macular degeneration, retinal disorders (retinopathy), and glaucoma.

In another aspect of this embodiment, OPS imaging technology can be used to visualize and characterize the optic disk, retina, sclera, conjunctiva, and changes in the vitreous humor.

In another aspect of this embodiment, OPS imaging technology can be used for early diagnosis and treatment of diabetes by looking at the ocular microcirculation, especially changes or differences in the sclera and/or aqueous humor of the eye.

In another embodiment of the present invention, the OPS imaging probe is used during normal or complicated pregnancy to monitor the woman's microvascular function.

In one aspect of this embodiment, a standard or high contrast OPS imaging probe is used to detect or monitor women whose pregnancy is complicated by preeclampsia (PE).

In another embodiment of the present invention, the OPS imaging probe can be used in neonatology monitoring.

- 21 -

In one aspect of this embodiment, a standard or high contrast OPS imaging probe is used to quantitatively measure changes in the microcirculation of neonates during different disease states like sepsis and meningitis, and therefore be used to diagnosis those conditions. Hemoglobin levels of the neonates can be monitored non-invasively.

In another embodiment of the present invention, OPS imaging can be used in high altitude studies or to study space physiology.

In one aspect of this embodiment, a standard or high contrast OPS imaging probe is used to observe and evaluate changes in the microcirculation at high altitudes to study, diagnose, and/or treat high altitude sickness.

In another embodiment of the present invention, the OPS imaging probe can be used *in vivo* in critical care or intensive care medicine.

In one aspect of this embodiment, a standard or high contrast OPS imaging probe is used as a sublingual measuring or monitoring device on critically ill patients to diagnose, treat, or prevent sepsis and shock (hemorrhagic or septic).

In another embodiment of the present invention, the OPS imaging probe is used in the field of pharmaceutical development.

In one aspect of this embodiment, a standard or high contrast OPS imaging probe is used to study the effects of different pharmaceuticals on the microcirculation, such as anti-angiogenesis drugs to determine if circulation to a tumor is cut off; or angiogenesis drugs to determine if vessel growth to an organ and thus circulation has improved; or anti-hypertensive agents to determine mechanisms of action of new treatments or hypertension etiology at the microvascular level.

In another aspect of this embodiment, a standard or high contrast OPS imaging probe is used to look at hemoglobin-based oxygen carriers (*i.e.*, DCL Hb, a synthetic hemoglobin) to determine their effects on the microcirculation, such as, *e.g.*, whether there is an increased flow of RBC's as a result of using the product.

- 22 -

In another aspect of this embodiment, the OPS imaging probe can be used to study the effect of ultrasound enhancers (*i.e.*, injectable dyes) on the microcirculation.

In another aspect of this embodiment, the OPS imaging probe can be used to visualize and detect leakage of injectable dyes or other injectable contrast-generating agents, from the blood vessels into tissues.

In another embodiment of the present invention, a standard or high contrast OPS imaging probe is used to visualize and characterize capillary beds in the nailfold, as has been done before using standard capillaroscopy.

In one aspect of this embodiment, a standard or high contrast OPS imaging probe is used to study, diagnose, and evaluate patients with circulation disturbances, such as, for example, Raynaud's phenomenon, osteoarthritis, or systemic sclerosis.

In another embodiment of the present invention, the OPS imaging probe is used in the area of anesthesiology.

In one aspect of this embodiment, a standard or high contrast OPS imaging probe is used to monitor blood loss during surgery. For example, an OPS imaging probe can be used to non-invasively and continuously monitor the hemodynamic parameters of an anesthetized patient, such as, *e.g.*, hemoglobin concentration and hematocrit.

In another aspect of this embodiment, a standard or high contrast OPS imaging probe is used on an anesthetized patient to monitor the clumping of red blood cells, and the early formation of microemboli during surgery.

In another embodiment of the present invention, a standard or high contrast OPS imaging probe is used to visualize, characterize, identify, and/or monitor disseminated intravascular coagulation (DIC) in a patient, which may occur as a secondary complication of infection, obstetrics, malignancy, and other severe illnesses.

In one aspect of this embodiment, a standard or high contrast OPS imaging probe is used to visualize, characterize, identify, and/or monitor DIC, due to infection, and more particularly due to meningitis.

- 23 -

In another embodiment of the present invention, a standard or high contrast OPS imaging probe is used to visualize, characterize, and monitor changes in leukocyte-endothelial cell interactions, such as occurs during inflammation or infection.

In another embodiment of the present invention, the OPS imaging probe is used for *in vitro* or *in vivo* basic or clinical research in any or all of the areas mentioned above (*i.e.*, cardiology, cardiac surgery, wound care, diabetes, hypertension, opthalmology, neurosurgery, plastic surgery, transplantation, anesthesiology, and pharmacology).

In another embodiment of the present invention, the OPS imaging probe is used as a teaching tool for medical students and/or science students studying, for example, physiology, anatomy, pharmacology, the microcirculation, and disease states affecting the microcirculation.

It is to be understood that both the foregoing general description and the following detailed description are exemplary and explanatory and are intended to provide further explanation of the invention as claimed.

Brief Description of the Figures

The accompanying figures, which are incorporated herein and form part of the specification, illustrate embodiments of the present invention and, together with the description, further serve to explain the principles of the invention and to enable a person skilled in the pertinent art to make and use the invention. In the figures, like reference numbers indicate identical or functionally similar elements.

Figure 1 shows a block diagram illustrating one particular embodiment of an OPS imaging probe for non-invasive *in vivo* analysis of a subject's vascular system. In this particular embodiment, the objective lens is 8 inches long. This embodiment would be particularly useful for imaging cervical tissue.

Figure 2 is an OPS image of arterioles (A) and venules (V) in normal brain tissue after opening of the dura during neurosurgery. Bar indicates 100 μm.

- 24 -

Figure 3 is an OPS image showing the site of interest in the brain dominated by capillaries. Bar indicates 100μm.

Figure 4 is an OPS image of cortical microvessels in a patient with subarachnoid hemorrhage. Extravasation of red blood cells is seen as black dots in the extravascular space. The arteriole (A) shows the pearl string sign of multiple segmental microvasospasm (arrows). No microvasospasm is seen in the venule (V). Bar indicates 100μm.

Figure 5 is an OPS image of the opaque endothelial layer in several vessels close to the area of brain tumor resection. The underlying pathophysiology is unknown. The observation may represent endothelial swelling or a plasma layer streaming along the endothelium. Bar indicates 100 μm.

Figure 6 is an OPS image depicting tumor angiogenesis in a patient with a glioblastoma multiforme WHO IV. Typical tortuous, irregular shaped conglomerate of newly built tumor vessels. Bar indicates 100 μm.

Figure 7 is a bar graph depicting functional capillary density before and after tumor resection/clipping of aneurysm. Mean±SEM.

Figure 8 is a bar graph depicting the distribution of arteriolar and venular diameters before and after tumor resection/clipping of aneurysm. The box and bars indicate the median and the $10^{th}, 25^{th}, 75^{th}$ and 90th percentiles.

Figure 9 is a bar graph depicting the frequency distribution of red blood cell velocities in arterioles and venules before and after tumor resection/clipping of aneurysm given in percentages of total number of vessels. nm = no measurement.

Figure 10 depicts changes of portal venous blood flow in Sham and endotoxemic (ETX) animals during the investigation period. All data are expressed as boxplots including median, $10^{th}, 25^{th}, 75^{th}$ and 90th percentiles, as well as the highest and the lowest value. # denotes significant difference versus baseline, § indicates significant difference between the two groups.

Figure 11 depicts changes of the gastrointestinal mucosal-arterial pCO_2-gap (r-aPCO_2) in Sham and endotoxemic animals during the investigation period. All data are expressed as boxplots including median, $10^{th}, 25^{th}, 75^{th}$ and 90th

- 25 -

percentiles, as well as the highest and the lowest value. # denotes significant difference versus baseline, § indicates significant difference between the two groups.

Figure 12 depicts changes in the numbers of perfused/heterogenously perfused/unperfused villi in Sham and endotoxemic animals during the investigation period.

Figure 13 depicts relative changes of perfused/heterogenously perfused/unperfused villus count in Sham and Endotoxin animals during the investigation period. Data are shown in % of counted villi.

Figure 14 is a schematic picture of the OPS imaging device and an image of the capillaries of the nailfold.

Figures 15A-15B: Figure 15A depicts change in flux (%) during venous occlusion and after arterial occlusion (peak flux) compared to flux at rest measured at the palmer side. One subject of the preeclamptic group had an increase in peak flux that was an increase of 178% compared to rest value.

Figure 15B depicts change in flux (%) during venous occlusion and after arterial occlusion (peak flux) compared to flux at rest measured at the dorsal side. One subject of the control group had an increase in flux of 411% during venous occlusion.

Figure 16 shows percentual change in velocity during venous occlusion compared to velocity at rest.

Figure 17 depicts an OPS image of the sublingual area in a healthy volunteer. Note the dense venular and capillary network.

Figure 18 is an OPS image of the sublingual area of a patient with septic shock (mean arterial pressure 68 mmHg, lactate 3.8 mEq/L, dopamine 20 mcg/kg.min, norepinephrine 0.13 mcg/kg/min). Note the decrease in capillary density with stop flow and transient flow in numerous capillaries.

Figure 19 is an OPS image of the sublingual area of a patient with severe cardiogenic shock (mean arterial pressure 50 mmHg, lactate 10.5 mEq/L, dobutamine 20 mcg/kg.min, dopamine 20 mcg/kg.min, norepinephrine 3

- 26 -

mcg/kg.min). Note the decreased capillary density and the red blood cell conglomerates in large vessels representative of stagnant flow.

Figure 20 is an OPS image of necrotic ileostomy. Note the decreased number of gut mucosal capillaries, most of them not perfused.

5
Detailed Description of the Embodiments

The present invention relates to medical applications of OPS imaging technology for visualizing and characterizing the microcirculation. Such applications may result in the development of new diagnostic tests for human microvascular pathologies.

10   Accordingly, the present invention provides a method of detecting a circulation disturbance comprising: (a) obtaining a single captured image or a sequence of images of the microcirculation of an individual afflicted with, or suspected of being afflicted with a circulation disturbance, using an orthogonal polarization spectral ("OPS") imaging probe, comprising the steps of: (i)

15   illuminating a tissue in the microcirculatory system of said individual with light polarized in a first plane of polarization, and (ii) capturing at least one image or a sequence of images reflected from said tissue, wherein said reflected image(s) are passed through an analyzer having a plane of polarization substantially orthogonal to said first plane of polarization to produce a raw reflected image(s),

20   thereby obtaining the captured image(s); and (b) analyzing said captured image(s) to identify characteristics of the microcirculation, thereby detecting said circulation disturbance.

In addition, the invention provides a method of monitoring the microcirculation of an individual before, during, or after a medical procedure

25   comprising:(a) obtaining a single captured image or a sequence of images of the microcirculation of an individual before, during, or after a medical procedure, using an OPS imaging probe, comprising the steps of: (i) illuminating a tissue in the microcirculatory system of said individual with light polarized in a first plane of polarization, and (ii) capturing at least one image or a sequence of images

- 27 -

reflected from said tissue, wherein said reflected image(s) are passed through an analyzer having a plane of polarization substantially orthogonal to said first plane of polarization to produce a raw reflected image(s), thereby obtaining the captured image(s); and (b) analyzing said captured image(s) to monitor the microcirculation of said individual before, during, or after a medical procedure. As used herein, the term "tissue" is intended to include blood.

The small size of the optical probe will facilitate its use as a non-invasive diagnostic tool in both experimental and clinical settings to evaluate and monitor the microvascular sequelae of conditions known to impact the microcirculation, such as shock (hemorrhagic, septic), hypertension, high altitude sickness, diabetes, sickle cell anemia, and numerous other red blood cell or white blood cell abnormalities. In addition to non-invasive applications, imaging and quantitative analysis of the microcirculation during surgery (transplant, cardiac, vascular, orthopedic, neurological, plastic, etc.), wound healing, tumor diagnosis and therapy and intensive care medicine are also applications of OPS imaging technology.

The ability to obtain high contrast images of the human microcirculation using reflected light will allow quantitative determination of one or more parameters, such as, capillary density, vessel (and microvessel) morphology, vessel density, vasospasm, red blood cell (RBC) velocity, cell morphology, vessel diameter, leukocyte-endothelial cell interactions, vascular dynamics (such as vasomotion), functional vessel density, functional capillary density, blood flow, area-to-perimeter ratio, hemoglobin concentration, and hematocrit, at many previously inaccessible sites. Preferably, two or more parameters will be determined using OPS imaging technology. These measurements will be instrumental in developing precise tools to evaluate perfusion during clinical treatment of those diseases that impact tissue viability and microvascular function. Using this methodology, physicians may now be able to follow the progression and development of microvascular disease and directly monitor the effects of treatment on the microcirculation.

- 28 -

As used herein, the term "capillary density" means the ratio of the length of capillaries to the total area of observation, expressed as cm/cm^2.

As used herein, the term "vessel (and/or microvessel) morphology" means the physical or structural characteristics of a vessel (or microvessel). This term can refer to an individual vessel or to a network of vessels.

As used herein, the term "vessel density" means the area occupied by vascular structures. Vessel density is expressed as a ratio of the area occupied by vessel structures to the total observation area. The number can be expressed as a percentage. Vessel density can also be referred to as "vascularization index."

As used herein, the term "vasospasm" means prolonged abnormal constriction of vessels, usually in response to trauma and/or the presence of extracellular blood in the area adjacent to the vessel. For example, vasospasms are a well-known consequence of a sub-arachnoid hemorrhage in the brain.

As used herein, the term "red blood cell (RBC) velocity" means the observed velocity of red blood cells within a blood vessel.

As used herein, the term "cell morphology" means the cell shape characteristics of white blood cells, red blood cells, and/or epithelial cells.

As used herein, the term "vessel diameter" means the distance between the observable walls of a blood vessel.

As used herein, the term "leukocyte-endothelial cell interactions" means any interaction between a leukocyte (white blood cell) and the inner surface of a blood vessel (the endothelial cell layer). These interactions can include rolling along the wall of the vessel at a rate slower than the RBC velocity, sticking in one place for a period of time, or migrating out through the vessel wall, perhaps to a site of inflammation.

As used herein, the term "vascular dynamics" means a temporal (time dependent) change in vessel diameter. This may be a spontaneous change (e.g., vasomotion) or in response to a neuronal, hormonal, or pharmacological stimulus. In addition, the normal response of a vessel to a given stimulus may be influenced by other factors. These other factors would then be described as influencing the vascular dynamics.

- 29 -

As used herein, the term "functional vessel density" means a ratio of the length of perfused vessels to the total observation area. A perfused vessel is one through which RBC's can be observed to flow.

As used herein, the term "functional capillary density" means a ratio of the length (or number) of perfused capillaries to the total observation area. A perfused capillary is one through which RBC's can be observed to flow. This is expressed as cm/cm^2 (or $number/cm^2$).

As used herein, the term "blood flow" means the observed movement of red blood cells through a vessel.

As used herein, the term "area-to-perimeter ratio" means a measure of the clumping or heterogeneity of red blood cells in a vessel. The ratio is defined as the ratio of the area of red blood cell conglomerates detected within a vessel to the length of the perimeter or outline of the red blood cell conglomerates. A fully perfused vessel without plasma spaces leads to a higher area-to-perimeter ratio. Plasma spaces or partially filled vessels will result in a smaller area-to-perimeter ratio value. This parameter might be used to assess stagnant flow or clumped cells, for example.

As used herein, the term "hemoglobin (or Hb) concentration" means the concentration of the iron-containing protein pigment (hemoglobin) found in red blood cells. Hemoglobin, the main component of the red blood cell, is a conjugated protein that serves as a vehicle for the transportation of oxygen and CO_2, throughout the body. When fully saturated, each gram of hemoglobin holds 1.34 ml of oxygen. The red cell mass of the adult contains approximately 600 g of hemoglobin, capable of carrying 800 ml of oxygen. The main function of hemoglobin is to transport oxygen from the lungs, where oxygen tension is high, to the tissues, where it is lower.

As used herein, the term "hematocrit" means the ratio of the volume of erythrocytes (red blood cells) in a sample of blood to that of the whole blood. It is expressed as a percentage or, preferably, as a decimal fraction.

Thus, the present invention is directed to new medical applications of the OPS imaging probe apparatus described in U.S. Patents 5,983,120 and 6,104,939

- 30 -

(also called herein, the "standard" probe), as well as the OPS imaging probe described in copending U.S. Patent Application No. 09/401,859, filed September 22,1999 (also called herein, the "high contrast" probe). It is believed that the medical applications described herein will be applicable to both the standard and high contrast versions of the OPS imaging system. In certain medical applications, however, the high contrast OPS image will be preferred.

The OPS imaging technology described herein is useful for imaging human subjects and animal subjects, as well as *in vitro* applications in research and teaching.

The apparatus used includes a light source, an illumination system, and an imaging system. The light source provides an illumination beam that propagates along an illumination path between the light source and the plane in which the object is located (the object plane). The illumination system transforms the illumination beam into a high contrast illumination pattern and projects that illumination pattern onto the sub-surface object. The illumination pattern has a high intensity portion and a low intensity portion. The imaging system includes an image capturing device that detects an image of the sub-surface object, such as blood and/or tissue under the skin of a patient, from sublingual sites, as well as from the surface of solid organs (heart, brain, colon, lungs) exposed during surgery, or epithelial or intraepithelial tissue (*i.e.*, cervix). Intravital imaging by transmission microscopy is not possible in humans or animals for inaccessible sites or solid organs. The OPS imaging method employs a small sized optical probe and produces clear images of the microcirculation by reflectance from the surface of solid organs and from sites such as the sublingual area in the awake human. OPS imaging could thus reveal differences between normal and pathological microvascular structure and function non-invasively. The diagnosis and progression of disease, and the effectiveness of treatment could be monitored for disorders in which altered microvascular function has been noted.

The image of the microcirculation may be a single captured OPS image or a sequence of images, depending on the parameter to be determined.

- 31 -

Parameters which can be measured from a single captured OPS image include: vessel diameter (vessel can include arteriole, capillary, and venule); vessel morphology; cell morphology, capillary density; vessel density; area-to-perimeter ratio; and vasospasm.

Parameters which are dynamic and can only be measured from a sequence of images include: red blood cell velocity; functional capillary density; functional vessel density; blood flow; leukocyte-endothelial interactions (includes rolling leukocytes and sticking (or adherent) leukocytes); and vascular dynamics, such as vasomotion.

The present invention is illustrated by numerous examples and experimental data presented below. This information is provided to aid in the understanding and enablement of the present invention, but is not to be construed as a limitation thereof.

Cancer Applications

In this embodiment of the present invention, a high contrast OPS imaging probe is used for *in vivo* cancer diagnosis, prognosis, or as an aid in cancer surgery.

In one aspect of this embodiment, a standard or high contrast OPS imaging probe is used for the direct diagnosis of epithelial or intraepithelial neoplasms or pre-cancerous conditions. Examples of epithelial or intraepithelial neoplasms that could be diagnosed by OPS imaging include cervical, dermal, esophageal, bronchial, intestinal, or conjunctival neoplasms.

Regarding cervical intraepithelial neoplasms (CIN), although there has been a significant decline in the incidence and mortality of invasive cervical carcinoma over the last 50 years, there has been an increase in both the reported and actual incidence of CIN. As a result, it has been estimated that the mortality of cervical carcinoma may rise by 20% in the years 2000-2004 unless screening techniques for CIN are improved.

- 32 -

Present screening for CIN and cervical cancer is relatively inexpensive but labor intensive because it initially relies on the results of a Pap smear; a false negative error rate of 20-30% is associated with insufficient cell sampling and/or inexpert reading of Pap smears. On the other hand, false positive results on a Pap smear, such as occurs in 70-80% of women with the Pap smear classification "ASCUS" (which stands for Atypical Cells of Undetermined Significance under the newer "Bethesda" classification system), may lead to unnecessary, time-consuming, and costly follow-up testing (such as colposcopyand/or biopsy) and needless worry for the patient.

Thus, a more reliable method to classify cervical tissue as normal or abnormal, and in the latter case to distinguish inflammation or benign HPV infection from CIN, is needed.

It was noted that the excellent images of the microcirculation obtained through OPS imaging technology were overlain by a "mosaic" of tesserae that were epithelial cell-shaped. They were rhomboidal, penta, hexa, septahedronal and quite flat and regular. Their diameters were approximately 10-40 microns based on a comparison with the RBCs and arterioles and venules in the same fields. They were clearly overlaying the vascular structures. Their cell margins were illuminated (refractile). The cells were quite "flat," suggesting that they were superficial rather than deeper epithelium, and definitely not basal layer cells which are more cuboidal. In addition, the size and shape of cell nuclei could also be distinguished. These characteristics are particularly important in an assessment of premalignant and malignant states.

With the information that the focal "plane" of the system as configured was ≈150-200 microns from the surface of the optical probe, which corresponds to the depth at which the vasculature exists, it was theorized that the depiction of superficial epithelium must arise from a mechanism of light scattering and back illumination, or other effects. It was then realized that the optics of the OPS imaging probe could be optimized to make the epithelium the main feature of the image. Thus, by using the OPS imaging probe to bring out the epithelial image at

- 33 -

different depths, then the direct diagnosis of intraepithelial lesions, including carcinoma-in-situ or early invasive carcinoma can be achieved.

In gynecological oncology, recognizing and treating carcinoma-in-situ is challenging. Current practice usually begins with a Pap smear test, sometimes associated with papilloma virus detection, followed by colposcopy with biopsy and then a surgical removal. This is time-consuming, involving multiple visits by the patient for pelvic examination, cytologic and wet laboratory (for papilloma virus) testing and pathological examination of biopsy specimens. This is also quite expensive.

In this embodiment of the invention, OPS imaging technology, or derivatives of it, can be employed to directly visualize, characterize, and also quantify pre-malignant and malignant epithelial lesions. For example, in the case of carcinoma-in-situ of the cervix, a gynecological examination by eye could be immediately followed by employing an OPS imaging probe that reveals epithelial cell layers. The lesions mentioned above are defined as disruptions of the regular pattern, by cells with distinguishable characteristics that include abnormal size, shape and cellular features such as nuclear: cytoplasmic ratios. They produce an abnormal "architecture," in histopathological terms, that has heretofore required examination by a pathologist of biopsy material. Distinguishing the abnormal disruptive architecture of pre-malignant and malignant epithelial lesions from normal cells could be done by reconstructing 3-dimensional images of the tissue from OPS images gathered while focusing through the tissue.

Using an OPS imaging probe, a direct diagnosis could be made by comparing uninvolved, normal, portions of the cervix with "suspicious" regions. Image analysis of the mosaic could lead to characterizable differences in the regularity of the mosaic. Cell dimensions, shapes and other morphological characteristics could be quantified; alterations in blood flow and velocity between normal and suspicious areas, or even between different tumor types may also be observed and quantified. This has never been done before and pathological diagnosis is still impressionistic and subjective rather than statistical. Direct

- 34 -

diagnosis using OPS imaging technology, of course, does not preclude conventional biopsy.

The approach to intraepithelial diagnosis might well require optimization of the OPS imaging probe. For example, image analysis of mosaic patterns, different magnifications, different and perhaps continuously variable focus, different dimensions of light source, masking of the aperture for dark field and perhaps epi-illumination (perhaps also at different angles) to accentuate the epithelial cell boundaries and interior structure, image quantification of the normal vs. inspected abnormal region, etc, may need to be optimized by those skilled in the art.

FIG. 1 shows a block diagram of an OPS imaging probe 200, having an elongated objective 214 (approximately 8 inch), that could be used for the screening and/or diagnosis of cervical neoplasms or cervical pre-cancerous lesions. Probe 200 includes a light source 202, collection lenses 204, relay lenses 208, a detector 260, and an objective 217. One or more band pass filters 206 may be placed in the light path to enhance the quality of the image obtained. The type of filter used is a function of the object being imaged, as is well-known to skilled workers in the relevant arts.

Light source 202 illuminates a tissue region of a subject (shown generally at 224). Although one light source is shown in FIG. 1, it is to be understood that the present invention is not limited to the use of one light source, and more than one light source can be used. In an embodiment where more than one light source is used, each light source can be monochromatic or polychromatic. Light source 202 can be a light capable of being pulsed, a non-pulsed light source providing continuous light, or one capable of either type of operation. Light source 202, can include, for example, a pulsed xenon arc light or lamp, a mercury arc light or lamp, a halogen light or lamp, a tungsten light or lamp, a laser, a laser diode, or a light emitting diode (LED). Light source 202 can be a source for coherent light, or a source for incoherent light.

A folding mirror or beam splitter 218 is used to form a light path between light source 202 and subject 224. According to one embodiment of the present

- 35 -

invention, beam splitter 218 is a coated plate having 50% reflection of illumination beam 209. Other embodiments of beam splitter 218 are well known to persons skilled in the relevant arts.

In a preferred embodiment, a first polarizer 210 is placed between light source 202 and subject 224. First polarizer 210 polarizes light from light source 202. A second polarizer or analyzer 220 is placed between object 224 and image capturing means 260 along image path 207. Polarizers 210 and 220 preferably have planes of polarization oriented 90° relative to each other. Polarizers, such as polarizers 210 and 220, having planes of polarization oriented 90° relative to each other are referred to herein as "crossed-polarizers."

Preferably, the image from object 224 emanates from a depth less than a multiple scattering length and travels along image path 207 to image capturing means 260. However, the imaging system of the present invention can also capture images formed from a depth greater than a multiple scattering length. Objective 217 is used to magnify the image of object 224 onto image capturing means 260. Objective 217 is placed co-axially in illumination path 209 and image path 207. Image capturing means 260 is located in a magnified image plane of objective 217. Objective 217 can comprise one or more optical elements or lenses, depending on the space and imaging requirements of apparatus 200, as will be apparent to one of skill in the art based on the present description.

Suitable image capturing means 260 include those devices capable of capturing a high resolution image as defined above. The image capturing means captures all or part of an image for purpose of analysis. Suitable image capturing means include, but are not limited to, a camera, a film medium, a photosensitive detector, a photocell, a photodiode, a photodetector, or a CCD or CMOS camera.

Image capturing means 260 can be coupled to an image correcting and analyzing means (not shown) for carrying out image correction and analysis. The resolution required for the image capturing means can depend upon the type of measurement and analysis being performed by the *in vivo* apparatus.

Preferably, objective 217 can be one or more lenses that are selected with the lowest magnification level required to visualize the illuminated object. The

- 36 -

magnification required is a function of the size of the object in the illuminated tissue to be visualized, along with the size of the pixels used for the image.

According to a preferred embodiment, illumination path 209 and image path 207 share a common axis. This coaxial nature allows for objective 217 to be utilized for more than one purpose. First, objective 217 acts as the objective for image capturing means 260. In other words, it collects the image beam emanating from object 224 onto image capturing means 260. Second, objective 217 acts to focus the high contrast illumination pattern onto the object plane. The high intensity portion of illumination beam 209 is directed outside the field of view (FOV) of the image capturing means 260.

The combination of the optical characteristics of objective 217 and image capturing means 260 determine the FOV of device 200. The FOV of the image capturing means can be limited by many parameters including the numerical aperture of its objective (here objective 217), entrance pupils, exit pupils, and the area of the detector comprising image capturing means 260.

While the cervix is a particularly important target because of the frequency of disease and the regularity of examination for carcinoma, and also because the cervical epithelium is thick, flat based and regular, other intraepithelial lesions and immediate sub-epithelial extensions of epithelial malignancies through the basal layer and basal membrane are also good targets for this approach to diagnosis. For example, the difference between a benign activated nevus and a malignant melanoma presents a serious diagnostic dilemma that usually results in a biopsy. With the OPS imaging technique of this invention, such skin lesions, or their precancerous precursors could be diagnosed, and distinguished, directly. An "inventory" of pigmented lesions could be recorded by sight on an individual's body and archived images and quantitative measures be employed as "baseline."

In another aspect of this embodiment, a high contrast OPS imaging probe is used to assess tumor boundaries or tumor margins, prior to, during, or following cancer therapy. For example, OPS imaging can be used to visualize and characterize true skin cancer margins that may not be clinically visible to the

- 37 -

dermatologist with the unaided eye. This may reduce the need for additional surgery.

In another aspect of this embodiment, a high contrast OPS imaging probe is used to diagnosis different types of tumors based on their vascular structure.

In another aspect of this embodiment, a high contrast OPS imaging probe is used to monitor the microvascular effects of cancer radiation therapy, such as the occurrence of telangiectasia (the dilation of smooth blood vessels). A high contrast OPS imaging probe could also be used to study other microvascular or vascular effects on irradiated tissue, such as changes in perfused microvessel density following varying doses of radiation.

Applications in Wound Care and Wound Healing Management

In this embodiment, the OPS imaging probe is used in the visualization, characterization, assessment, and management of different types of wounds-- venous ulcers (caused by chronic venous insufficiency or diabetes); decubitis ulcers (also known as pressure sores, which form when chronic pressure inhibits blood flow, cutting off oxygen and nutrients and leading to tissue ulceration and death); traumatic wounds (wounds sustained during an accident or violent episode); non-healing surgical wounds (incisions made during a surgical procedure that do not heal within the expected timeframe) and burn wounds. Since venous ulcers are formed as a result of an underlying circulatory problem, knowledge about the microcirculation would be essential to effective treatment.

In each of the following aspects of this embodiment, one or more parameters, such as, capillary density, vessel (and microvessel) morphology, vessel density, vasospasm, red blood cell (RBC) velocity, cell morphology, vessel diameter, leukocyte-endothelial cell interactions, vascular dynamics (such as vasomotion), functional vessel density, functional capillary density, blood flow, area-to-perimeter ratio, hemoglobin concentration, and hematocrit, may be quantitatively determined. Preferably, two or more parameters are determined.

- 38 -

In one aspect of this embodiment, a standard or high contrast OPS imaging probe is used to visualize and characterize microvessels in and around wounds.

In another aspect of this embodiment, a standard or high contrast OPS imaging probe is used to visualize, characterize, and quantify the perfused microvessel density in venous stasis ulcers or diabetic ulcers. Using OPS imaging on chronic wounds in diabetic patients, a relative lack of microvessels in the wound bed or in the adjacent tissue has been observed compared to uninvolved skin.

In another aspect of this embodiment, a standard or high contrast OPS imaging probe is used to observe necrotic tissue and determine the degree of debridement a wound would require.

In another aspect of this embodiment, a standard or high contrast OPS imaging probe is used to assess the margins of a wound to determine the likelihood it is going to heal.

In another aspect of this embodiment, a standard or high contrast OPS imaging probe is used to assess the viability of wound tissue to successfully support a skin graft.

In another aspect of this embodiment, a standard or high contrast OPS imaging probe is used to more accurately and objectively determine the line of amputation.

In another aspect of this embodiment, a standard or high contrast OPS imaging probe is used to measure and compare the revascularization and healing of a wound using different wound healing therapies.

In another aspect of this embodiment, a standard or high contrast OPS imaging probe is used to monitor capillary "budding" (i.e., the creation of new capillaries) during wound healing.

In the following study, the microcirculation of the skin was visualized and characterized using OPS imaging. The aim of this study was to validate the use of OPS imaging (Groner, W., et al., Nat. Med. 5:1209-1213 (1999)) for making microvascular measurements in the skin against standard fluorescent videomicroscopy, under normal conditions and in a disease state (in this case

during the process of wound healing). Clearly, the assessment of cutaneous microcirculation would have important clinical implications since several dermatological pathological states are associated with changes in the microvasculature. Through quantitative analysis of skin microcirculation, vascular pathologies, angiogenesis during wound healing and impaired blood flow after skin flap creation could be identified.

Materials and Methods: Experiments were carried out on ears of hairless (SKH-1*hr*) mice (n=9). A circular wound was created according to Bondar and coworkers (Bondar, 1., *et al.*, *Res. Ex. Med.* *191*:379-388 (1991). The OPS imaging device (CYTOSCAN™ A/R) was attached to the intravital microscope to take advantage of the computer controlled XY-plate. Observations were made using both the intravital fluorescence microscopy (IVM) and OPS imaging in the exact same regions of interest at baseline as well as 4, 7, 10 and 15 days after wound creation. For the measurements with IVM, 0.02 ml of a 3% solution of FITC-Dextran i.v. was used as a plasma marker. The images obtained from both instruments were analyzed during playback of the videotapes using a computer assisted analysis system (CapImage™) (Klyscz, T., *et al.*, *Biomed. Tech. (Berl)* *42*:168-175 (1997)). Measurements of arteriolar diameter, venular diameter, red blood cell velocity and functional capillary density (FCD) were made under baseline conditions, as well as during wound healing.

Conclusions: OPS imaging produced high quality images of skin microcirculation with optical contrast comparable to that achieved with IVM. Further, using OPS imaging, it was possible to make accurate quantitative measurements of vessel diameter, venular RBC velocity, and functional capillary density during the physiological conditions and during the process of wound healing. The small size and portability of the instrument, as well as the quality of the images obtained without the need of a fluorescent dye, indicate that OPS imaging offers a great potential to be used for diagnostic measurements in human skin.

In another study, wound induced angiogenesis was observed using OPS imaging.

Introduction: The trauma associated with wounding creates the first signals for the tissue to begin to repair itself. This initial trauma initiates inflammation, which leads to a cascade of molecular signals, encouraging angiogenesis. Conheim was one of the first in modern history to describe the initial changes in the vasculature that occur following wounding (Conheim, J., "The pathology of the circulation," Section 1 in *Lectures in General Pathology: A Handbook for Practitioners and Students*, trans. by A.B. McKee, ed.., New Sydenham Society, London. V. 126, 129, 133, pp. xvii-528, 1889-1890 (1889)). More recently, Clark and Clark suggested that angiogenesis was an important step in the initiation of the healing of wounds (Clark, E.R. and Clark, E.L., *Am J Anat* 64:251-299 (1939)).

One of the experimental models that have been widely used to study wound healing is the window chamber. Hashomoto and Prewitt placed a chamber in the rabbit ear and documented the changes that occur in this model of a healing wound (Hashimoto, H., *et al., Int. J. Microcirc: Clin. Exp. 5*:303-310 (1987)). Numerous investigators, such as Dewhirst *et al.* (Dewhirst *et al., Rad. Res. 112*:581-591 (1987)), have placed a window chamber in the dorsal skin fold of rats and indicated that this is an excellent model for the study of early angiogenesis. However, such a chamber is not feasible for clinical use in humans. This study utilized a similar principle of using a wound to stimulate angiogenesis.

A reproducible model for the assessment of angiogenesis would be of value in a variety of clinical situations, such as testing the efficacy of a particular therapy for inhibiting angiogenesis in cancer patients. Auerbach *et al., Pharmacol Therapeutics 51*:1-11 (1991) indicated in a recent review that understanding of angiogenesis has been important in the increased knowledge of wound healing. Similarly, Folkman proposed that understanding angiogenesis would permit the development of therapies to inhibit normal angiogenesis (Folkman, *Adv. Cancer Res.19*:351-358 (1974)). The goal of this study was to characterize the development of microvessels surrounding full thickness wounds in humans.

- 41 -

Materials and Methods: Subjects received local anesthesia on the volar aspect of their forearm, followed by a full thickness 4 mm diameter cutaneous punch biopsy extending down to fat or fascia. The wound was dressed with antibiotic ointment and dressed. Every other day, the wound was examined with a variety of optical devices, including an operating microscope with video camera and a CYTOSCAN™ A/R. On each day of observation, the dressing was removed and the cutaneous tissue adjacent to the wound was recorded for several seconds in each position, moving around the biopsy margin in a clock-wise motion. Approximately five minutes were needed to complete one cycle of the wound margin. The video images were stored in either analog or digital form.

For analysis, a semi-quantitative scale with four grades was established. Grade 0 was characterized by a total lack of vascular elements and color. Grade 1 was characterized by a diffuse pink or red color with very few clearly visible microvessels in the tissue adjacent to the wound, with no identifiable organization or pattern. Grade 2 was typified by short, vertical microvessel loops seen on end that were poorly organized with no preferential orientation and little branching. Grade 3 was characterized by longer microvessels that were generally curved but were beginning to orient radially extending out from the edge of the wound. Some minimal branching was also visible. Grade 4 consisted of long microvessels that were aligned radially like the rays of the sun with some interconnected loops or anastomoses. Some limited branching was also observed. Once the semi-quantitative scale had been defined, blinded observers viewed the images and scored them using these detailed criteria.

Results: The grading of the vascular pattern observed was reproducible based on the well-defined criteria. The coefficient of variation was approximately 10% or less. It took only a few days for the vascular grade to increase to an average of 1.5. A score of 2.0 was achieved in less than five days following wounding. The change from an average grade of 2.0 to a grade of 2.5 was slower, requiring approximately 10 days after wounding. Then, the newly formed vessels appeared to quickly elongate and begin to align radially, achieving a grade

- 42 -

of 3.0 less than one full day later. The score of 1.0 was achieved soon after initial wounding.

Microvascular architecture was also observed in patients with diabetic or venous ulcers. The CYTOSCAN™ A/R was used to perform video microscopy of each patient prior to treatment and during several weeks of conservative non-surgical therapy. A pattern of vascular grades was observed. The most difficult wounds showed a general lack of vascularity adjacent to the wounds (as in grade 1). The diabetic patients, in particular, showed a very low number of visible microvessels in the superficial skin immediately adjacent to the wound. Wounds that were progressing toward healing showed some increased number of microvessels with no obvious orientation (as in grade 2). Microvessel lengthening and the emergence of a preferential microvessel orientation (as in grades 3 and 4) paralleled a clinical improvement in the wound.

Discussion: The semi-quantitative assessment of angiogenesis induced by wounds appears to be possible using instruments permitting intravital microscopy, such as the CYTOSCAN™ A/R. For hundreds of years, numerous investigators have observed microvessels associated with various types of wounds. However, clinical studies in patients were extremely difficult to execute due to the extensive and cumbersome equipment required. Even in experimental animals, intravital microscopy has been difficult. OPS imaging greatly facilitates the acquisition of microscopic images of the living microvasculature. Minimal training of personnel was required before they were able to accurately conduct the video microscopy protocols for these clinical studies.

In the following case report, OPS imaging was used to assess the microcirculation in a burn wound.

Introduction: The treatment of choice of deep second and third degree burns is toward early excision and grafting. As a prerequisite for such an aggressive surgical treatment, an accurate diagnosis of the burn lesion is required. This underscores the importance of accurate assessment of the severity of a burn wound as the key in early decision making. Clinical examination, based on wound appearance, remains the unchallenged method for such procedures, even though

- 43 -

it has been reported that clinical assessment of burns performed by clinically experienced burn surgeons is not always satisfying (Robson, M.C., *et al., Clin.Plast.Surg. 19*:663-671 (1992); Heimbach, D.M., *et al., J.Trauma. 24*:373-378 (1984)). Thus, adjunct diagnostic techniques might help surgeons to accurately analyze the severity of a burn and therefore might help for rapid decision making at bedside. However, despite all technical innovations an ideal device for such an application has not been established for routine use as yet.

Recently, a novel microscopic technique, orthogonal polarization spectral (OPS) imaging, has been introduced (Groner, W., *et al., Nat.Med. 5*:1209-1212 (1999); Messmer, K., ed., Orthogonal Polarization Spectral imaging: a New Tool for the Observation and Measurement of the Human Microcirculation, *Prog. Appl. Microcirc.*, Karger, Basel (2000), pp 1-117). OPS imaging provides a method which can be used to directly visualize the organ microcirculation in animals and in human beings. OPS imaging uses polarized reflected light at a wavelength of 548 nm to visualize hemoglobin carrying microvessels without the use of fluorescent dyes, thereby avoiding phototoxic effects (Saetzler, R.K., *et al., J.Histochem.Cytochem. 45*:505-513 (1997)). The OPS imaging technique has been validated for the measurement of functional capillary density against the standard method for such measurements, the fluorescence intravital microscopy (Harris, A., *et al., J. Vasc. Res.* (In Press) (2000)). Functional capillary density is a parameter reflecting capillary tissue perfusion and is given as the length of the red cell perfused capillaries per observation area (Harris, A.G., *Am. J. Physiol. 271*:H2388-H2398 (1996)).

Tissue blood flow in human burns had been the subject of several studies and it was hypothesized that the degree of reduction of dermal blood flow in the thermally injured skin correlates with the level of its destruction (Micheels, J., *et al., Scand. J. Plast. Reconstr. Surg. 18*:65-73 (1984); Alsbjorn, B., *et al., Scand. J. Plast. Reconstr. Surg. 18*:75-79 (1984); O'Reilly, T.J., *et al., J.Burn.Care Rehabil. 10*:1-6 (1989)). However, a direct visualization of the microcirculation in a human burn, was not yet possible due to methodological difficulties. In this

- 44 -

case study, OPS imaging was introduced as a novel technique for the assessment of the microcirculation in a burn wound.

Patient: The patient was a 26 year old male patient with a burn injury on his left hand. The burn was inflicted by boiling oil during cooking and was immediately rinsed with cold water prior to the emergency room admission. A second degree burn was diagnosed by clinical observation after initial debridement of devitalized tissue. Blisters were opened but left intact. The burn was managed conservatively using topical 1% silversulfadizine in a semi-solid oil in water emulsion and the fingers were wrapped separately in a soft gauze dressing. The hand was elevated for the first 48 hours after the burn and analgesics were given orally for pain control.

Study Protocol: The OPS imaging technique has been incorporated into a small, easy-to-use device called the CYTOSCAN™ A/R (Cytometrics Inc., Philadelphia, PA). After obtaining informed consent, observations of the microcirculation were performed with OPS imaging starting day 3 following the injury. Measurements were carried out at constant room temperature (27°C) in our outpatient clinic. Approximately 10 minutes after cleaning of the wound by irrigation with sterile saline solution to remove the topical agent, the OPS imaging probe was applied to 6 different areas of interest at the dorsal surface of the hand including the fingers. Images of the microcirculation were recorded on super-VHS videotapes (Sony, Cologne, Germany). The working distance of the OPS imaging probe, which was covered with a disposable sterile plastic cap, was approximately 2 mm. Sterile ultrasound gel was applied in between the probe and the tissue, and helped to improve index matching. The patient never showed signs of pain or discomfort during the application of the OPS imaging probe which required approximately 5 minutes of duration. A custom made holder helped to prevent the probe from moving during the observations, as well as from compressing the capillary circulation. Subsequent measurements of the microcirculation were performed at days 6, 12, 20, 23, 26, and 30 after the burn, always returning to the same areas within the affected site. Quantitative analysis of the microcirculation was performed off-line during play back of the videotapes

- 45 -

using the CapImage™ computer program (Klyscz, T., *et al., Biomed. Tech. (Berl.)* *42*:168-175 (1997)). Functional capillary density was assessed from single images which were digitalized from the running video sequence. Capillaries which were in focus and could be clearly identified as red blood cell perfused were included into the evaluation. Data is given as the number of perfused capillaries per observation area [n/cm^2] as described earlier in studies of clinical capillaroscopy (Bollinger, A. and Fagrell, B., *Clinical Capillaroscopy-A Guide to its Use in Clinical Research and Practice*, Toronto, Hofgrefe & Huber Publishers, pp.1-166 (1990).

Results: OPS imaging produced high quality images of the microcirculation in a burn wound using a total on-screen magnification of 254x. Capillary morphology was clearly identified and from these images the quantitative analysis of the number of red blood cell perfused capillaries was feasible. The functional capillary density (FCD) which was measured at day 3 following the injury was 11.2 ± 4.6 n/mm^2 (mean $\pm$ SEM). During the initial phase of healing, microcirculatory changes were characterized by a moderate but steady increase of FCD, and showed marked increase beginning from day 12 following the burn (16.6 ± 6.9). Maximal FCD measured at day 23 (48.2 ± 19.7) decreased from this point in time to finally reach 25.2 ± 10.3 n/mm^2 at the end of observation. The patient tolerated the measurements very well, and was enthusiastic about seeing his own capillaries in the healing wound. The wound, which presented a surface area of 122 cm^2 at the day of injury, calculated by digital planimetry, showed an uncomplicated healing within 3 weeks without leaving residual scars.

Discussion: The ability to determine precisely and as early as possible the severity of a thermal injury is prerequisite for planning surgical treatment thus to optimize patients functional and cosmetic results (Kao, C.C. and Garner W.L., *Plast. Reconstr. Surg. 105*:2482-2492 (2000); Heimbach, D., *et al., World J. Surg. 16*:10-15 (1992); Germann, G., *et al., Pediatr. Surg. Int. 12*:321-326 (1997)). Early burn wound excision and closure by grafted skin confers several advantages (Heimbach, D., *et al., World J. Surg. 16*:10-15 (1992); Engrav, L.H., *et al., J. Trauma. 23*:1001-1004 (1983); Gray, D.T., *et al., Am.J.Surg. 144*:76-80

- 46 -

(1982); Schiller, W.R., *et al., J.Trauma. 43*:35-39 (1997)), however clinical evaluation is often inaccurate and estimated not to be better than 64% even for experienced burn surgeons (Heimbach, D., *et al., supra*). Due to the limitations of clinical observation, it is not surprising, that for decades interest has been focused on devices and methods that could support clinical observation, particularly to distinguish between burns which heal without complications and those which need surgery. Numerous modalities such as vital dyes, fluorescein fluorometry and nuclear magnetic resonance imaging are available to classify burns (Heimbach, D., *et al., supra*). However, none of these techniques has been accepted for widespread clinical application so far. One reason for that is the additional injury some of these invasive approaches inflict, however, the main reason is that, except for the laser doppler (LD) technique, they have not proven to give reliable results. For a review, see, Heimbach, D., *et al., World J. Surg. 16*:10-15 (1992) and Shakespeare, P.G., *Burns 18*:287-295 (1992).

The LD technique was first used for assessing the extent of skin destruction in human burns by Micheels and coworkers (Micheels, J., *et al., Scand. J. Plast. Reconstr. Surg. 18*:65-73 (1984)). The principle of the use of LD for such investigations is the hypothesis that the amount of skin blood flow correlates with the level of its destruction (O'Reilly, T.J., *et al., J.Burn.Care Rehabil. 10*:1-6 (1989)). As described by Braverman, the nutritive components of the skin are formed by the dermal papillary loops which are situated 1-2 mm below the dermal surface (Braverman, I.M., *Microcirculation 4*:329-340 (1997)). Thus, if the papillary loops are destroyed (as is the case in deep dermal burns), a standstill, or at least a reduction of the microcirculatory blood flow must be present.

Given this, LD measurements might be useful to obtain data of the amount of blood flow from which a predictive statement concerning the severity of the burn lesion can be made. This was already done in clinical investigations, and a significant relationship between burn blood flow and clinical ultimate fate has been demonstrated in adult patients (Alsbjorn, B., *et al., Scand. J. Plast. Reconstr. Surg. 18*:75-79 (1984); O'Reilly, T.J., *et al., J.Burn.Care Rehabil. 10*:1-6 (1989);

- 47 -

Schiller, W.R., *et al., J.Trauma. 43*:35-39 (1997); Green, M., *et al., J.Burn.Care Rehabil. 9*:57-62 (1988); Niazi, Z.B., *et al., Burns. 19*:485-489 (1993); Yeong, E.K., *et al., J.Trauma.* 40:956-961 (1996)) as well as in children (Atiles, L., *et al., J.Burn.Care Rehabil. 16*:596-601 (1995)). However, despite these encouraging

5   results, the use of LD is limited to unexcited and cooperative patients, since movements or agitation make the measurements difficult to interpret or even useless (Micheels, J., *Scand. J. Plast. Reconstr. Surg. 18*:65-73 (1984); Park, D.H., *et al., Plast.Reconstr.Surg. 101*:1516-1523 (1998)). In addition, since the measurements are reported to be relatively time-consuming for the patient and the

10   research staff (Micheels, J., *Scand. J. Plast. Reconstr. Surg. 18*:65-73 (1984)), not all of the patients are suitable for such kind of examinations. Importantly, additional staff is required, unquestionably raising costs of patient care. Further limitations of the LD technique are the pressure exerted by the probe on the skin, meaning that the measurement itself influences the parameter which is under study

15   (Obeid, A.N., *et al., J.Med.Eng.Technol. 14*:178-181 (1990)).

In clinical investigations using LD on wounds which ultimately healed, a steady increase of the average perfusion level was found during the first post burn days. In deeper burn wounds, on the other hand, such a clear pattern of recovery of blood flow has not been detected (O'Reilly, T.J., *et al., J.Burn.Care Rehabil.

20   10*:1-6 (1989); Green, M., *et al., J.Burn.Care Rehabil. 9*:57-62 (1988); Atiles, L., *et al., J.Burn.Care Rehabil. 16*:596-601 (1995)). From these investigations, it became evident that one limiting factor in the healing of a burn is the amount of damage that occurred to the microvessels of the skin.

The rheologic changes in the microvascular network following a scald burn

25   have also been studied in an animal model using intravital fluorescent microscopy and a fluorescent agent for contrast enhancement (Boykin, J.V., *et al., Plast.Reconstr.Surg. 66*:191-198 (1980)). These studies allowed for a close insight into the dynamic alterations of the microcirculation following a burn injury, however, this kind of investigation is limited to the laboratory so far.

30   In this case report, the microcirculation of a human burn wound was assessed for the first time by means of OPS imaging. This technique allowed for

- 48 -

direct and noninvasive visualization of the cutaneous and dermal microcirculation repeatedly during the healing process. The observations were performed within minutes and the patient was spared to undergo a period of adaptation to specific environmental conditions as needed for investigations using LD (Micheels, J., *et al., supra*). There was no need for surface contact of the OPS imaging probe thus excluding pressure artifacts. In contrast to LD measurements, using OPS imaging, the individual capillaries in the burn wound were visualized in order to study their morphology, and to quantitatively assess their dynamics during the process of healing from the video recordings.

Microcirculatory data obtained from OPS imaging showed that there was a similar recovery of FCD in the healing process as reported in previous studies for perfusion data using LD (O'Reilly, T.J., *et al., J.Burn.Care Rehabil. 10*:1-6 (1989); Heimbach, D., *et al., World J. Surg. 16*:10-15 (1992); Green, M., *et al., J.Burn.Care Rehabil. 9*:57-62 (1988)). Given that, from LD measurements, a correlation between perfusion and the burn wound's ability to heal was made, it is likely that FCD might also be a useful parameter to predict whether a burn lesion will heal or not.

The results obtained in the patient reported here have shown that OPS imaging should provide a reliable tool for quantitative estimation of the functional capillary density in burn wounds. The device is convenient to operate, portable, and does not require special skills. Moreover, the probe can be wrapped in sterile plastic foil also allowing for measurements during surgery. These results on the use of OPS imaging to assess the microcirculation in burns appear promising, and it is anticipated that this technique will permit our knowledge of the dynamics of the microcirculation in the pathophysiology of thermal injury to grow. Beyond this, OPS imaging, in conjunction with the clinical observation, seems to be an encouraging diagnostic tool for the assessment of the severity of burn lesions.

- 49 -

Applications in Plastic Surgery

In this embodiment of the present invention, a high contrast OPS imaging probe is used *in vivo* during plastic surgery.

In each of the following aspects of this embodiment, one or more parameters, such as, capillary density, vessel (and microvessel) morphology, vessel density, vasospasm, red blood cell (RBC) velocity, cell morphology, vessel diameter, leukocyte-endothelial cell interactions, vascular dynamics (such as vasomotion), functional vessel density, functional capillary density, area-to-perimeter ratio, blood flow, hemoglobin concentration, and hematocrit, may be quantitatively determined. Preferably, two or more parameters are determined.

In one aspect of this embodiment, a high contrast OPS imaging probe is used to monitor blood flow (perfusion) during and following plastic, reconstructive, reattachment, or microsurgery.

In another aspect of this embodiment, a high contrast OPS imaging probe is used to determine healthy versus necrotic or dead tissue around a skin flap. During skin flap reconstruction, one's own tissue is used to reconstruct or replace tissue lost during surgical tumor removal or trauma. It is important for the plastic surgeon to monitor blood flow (perfusion) to the flap both intraoperatively, and especially postoperatively to insure that there is good perfusion in the tissue. This could be accomplished using functional capillary density measurements, RBC velocity, and diameter.

In the following study, skin flap perfusion was monitored using OPS imaging. Despite recent advances in technology, there is currently no monitoring system for a reliable detection of perfusion failure in human skin flaps. There is, however, a large need for an objective method that identifies perfusion inadequacy within transferred tissues. OPS imaging allows for the direct visualization and characterization of the microcirculation using polarized light. The aim of this study was to validate OPS imaging for microvascular measurements in skin flaps. The validation was performed against the standard technique for quantitative microcirculatory measurements, intravital fluorescence microscopy (IFM).

- 50 -

Material and Methods: An established skin flap model of male hairless mice (hr/hr) was used (Galla, T.J., *et al., Br. J. Plastic Surg. 45:*578-585 (1992). After flap creation (n=9), examinations of the skin microcirculation were performed at 1 hour, 6 hours and 24 hours following flap creation with both OPS imaging and IFM. Application of FITC-Dextran (5mg/kgBW) was a prerequisite for IFM measurements, but not for OPS imaging. For direct comparison of the two techniques the identical regions of interest were sequentially monitored. The flaps were scanned from the distal part to their base. A total of 60 regions of interest were captured on videotape of each time point. Functional capillary density (FCD) was measured off-line using the CapImage™ computer program. All procedures were performed under general isoflurane anesthesia.

Results: Using OPS imaging it was possible to visualize and characterize the skin flap microcirculation without the use of tracers (FITC-Dextran). From these images quantitative analysis of FCD was feasible. FCD was significantly lower in the distal part of the flap compared to the base (171.8 ± 34.7 vs 62.0 ± 25.6, mean$\pm$SD; 1h data). Comparison of OPS imaging and IFM revealed a significant correlation of FCD values ($p < 0.001$, Spearman rank sum test) at all time points. Bland-Altman plots revealed a good agreement between the two methods.

Discussion: OPS imaging allows for quantitative analysis of skin flap perfusion. Given the success of this validation study on mouse skin flaps, further investigations have to certify that OPS imaging can also successfully be used in humans. Implementation of this novel technique in reconstructive surgery will improve our knowledge of the function of skin flap microcirculation and provide a novel tool for inter- and postoperative monitoring of skin flap perfusion.

In another aspect of this embodiment, a standard or high contrast OPS imaging probe is used to visualize and characterize the microcirculation in cutaneous and myocutaneous free flaps, as well as free flaps that develop complications. For example, in questionable free flaps, the direct observation of red blood cell flow in capillaries, by using OPS imaging, gave indication that the flap was viable.

- 51 -

In another aspect of this embodiment, a standard or high contrast OPS imaging probe is used after plastic or microsurgery to continuously monitor the microcirculation and identify any potential problems with reperfusion. Early indication of reperfusion problems may help avoid the need for repeat surgery.

5   *Cardiac Applications*

In this embodiment of the present invention, a high contrast OPS imaging probe is used *in vivo* in the field of cardiology and/or cardiac surgery.

In each of the following aspects of this embodiment, one or more parameters, such as, capillary density, vessel (and microvessel) morphology,

10   vessel density, vasospasm, red blood cell (RBC) velocity, cell morphology, vessel diameter, leukocyte-endothelial cell interactions, vascular dynamics (such as vasomotion), functional vessel density, functional capillary density, blood flow, area-to-perimeter ratio, hemoglobin concentration, and hematocrit, may be quantitatively determined. Preferably, two or more parameters are determined.

15   In the following study, OPS imaging was applied to a beating pig heart using an epicardial stabilization device, to see if it could be used to detect, visualize, and characterize changes in the epicardial microcirculation during regional induced ischemia.

Methods: Eight pigs (70 kg body weight) underwent median sternotomy

20   under general anesthesia. After exposure of the heart, an epicardial suction device (Octopus, Medtronic Inc.) was applied. The two fork-like extensions of the device were placed on top of the left anterior descending (LAD) artery, and the myocardial area was stabilized by applying 400mmHg of suction. The OPS imaging probe was placed in this stablized region to visualize the epicardial

25   microvessels. Regional ischemia of this area was achieved with a monofilament tourniquet suture around the proximal LAD.

Results: It was possible to obtain microvascular images of the epicardium in all 8 animals. Semiquantitative analysis showed a decrease in microvascular blood flow on occlusion of the LAD.

- 52 -

Conclusions: OPS imaging in conjunction with regional myocardial wall immobilization device allows the visualization and characterization of the microcirculation of the epicardium. From the images obtained, it is possible to quantify changes in epicardial blood flow and allow a unique assessment of the microcirculatory changes during regional ischemia. The ability to detect and visualize changes in the epicardial microcirculation on the beating heart may be of particular interest and a valuable tool during coronary revascularization.

In one aspect of this embodiment, a high contrast OPS imaging probe is used to increase visualization and characterization of the cardiac microcirculation to confirm reperfusion during minimally invasive cardiac surgical procedures that avoid the heart-lung bypass machine, such as "keyhole" surgeries (*i.e.*, Heartport) and thoracotomies.

In another aspect of this embodiment, a high contrast OPS imaging probe is used for monitoring and detecting changes in patient blood flow (the microcirculation) during open heart surgery while the patient is on the heart-lung machine. The OPS imaging probe would be in the patient's mouth during monitoring. Differences in blood flow were observed after the patient was placed on the heart-lung machine and after coming off of it, when compared to prior to the start of surgery. An increased incidence of vessels were also observed where leukocytes can be observed. In particular, the longer the patient is on the heart-lung machine the worse the flow in the microcirculation is. Thus, the OPS imaging probe could be used to monitor the progress of the patient while on the heart-lung machine, as well as when "off" the machine.

In the following study, OPS imaging was used to directly visualize and characterize microvascular changes in human patients undergoing cardiac surgery.

Methods: OPS imaging was used on 12 male patients (mean age 61.1 years) undergoing cardiopulmonary bypass (CPB) surgery to examine the changes in microvascular perfusion during CPB. Leukocyte-endothelial cell interaction was also examined. Microvascular diameter (DIA [μm]), red cell velocity (VEL [mm/s]), as well as functional capillary density (FCD [cm/cm^2]) were measured in images taken from the sublingual mucosa, immediately after induction of

- 53 -

anaesthesia (T1), in the early phase of CPB (T2), the late phase of CPB (T3), and one hour after reperfusion (T4).

Results: DIA was significantly increased at T3 and T4. VEL was decreased at T2 and increased at T3. FCD did not change significantly (Table 1).

Table 1

	T1	T2	T3	T4
VEL (mm/s)	0.55 (0.37-0.81)	0.49* (0.33-0.69)	0.66* (0.45-1.09)	0.59 (0.40-0.79)
DIA (μm)	20.8 (15.5-28.9)	23.0 (15.4-32.2)	23.8* (18.2-32.0)	25.6* (19.0-34.0)
FCD (cm/cm^2)	152 (123-175)	135 (98-164)	126 (100-154)	139 (109-172)

median (25%-75%); *$p < 0.05$ vs. T1

Conclusions: This data provides evidence for microcirculatory changes during CPB. However, nutritive blood flow seems to be well-maintained during uncomplicated CPB, since FCD only showed a non-significant decrease.

In another study, described below, OPS imaging was used to visualize and characterize the changes in epicardial microcirculation during cardiopulmonary bypass in humans.

Methods: In a pilot study, OPS imaging was used in 3 humans who underwent median sternotomy under general anesthesia and were placed on cardiopulmonary bypass for different cardiac procedures. The area perfused by LAD was visualized in all patients during each period of cardioplegic perfusion with blood cardioplegia. Microvascular diameter (DIA [mm]) and red cell velocity (VEL [mm/s]) were measured in images taken directly from the heart surface.

Results: Using OPS imaging, microvascular images of the epicardium were obtained in all patients. The diameters of arterioles and venules ranged between 10 and 70m. The red cell velocities reached a maximum of 0.6 mm/sec in these vessels during the application of the cardioplegic solution. Evidence of vasomotion was also found since arteries and arterioles were contracting and dilating. Frequently, areas with no apparent flow of erythrocytes were identified, which may suggest that the cardioplegic solution had not reached this part of the myocardium.

- 54 -

Conclusions: This data provides the first intravital microscopic images of the surface of the human heart during the application of cardioplegic solution in humans. The semiquantitative analysis done so far suggests remarkable differences in microvascular blood flow. OPS imaging may become of great importance during cardiac surgery, since it allows direct assessment of microvascular changes in the human heart.

In another aspect of this embodiment, the OPS imaging probe also can be used during coronary artery bypass graft (CABG) surgery to determine if the area supplied by the graft is getting good blood flow. That is, a cardiac surgeon could use the OPS imaging probe, directly contacting the heart, to monitor the blood flow to the capillaries after bypass surgery.

In another aspect of this embodiment, the OPS imaging probe can be used to monitor a patient's microcirculation during cardiac surgery to repair congenital heart defects. For example, the OPS imaging probe has been used during pediatric cardiac surgery to image the surface of the heart of two infants during ventricular septal defect (VSD) repair. The OPS imaging probe, which has the size of a large pen, was applied to the surface of the heart. The probe was hand-held and focused manually in response to the images seen on a high resolution monitor. Images were recorded during the application of cardioplegic solution (Brettschneider solution), which is used to protect the heart during the ischemia associated with open heart surgery. Initially, the heart was still beating with < 20 beats/minute followed by a period of cardioplegia. The well-established CapImage™ analysis program was used for quantification of the intravital microscopic images.

Using OPS imaging, it was possible to obtain images from the surface of the heart, and calculate the diameters of the microvessels observed. Despite the fact that the Brettschneider solution does not contain erythrocytes, it was possible to visualize the vessels due to the remaining erythrocytes within the vessel. In general, the cardioplegic solution reached most of the microvessels, however some microvessels were not reached as they still contained columns of erythrocytes with no evident erythrocyte flow. Thus, certain areas of the heart that did not receive the cardioplegic solution, remained unprotected from the surgery induced

- 55 -

ischemia. Moreover, profound vasomotion in arterioles was observed during the application of the cardioplegic solution with a diameter change from 70 μm to 32 μm.

Thus, in view of these findings, as well as the prior report, in yet another aspect of this embodiment, OPS imaging can be used to make both qualitative and quantitative assessments of the effectiveness of cardioplegic solution perfusion when applied during any cardiac surgery procedure. Further, microvascular phenomena like vasomotion can be studied with OPS imaging technology.

In another aspect of this embodiment, the OPS imaging probe can be used to monitor a patient's microcirculation during any type of cardiac surgery. Examples include surgery for heart valve replacement or heart valve repair.

In another aspect of this embodiment, the OPS imaging probe can be used for cardiac risk monitoring. The use of the OPS imaging probe to visualize and characterize the microcirculation may assist in non-invasively determining a high risk cardiac profile. The microvascular sequalae of hypertension could be studied and also be used in determining cardiac risk.

Pulmonary Medicine Applications

In this embodiment, the OPS imaging probe is used in the visualization, characterization and assessment of lung tissue.

In each of the following aspects of this embodiment, one or more parameters, such as, capillary density, vessel (and microvessel) morphology, vessel density, vasospasm, red blood cell (RBC) velocity, cell morphology, vessel diameter, leukocyte-endothelial cell interactions, vascular dynamics (such as vasomotion), functional vessel density, functional capillary density, blood flow, area-to-perimeter ratio, hemoglobin concentration, and hematocrit, may be quantitatively determined. Preferably, two or more parameters are determined.

The lung from a pig was visualized using the CYTOSCAN™ A/R with two objectives; one objective having an optical magnification of 5x, the other objective having an optical magnification of 10x.. Using the A/R 10x, much detail

- 56 -

was observed, such as the corner vessels (the vessels that surround the air sac), and also the capillaries providing gas exchange within the alveolus. The plural vessels were also visualized through the thin membrane overlying the lung proper. With the A/R 5x, the air sacs were visualized much more clearly, but the "corner" vessels were now almost too small to quantitate (~10-15 microns). The greater definition seen at 5x vs. 10x may be due to the different depth of field between the two objectives.

Neurosurgical Applications

In this embodiment of the present invention, a high contrast OPS imaging probe is used *in vivo* prior to or during neurosurgery.

In each of the following aspects of this embodiment, one or more parameters, such as, capillary density, vessel (and microvessel) morphology, vessel density, vasospasm, red blood cell (RBC) velocity, cell morphology, vessel diameter, leukocyte-endothelial cell interactions, vascular dynamics (such as vasomotion), functional vessel density, functional capillary density, blood flow, area-to-perimeter ratio, hemoglobin concentration, and hematocrit, may be quantitatively determined. Preferably, two or more parameters are determined.

In one aspect of this embodiment, a high contrast OPS imaging probe is applied directly to the brain during diagnostic or therapeutic neurosurgery to view the cortical or pial microcirculation, and measure parameters such as vessel diameter, flow velocity, and functional capillary density.

Using a specially prepared OPS imaging device, the pial microcirculation was imaged in anesthetized humans just prior to neurosurgery. To allow the surgeon to position the light guide on the brain surface and to hold the image guide in place for stable video recordings, a stainless steel surgical arm was developed having three pivot points. The arm could be made rigid by twisting a number of securing knobs. Before surgery, the arm with the OPS imager was secured to the rails of the operating table. The arm was covered by sterile foil used for covering endoscopes, which in turn was attached to the sterile Teflon

- 57 -

sleeve covering the light guide. Following craniotomy, the imager was gently positioned on the surface of the pial mater. The surgeon was able to observe the microcirculation of the brain on the TV monitor.

Although difficult to see in a static image, during video playback, red blood cells could be observed flowing in single file through the capillaries. Vessels could be readily identified as arterioles, capillaries, or venules. Video images were of sufficient quality to allow quantification of red cell flux using commercially available image processing software originally developed for analysis of video images obtained from intravital microscopy (Klyscz, T., et al., Biomed. Tech. (Berl.) 42:168-175 (1997)). Equally revealing images of other human microcirculatory beds in the esophagus and the stomach have also been obtained.

In another aspect of this embodiment, a high contrast OPS imaging probe is used to detect vasospasm following an aneurism or subarachnoid hemorrhage.

In another aspect of this embodiment, a high contrast OPS imaging probe is used to detect boundaries of tumors in the brain. Brain tumors typically do not lie at the surface, so they cannot be seen. In another neurosurgical application of OPS imaging, the OPS imaging probe can be used during surgery to detect changes in functional capillary density in "normal" tissue resting above the tumor, and therefore can be used to assess brain tumor margins.

Microcirculatory abnormalities in human brain tumors have been observed using OPS imaging technology. Thus, in another aspect of this embodiment, a high contrast OPS imaging probe is used for the determination and typing of brain tumors based on the vascular structure and differences in the microcirculation of different brain tumors.

The microcirculation of human tumors is a highly researched area due to the importance of tumor hypoxia and angiogenesis. In the following study, OPS imaging was used to visualize and characterize the microcirculation of human brain tumors in 11 patients (55.9 ± 5.17 years old; mean ± SEM) during surgery. These patients were selected because of the superficial position of the tumor in the brain. In this way, the microcirculation of the tumor could be observed with minimal manipulation of the tumor and surrounding tissue. Comparisons between

- 58 -

the microcirculation of the patients' healthy cortex and their tumor were made by visualizing different random areas.

Three types of brain tumors were examined: benign meningioma (n = 5), glioblastoma multiforme (n = 4), and metastasis (n = 2). The meningiomas had a dark background compared to normal, almost no blood flow, chaotic and dilated vascular pattern. The glioblastoma had a background similar to normal, low blood flow, and few vessels compared to normal. The metastases had a very dark background compared to normal, almost no blood flow, and a chaotic vascular pattern. This study showed the feasibility of *in situ* identification of pathologic microcirculation in brain tumors during surgery using OPS imaging.

Evaluation of microcirculatory parameters was performed using a computer asssisted microcirculatory analsysis system (CapImage™, Dr. Zeintl Ingenieurbüro, Heidelberg, Germany). Significant differences in microcirculatory parameters (such as red blood cell velocity (RBCV) and functional vessel density (total vessel length per area)) were found between the different brain tumors and healthy cortex. The RBCV in the glioblastoma was 0.40 ± 0.10 mm/s compared to 1.59 ± 0.32 in the arterioles and 0.64 ± 0.09 in the venules. Differences ($p<0.05$) in vessel length per area (vessel density) were found between the healthy cortex and the different tumor types: Meningioma (control; tumor): 68.10 ± 5.65 cm/cm^2; 41.75 ± 6.39; Glioblastoma multiforme (control; tumor): 88.47 ± 5.70; 50.02 ± 6.91; Metastasis (control; tumor): 72.96 ± 17.04; 25.04 ± 6.02). This study showed the first recording of human brain tumor microcirculation. It is expected that OPS imaging will provide more insight into the pathogenesis and possibly treatment of brain tumors.

The following study reports on intraoperative observation of human cerebral microcirculation using OPS imaging.

Our knowledge of human brain microcirculation is mainly derived from histological studies (Hunziker, O., *J. Geront. 34*:345-50 (1979); Craigie, E.H., *Biol. Rev. 20*:133-146 (1945)), or conclusions drawn from *in vivo* observations in animals (Uhl, E., *et al., Stroke 30*:873-879 (1999)). With the implementation of the OPS imaging method into a small hand held device (CYTOSCAN™ A/R),

- 59 -

it is now possible to observe human brain microcirculation during neurosurgical procedures (Groner, W., *et al., Nature Medicine* 5:1209-1213 (1999)). The technique is based on the illumination of the tissue with linearly polarized light, while the reflected light is imaged using a orthogonally polarized analyzer. The application of fluorescent dyes is not required. The aim of the current study was to test the feasibility of OPS imaging during neurosurgical procedures and to obtain basic quantitative data of human cortical microcirculation under normal and pathological conditions.

Patients and Methods: The study was approved by the local ethical committee and informed consent was obtained of each patient prior to surgery. So far, 12 patients (6 male, 6 female patients) have been entered in the study. Four patients were operated on an incidental intracerebral aneurysm and served as control group. Three patients had suffered from a subarachnoid hemorrhage (SAH) due to a ruptured intracranial aneurysm and underwent surgery for clipping of the aneurysm. Five patients were operated on a brain tumor. The mean age was 47.3±9.7 years. None of the patients had been operated on before. The operations were performed under general anesthesia using a standard regimen with sufentanil (1μg/kg b.w. for induction of anesthesia), propofol (400-700mg/h) and remifentanil (0.25-0.5μg/kg/min). In addition, all patients received 8mg of dexamethasone and 250ml of 20% mannitol before trephination. Patients with SAH also received a continous infusion of nimodipine (0.5-2mg/h). Systemic parameters were routinely measured during the operation.

Intraoperative Measurements: Intravital microscopy was performed with the CYTOSCAN™ A/R equipped with a lens of 5x magnification and a CCD camera. The technical details of the system have been described elsewhere (Groner, W., *et al., Nature Medicine* 5:1209-1213 (1999)). The device, which was covered with a sterile plastic cap (CYTOLENS™, Cytometrics Inc., Philadelpha, PA) and a sterile plastic foil, was adapted to a Leyla-retractor which allowed stable positioning of the probe on the brain surface during the measurements. Online observations of the cortical microvessels were performed right after opening the dura, before clipping the aneurysm or resection of the

- 60 -

tumor, respectively. A second measurement was performed at the end of the operation before closing the dura. The time between the first and the second measurement differed depending on the type and difficulty of the surgical approach. In each patient, at least five sites of interest (SOI) on the cortical surface were randomly selected. Each SOI was scanned for 30 seconds and the images stored on video tape for off-line evaluation. Due to the intraoperative shift and resection of brain tissue it was not possible to evaluate identical vessel segments. Evaluation of microcirculatory parameters was performed using a computer asssisted microcirculatory analysis system (CapImage™, Dr. Zeintl Ingenieurbüro, Heidelberg, Germany) at a final magnification of x260 (Klyscz, T., *et al., Biomed. Tech (Berl) 42*:168-175 (1997)). Vessel diameters [μm], red blood cell velocity [mm/s] in arterioles and venules as well as functional capillary density [cm⁻¹] were measured. The latter is defined as the length of all capillaries per cm², which are perfused with red blood cells at the time of observation.

The results were as follows:

Morphological Aspects of Cortical Vessels: With the OPS system, arterioles with their typical structure, capillaries, and draining venules were able to be clearly distinguished (FIGS. 2 and 3). Capillaries were found to have an irregular, however mostly circular shape. The number of capillaries can vary within a certain area and decreases in the vicinity of the junction of venules and arterioles. In SAH extravasation, red blood cells in the subarachnoid space were observed (FIG. 4). In these patients, segmental vasospams in arterioles were detected leading to a reduction of the vascular diameter of up to 50%. In some arterioles this vasospasm was limited to one segment only, in others multiple spasms led to a pearl string like appearance of the vessel (FIG. 4). In addition, changes of the vascular endothelium were observed initially in patients with SAH as well as in patients with brain tumor at the border of tumor resection (FIG. 5). In these vessels, an opaque layer was observed along the luminal vessel surface which led to a reduction of the intraluminal space resulting in a reduced flow of red blood cells.

- 61 -

In cases of the tumor reaching the surface, angiogenetic tumor vessels could be distinguished from normal brain microcirculation. The tumor vessels had an irregular and tortuous shape with sometimes sinusoidal aspect, forming a conglomerate of vessels at certain areas with normal microcirculation in between
5   (FIG. 6). These tumor vessels had close contact to venules whereas there was no obvious relation to the arterioles in this area.

Functional Capillary Density: The inital functional capillary density in control patients was $94.7 \pm 9.1 cm^{-1}$ (mean±SEM), in tumor patients 79.1 ± 5.7. In patients with SAH the initial value was lower than in the other patients reaching
10   a mean value of 61.7 ± 12.5. In all patients the functional capillary density had increased at the end of the operation as compared to the first measurement (FIG. 7) with the most pronounced increase observed after aneurysm surgery in patients with SAH.

Vessel diameter: The diameters of the observed vessels ranged between
15   10 and 150 μm in arterioles/small arteries, and 10 to 210 μm in venules/small veins. Since the vessels were randomly chosen it was not possible to measure the identical vessel segments at the beginning and the end of the operation. Therefore, actual changes of specific vessels could not be derived from our observations. Thus, the distribution of the data is presented rather than the mean (FIG. 8).
20   Except segmental microvasospasm in patients with SAH no dramatic change of the distribution of the vessel diameters during the course of the operation was observed.

Red blood cell velocity: With the line-shift diagram incorporated in the CapImage™ system it is possible to measure RBC-velocities up to 2mm/s. In
25   many cortical vessels, especially in arterioles, RBC-velocity exceeds this value and the exact value cannot be obtained. Therefore RBC-velocities were categorized in 6 classes and the percentage of the vessel classes with a certain RBC-velocity is given for each time point (FIG. 9). Vessels with RBC-velocities, that were too high to be measured, were comprised in the class of velocities higher than 2mm/s.
30   Our data show that in all 3 groups of patients, the number of vessels with a RBC-

- 62 -

velocity higher than 2mm/s had increased at the end of the operation with the most pronounced changes found in aneurysm surgery following SAH.

Discussion: This experience with the OPS imaging system shows that CYTOSCAN™ A/R is a suitable device for intraoperative observation of human cortical microcirculation. Brain capillaries, arterioles and venules were visualized, but also a quantitative analysis of microcirculatory parameters was obtained. In some patients at high magnification, however, brain movement, which mainly depends on respiration rather than on transmission of the cardiac pulse, did impair postoperative off-line quantification of the microcirculatory parameters despite excellent quality of the images. Although the brain with the translucent and thin pia mater is an ideal organ to be studied with a system that works on light reflectance the quality of the images strongly depends on the underlying pathology. Whereas in patients with incidental aneurysms and tumors the quality was good or excellent, visualization was impaired in patients with subarachnoid hemorrhage due to the extravasation of red blood cells and brain swelling. In addition to extravasated red blood cells we could observe distinct microvasospasm in arterioles (10-95μm) and small arteries (100-150μm) as described above. These microvasospams were observed in patients with normal transcranial Doppler values and without clinical signs of vasospasm at the time of the operation. Whether this intraoperative finding can be of prognostic value for the development of clinically relevant vasospasm later in the course of the disease should be evaluated in the future.

Furthermore, an opaque layer associated with the microvascular endothelium was observed in patients with SAH as well as at the border of resection in patients with brain tumor. The underlying pathology of this observation is not known. It may be speculated that this finding represents either endothelial swelling or a dense layer of plasma proteins along the inner surface of the endothelium leading to a reduced intraluminal space. The result is a reduced flow of red blood cells in the specific vessel.

In addition to the intraoperative visualisation of brain capillaries, arterioles and venules, a quantitative analysis of microcirculatory parameters was also

- 63 -

obtained. In all patients, FCD was found to be higher at the end of the operation, which is probably due to the reduction of intracranial pressure either by drainage of cerebrospinal fluid in patients with an aneurysm or by debulking of the tumor mass in patients with brain tumor. The resulting relaxation of brain tissue may also be the underlying reason for the higher number of microvessels, especially venules, with a RBC-velocity exceeding 2mm/s. In contrast to the mean vessel diameters, which essentially depend on the selection of SOIs by the observer, functional capillary density and red blood cell-velocity seem to be mainly independent and remain as the quanitative parameters of choice.

It is expected that OPS imaging will be a helpful tool in brain tumor surgery.

In another aspect of this embodiment, a high contrast OPS imaging probe is used to directly visualize and characterize the vascular consequences of neural trauma, and to determine the extent of neural trauma.

In the following study, it was shown that cortical hypoperfusion precedes hyperperfusion following controlled cortical impact injury in rats.

Impaired cerebral perfusion contributes to tissue damage following traumatic brain injury. In this longitudinal study, persistence of reduced cortical perfusion employing laser doppler flowmetry and intravital microscopy using OPS imaging (CYTOSCAN™ A/R) were investigated following controlled cortical impact injury (CCII).

Methods: Before, 30 minutes, 4, 24, and 48 hours after CCII, perfusion in pericontusional and non-traumatized cortex were determined by moving a laser doppler probe in 50 x 0.2 mm steps over the traumatized hemisphere in 6 rats. Diameter and flow velocity in arterioles and venules were assessed using orthogonal polarization spectral imaging in the same rats.

Results: At 4 hours after CCII, cortical perfusion was significantly diminished by 33% ($p < 0.05$) compared to pre-trauma levels. Despite normal $paCO_2$ values (mean: 42.1 +/- 1.0 mmHg) cortical perfusion was significantly increased by 43 and 107% ($p < 0.005$), respectively at 24 and 48 hours following CCII. Intravital microscopy revealed corresponding alterations. In the early phase

- 64 -

after trauma, vessel diameter was reduced in arterioles by 24% while the diameter in venules remained unchanged. Alterations in flow velocity were mostly sustained in venules as it was decreased by 39%. In the late phase, vessel diameter was significantly increased in arterioles (+ 39%) and venules (+ 75%) (p< 0.005). In venules flow velocity exceeded measurable values, being similar to velocities determined in arterioles at all time points.

Conclusions: Cortical hypoperfusion found within the early phase following CCII seems reversible as it precedes a long-lasting phase of hyperperfusion. Changes in tissue mediators (acidosis, NO, serotonin) could account for these findings.

Organ Transplantation Applications

In this embodiment of the present invention, a standard or high contrast OPS imaging probe is used *in vivo* during organ transplantation.

In one aspect of this embodiment, a standard or high contrast OPS imaging probe is used during transplant surgery to determine the amount of perfusion after the transplanted tissue/organ is connected. Any transplanted organ can be imaged, including, *e.g.*, liver, lung, pancreas, bowel, kidney, and heart. This would be especially useful during liver transplantation surgery, as perfusion would be difficult to assess otherwise (unlike kidney transplantation, for example). In liver, the number of perfused sinusoids could be measured. The OPS probe can be placed directly on the transplanted part of the organ.

One or more parameters, such as, capillary density, vessel (and microvessel) morphology, vessel density, vasospasm, red blood cell (RBC) velocity, cell morphology, vessel diameter, leukocyte-endothelial cell interactions, vascular dynamics (such as vasomotion), functional vessel density, functional capillary density, blood flow, area-to-perimeter ratio, hemoglobin concentration, and hematocrit, may be quantitatively determined. Preferably, two or more parameters are determined.

- 65 -

Vascular Grafting

In this embodiment of the present invention, a standard or high contrast OPS imaging probe is used *in vivo* during vascular grafting, such as in Peripheral Arterial Occlusive Disease (PAOD).

In each of the following aspects of this embodiment, one or more parameters, such as, capillary density, vessel (and microvessel) morphology, vessel density, vasospasm, red blood cell (RBC) velocity, cell morphology, vessel diameter, leukocyte-endothelial cell interactions, vascular dynamics (such as vasomotion), functional vessel density, functional capillary density, blood flow, area-to-perimeter ratio, hemoglobin concentration, and hematocrit, may be quantitatively determined. Preferably, two or more parameters are determined.

In one aspect of this embodiment, a standard or high contrast OPS imaging probe is used during vascular graft surgery to determine the amount of perfusion after the vascular graft is connected.

Orthopedic Surgery Applications

In this embodiment of the present invention, a standard or high contrast OPS imaging probe is used *in vivo* during orthopedic surgery, as well as in the field of orthopedic medicine.

In one aspect of this embodiment, a standard or high contrast OPS imaging probe is used during orthopedic surgery to identify and observe necrotic tissue, for surgical removal. The site of the probe would be on the area that has undergone trauma.

The probe can also be used to visualize bones, tendons, and ligaments.

In another aspect of this embodiment, a standard or high contrast OPS imaging probe is used to visualize and characterize the microcirculation around periosteum (bone). Differences in microcirculation were observed when the image was taken before or after a fracture.

- 66 -

One or more parameters, such as, capillary density, vessel (and microvessel) morphology, vessel density, vasospasm, red blood cell (RBC) velocity, cell morphology, vessel diameter, leukocyte-endothelial cell interactions, vascular dynamics (such as vasomotion), functional vessel density, functional capillary density, blood flow, area-to-perimeter ratio, hemoglobin concentration, and hematocrit, may be quantitatively determined. Preferably, two or more parameters are determined.

Gastrointestinal Applications

In this embodiment of the present invention, a standard or high contrast OPS imaging probe is used *in vivo* in the fields of gastroenterology and gastrointestinal (GI) or gastroesophageal surgery.

In each of the following aspects of this embodiment, one or more parameters, such as, capillary density, vessel (and microvessel) morphology, vessel density, vasospasm, red blood cell (RBC) velocity, cell morphology, vessel diameter, leukocyte-endothelial cell interactions, vascular dynamics (such as vasomotion), functional vessel density, functional capillary density, blood flow, area-to-perimeter ratio, hemoglobin concentration, and hematocrit, may be quantitatively determined. Preferably, two or more parameters are determined.

In one aspect of this embodiment, a standard or high contrast OPS imaging probe is used to visualize and characterize the large intestine and diagnose and treat inflammatory bowel disease (IBD), ulcerative colitis, Crohn's disease, or other gastrointestinal disorders affecting the microcirculation. OPS imaging technology can be used to distinguish Crohn's disease and ulcerative colitis, and therefore serve as an aid in accurate diagnoses. The probe can be inserted into the rectum to directly contact the wall of the large intestine.

In the following study, OPS imaging (CYTOSCAN™ A/R) was compared to intravital fluorescence microscopy for the visualization and characterization of colon microcirculation in a mouse model. In this study, the colon microcirculation of Balb/c mice under control conditions and after induction of DSS-induced colitis

was investigated (n=7 for each group studied). As microcirculatory parameters, postcapillary venular diameter, venular red blood cell velocity and functional capillary density were analyzed on the outer wall of the colon (serosa/muscularis), as well as on the luminal wall (mucosa). To examine the agreement between both methods, linear regression, Spearman's correlation coefficient and Bland-Altman-plots were analyzed.

All measured parameters correlated significantly between the two methods in both the control and colitis groups. It has been demonstrated that OPS imaging can be used to visualize and characterize the colon microcirculation without the use of fluorescent dyes, and allows quantitative measurement of relevant microcirculatory parameters of the mouse colon under physiological and pathophysiological conditions. The results obtained showed a significant correlation with those obtained with IVM. OPS images were of superior quality and sharpness compared to those obtained from IVM.

In the following study, OPS imaging detected microcirculatory shunting in the pig ileum after supra-mesenteric aortic cross-clamping.

Changes in the microcirculation due to ischemia and reperfusion injury are thought to cause "no-reflow" phenomenon and organ failure after aortic cross-clamping (AoX). Until now, *in vivo* observations of the microcirculation were only possible in rodents by the use of intravital microscopy. In this study, dynamic changes in the serosal microcirculation of the pig ileum after AoX were observed by using OPS imaging.

Six pigs were anesthetized and fully hemodynamically monitored. An ultrasonic flow probe was placed around the superior mesenteric artery (SMA). Following 60 minutes of stabilization, AoX was performed above the SMA for 45 minutes. The ileal serosal microcirculation was observed using OPS imaging during baseline, 5 minutes after AoX, and after 2 hours reperfusion. Video images were computer analysed by using CapImage™ software. The number of perfused vessels per imaged microcirculatory area (3 per pig) were determined. RBC velocity was calculated and graded in comparison to baseline flow. The number of perfused capillaries did not change from baseline 9 ±1.79 to 5 minutes after

- 68 -

unclamping 10.5 ±1.378, although the flow in the SMA nearly doubled. Two hours after reperfusion, the number of perfused vessels fell significantly to 5 ±2.1 (p< 0.05). The RBC velocity 5 minutes after AoX and after 120 minutes of reperfusion was significant lower (p< 0.05) than at baseline. These results indicate a decrease in capillary density and RBC velocity in the microcirculation of the ileum after AoX despite an increase in superior mesenteric artery flow. These results suggest the presence of shunting pathways during "no-reflow" phenomenon.

In the following study, it was shown by using OPS imaging, that endotoxin-induced ileal mucosal acidosis was associated with impaired villus microcirculation in pigs.

The following abbreviations are used: PA-cath. = pulmonary artery catheter for the measurement of mean pulmonary artery pressure and cardiac output; ECG = electrocardiogram to monitor heart rate; Flow V.portae = regional blood flow over the V. porta measured by ultrasonic flow probes; A.fem.-cath. = Arterial line in the A. femoralis to measure blood pressure and to take blood samples; PCO_2-Sensor = fiberoptic pCO_2 sensor for the continuous measurement of regional pCO_2 of the gut mucosa wall within an ileostoma; CYTOSCAN™ A/R = OPS imaging instrument to visualize and characterize the microcirculation of the gastrointestinal mucosa within an ileostoma.

Introduction: The tonometric determination of the gastrointestinal mucosal-arterial pCO_2-gap (Δr-aPCO_2) is used to monitor adequacy of the gastrointestinal perfusion and can indicate mucosal acidosis (Fiddian-Green, R.G., *Br. J. Anaesth.* 74:591-606 (1995); Brinkmann, A., *et al., Intensive Care Med.* 24:542-556 (1998)). Several different pathophysiological conditions, however, can influence regional pCO_2 homoeostasis such as changes of regional blood flow, oxygen delivery and consumption, CO_2 production and disturbencies of cellular energy metabolism (Schlichtig, R., *et al., J. Crit. Care 11*: 51-56 (1996); Vandermeer, T.J., *et al., Crit. Care Med 23*:1217-1226 (1995)). The role of the villus microcirculation for the development of an increased Δr-aPCO_2 and ileal mucosal acidosis, respectively, has never been investigated in longterm animal

- 69 -

models of larger species as no suitable intruments to visualize the gut mucosal microcirculation *in situ* had been available. The CYTOSCAN™ A/R, a new noninvasive method based on orthogonal polarization spectral (OPS) imaging enabled the visualization, characterization, and recording of the microcirculation at this previously inaccessible site.

Thus, the aim of this study was to analyze the influence of villi microcirculation on the development of mucosal gut acidosis in a hyperdynamic porcine endotoxic shock model and to compare this to the regional blood flow. In addition, the applicability and feasibility of the CYTOSCAN™ A/R for the analysis of the gastrointestinal microcirculation is discussed.

Material and Methods:

(1) Animal Model: The endotoxic pig model has been previously described in detail (Šantak, B., *et al.*, *Br. J. Pharmacol 124*:1689-1697 (1998)). In the present experiment, 16 pigs (mean body weight 48 kg) were investigated. All pigs were anesthesized and mechanically ventilated. A pulmonary artery catheter was inserted through the right jugular vein for the determination of mean pulmonary arterial pressure and cardiac output by the thermodilution principle. In one femoral artery a catheter was placed for continuous blood pressure recording and blood sampling. Ringer's lactate solution (10 ml $kg^{-1}h^{-1}$) was infused intravenously to maintain fluid balance.

A midline laparotomy was performed and a precalibrated Doppler-ultrasound flow probe (Transonic Systems, Ithaca, NY) was placed around the portal vein. The flow was continuously recorded by a T206 flow meter (Transonic Systems). An ileostomy was performed for the insertion of a fiberoptic CO_2 sensor (Multiparameter Intravascular Sensor; Pfizer, Karlsruhe) connected to a monitor (Paratrend 7; Pfizer), and intravital video records of the ileum microcirculation by the CYTOSCAN™ A/R.

After instrumentation, a stabilization period of 8 hours was allowed before baseline measurements.

- 70 -

(2) Protocol: The animals were randomly assigned to two groups: Endotoxin (ETX) (n=10) and Sham (n=6). After recording baseline measurements continuous i.v. endotoxin (Escherichia coli lipopolysaccharide B 0111:B4 [Difco Laboratories], 20 mg L^{-1} in 5% dextrose) or saline was started. The endotoxin infusion rate was incrementally increased until mean pulmonary arterial pressure (MPAP) reached 50 mmHg and then subsequently adjusted to result in moderate pulmonary hypertension with MPAP 35-40 mmHg. Hydroxyethylstarch was administered to stabilize hemodynamics and keep mean arterial pressure (MAP) above 60 mmHg. Further hemodynamic and $\Delta r\text{-}aPCO_2$ measurements as well as CYTOSCAN™ A/R recordings of the ileal mucosal microcirculation were obtained at 12 and 24 hours after the start of the endotoxin or saline infusion, respectively. At the end of the investigation, the animals were killed by KCl injection.

The $\Delta r\text{-}aPCO_2$ was calculated by the difference of ileal mucosal and arterial pCO_2. At each measurement time point, 6 video sequences of 1 minute duration each of the villus microcirculation from randomly chosen locations of the ileum mucosa were recorded using the CYTOSCAN™ A/R. All villi were counted and semiquantitatively classified as *perfused, heterogenously perfused (i.e.* existence of both perfused and unperfused capillaries within the same villus) and *unperfused.* Due to technical difficulties the microcirculation of two animals in the Sham-group were not recorded.

(3) Statistical analysis: All values shown are median and interquartile range unless otherwise stated. Intragroup differences were tested using a Friedman repeated measures analysis of variance on ranks and a subsequent Student-Newman-Keuls test for multiple comparisons. $P<0.05$ was regarded as significant. Intergroup differences were analyzed using the Mann-Whitney-Rank-Sum-Test for unpaired samples.

Results: Endotoxin caused a significant progressive fall of the mean arterial blood pressure from baseline to 12 and 24 hours of endotoxemia concomitant with a significant sustained increase in cardiac output, whereas there was no effect in the Sham animals (Table 2).

- 71 -

Table 2

		Baseline	12h shock	24h shock
MAP mmHg	ETX	102(93;107)	83(74;95)#	79(61;84)#
	Sham	95(91;97)	97(94;99)§	108(103;108)§
CO ml/minxkg	ETX	107(97;120)	160(148;170)#	162(131;200)#
	Sham	115(106;124)	107(103;115)§	116(110;130)§

# $p < 0.05$ vs. baseline; § $p < 0.05$ ETX alone vs. Sham

Table 2. Time-dependent variations of cardiac output (CO) and mean arterial pressure (MAP) in sham-operated and endotoxemic pigs. ETX means endotoxin group (n=10): animals which received an endotoxin infusion after recording of the baseline data; Sham means Sham-operated group (n=6): animals which were prepared like the above mentioned, but received saline instead of endotoxin.

Portal venous blood flow (FIG. 10) remained unchanged in both groups without intergroup difference. The (Δr-aPCO$_2$) increased significantly from baseline to 12 and 24 hours in the endotoxin group, while remained uninfluenced in the Sham-group (FIG. 11).

FIGS. 12 and 13 show the microcirculatory changes in the ileum mucosa during the investigation period: At baseline, all villi were perfused while 12 hours of endotoxin infusion lead to considerable heterogeneity of the microcirculation in the endotoxin-group: half of the villi were not or heterogenously perfused, whereas in the sham group, 5 % only of the classified villi were unperfused (p < 0.05). Virtually the same pattern was observed at 24 hours of endotoxemia.

Discussion: The aim of this study was to compare the influence of the macro- and microcirculation on the development of ileum mucosal acidosis during longterm hyperdynamic porcine endotoxemia mimicking the clinical features of septic shock in humans.

Earlier studies showed an ileal mucosal acidosis during endotoxemia in pigs although regional blood flow maintained, and thus, microcirculatory changes were expected. Unfortunately, up to now, there were no instruments available to visualize and characterize microcirculatory changes at the small bowel mucosa *in situ* which could be integrated in an experimental setting. Thus, the CYTOSCAN™ A/R was an optimal addition, as in comparison to capillary

- 72 -

microscopy, it is cheaper, easier to use, and it was not necessary to isolate the ileum from the animal. Using this techniques care should be taken not to press the probe too hard on the tissue, because this can compromise capillary perfusion.

The key finding was the marked heterogeniety of the villus microcirculatory status at 12 and 24 hours of endotoxemia, respectively, with about half of the counted villi being unperfused. For this finding it was favorable to use a lower magnification to identify as many villi as possible in one field of vision. Moreover, a reduced capillary network within the villus during endotoxemia was observed, which has also been found by other authors in smaller animal septic shock models and described as decreased capillary density (Farquhar I., et al., J. Surg. Res. 61:190-196 (1996)). Unfortunately, there exists no simple and time-sparing analytical device to quantitate these changes. Measurements of flow velocity within the villus capillaries were not possible, because of the gut peristaltic, which could not be corrected by movement control functions in the analytical software.

Besides this, microcirculatory changes during endotoxemia were so obvious, that perfused vs. not perfused villi was the focus of the evaluation.

These changes were accompanied by a significantly increased pCO_2-gap in the endotoxin group indicating intramucosal acidosis (Leverve, X.M., *Intensive Care Med.* 25:890- 892 (1999)). Taking into consideration the unchanged portal venous blood flow, *i.e.* the well-maintained macrocirculatory oxygen availability the progressive increase in Δr-$aPCO_2$ is mainly due to the heterogeniety of capillary villus perfusion. This finding is in striking contrast to data recently published by Knichwitz *et al.*, *Crit. Care Med.* 26:1550-1557(1998)) stating that a reduction of the arterial blood supply of at least 60-70 % is necessary to result in mucosal acidosis with increased pCO_2-gap.

In conclusion, it was demonstrated, by using the OPS imaging incorporated into the CYTOSCAN™ AR, that the development of ileum mucosal acidosis in a longterm hyperdynamic porcine endotoxic shock model was associated with marked alterations of the villus microcirculation, even when both portal venous blood flow of the gut wall were well-preserved.

In another aspect of this embodiment, the OPS imaging probe can be used during gastrointestinal (GI) surgery to visualize and characterize the colon during bowel resection.

In another aspect of this embodiment, the OPS imaging probe can also be used to determine the boundaries of a cancerous GI tumor and to visualize and characterize the necrotic tissue. Removal of the affected tissue from the stomach and/or esophagus area can thus be more easily accomplished during surgery.

In another aspect of this embodiment, the OPS imaging probe can also be used to visualize and characterize the rectal mucosal microcirculation, such as, for example, in patients with inflammatory bowel disease (IBD).

There is strong evidence that the microcirculation is involved in IBD. OPS imaging was used to visualize the microcirculation of the rectal mucosa of 11 healthy volunteers and 25 patients with IBD. Of these, a few patients (3 healthy; 6 IBD) were selected to apply a well-known image analysis algorithm in order to quantify the images. Macroscopic images were also made using conventional endoscopy, during which biopsies were taken. OPS imaging allowed detailed visualization of the rectal mucosa to be made and was well-tolerated by patients. Erythrocyte movement could be observed in capillaries and venules. Mucosal crypts, from which the mucosa is renewed and where mucus is formed, could be clearly identified. The normal rectal mucosa is characterized by a very distinct vascular pattern of the elevated crypts surrounded by hexagonal capillary rings. Marked differences were found between the rectal microcirculation of healthy volunteers and that of IBD patients. The distinct mucosal and capillary structures were completely distorted to the extent that the crypts were not identifiable anymore, and the capillaries were dilated and more tortuous than normal. Image analysis using a polyhedron-recognition algorithm (expressed in a Euler-number) showed a marked difference in results between normal (15.7), severe (-434) and mild (-36.3) IBD.

In another aspect of this embodiment, the OPS imaging probe can be used to assess and characterize the microcirculation of solid organs, such as the liver and pancreas. Other organs within the gut can be visualized as well using OPS

- 74 -

imaging, such as, kidney, small intestine, gall bladder, mesentery, bladder, diaphragm, stomach, and esophagus. In addition, the OPS imaging probe can be used to visualize the villi and microcirculation of the villi in the ileum, through an ileostomy.

5   The aim of the following study was to validate OPS imaging against standard intravital fluorescence microscopy (IFM) under normal and pathophysiological conditions in the rat liver.

Background: Quantitative analysis of the liver microcirculation using IFM in animals has increased our knowledge about ischemia/reperfusion injury.

10   However, because of the size of the instrumentation and the necessity of fluochromes for contrast enhancement the human liver microcirculation cannot be observed. OPS imaging is a recently introduced technique which can be used to visualize the microcirculation without the need for fluorescent dyes. It is a small, hand held device and could potentially be used to study the microcirculation of the

15   human liver in a clinical setting. However, before implementation into clinical use its ability to quantitatively measure microcirculatory parameters must be validated.

Methods: The livers of Spraque-Dawley rats (n=9) were exteriorized and images were obtained using OPS imaging and IFM of the identical microvascular regions prior to and after the induction of a 20 minute warm lobar ischemia.

20   Images were videotaped for later computer assisted off-line analysis.

Results: OPS imaging can be used to accurately quantify the sinusoidal perfusion rate, vessel diameter and venular red blood cell velocity. Correlation parameters were significant and Bland-Altman analyses showed good agreement for data obtained from the two methods at baseline as well as during reperfusion.

25   *Conclusion:* OPS imaging can be used to visualize the hepatic microcirculation and quantitatively measure microcirculatory parameters in the rat liver under both physiological and pathophysiological conditions. Thus, OPS imaging has the potential to be used to make quantitative measurements of the microcirculation in the human liver. As it can be seen from the correlation

30   parameters and the Bland-Altman analyses, there is a statistically significant agreement of the data obtained from OPS imaging and the standard method for

such measurements, the intravital fluorescent microcope. In contrast to the fluorescent method, OPS imaging can be used to visualize the microcirculation in humans since it does not require fluorescent dyes for contrast enhancement. Furthermore, the OPS imaging device is small and can easily be used in a clinical setting, *e.g.*, during surgery or transplantation.

One of the most frequent complications following liver transplantation is the dysfunction of the graft which results from severe deterioration of hepatic microcirculation. Therefore, the ability to assess blood flow in the human liver is of great clinical importance.

The following validation study has also been done using OPS imaging to image the rat pancreas. The quantification of capillary perfusion in human pancreas during transplantation and surgery could correlate the results of laboratory experiments and provide a new insight into the pathophysiology of acute pancreatitis and pancreatic ischemia/reperfusion damage.

Materials and Methods: Eight rats (n=8) were anaesthetized and monitored as described previously. Following transverse laparotomy, the short gastric arteries were ligated and dissected. For access to the pancreas the greater omentum was than removed from the greater curvature of the stomach. The microsurgical technique performed has been described previously in detail (Hoffmann *et al.*, *Res. Exp. Med. (Berl.)* *195*:125-144 (1995)). After mobilization, the pancreas and the attached spleen were gently exteriorized onto an adjustable stage and covered by a thin plastic foil to protect it from room air and drying. For visualization of the capillary networks 0.3 ml 5 % bovine serum albumin labeled with the plasmamarker FITC (fluorescein-isothiocyanate, Sigma-Aldrich Chemie, Deisenhofen, Germany) were injected intravenously. For comparison of the capillary perfusion using the two techniques the identical setup as for the liver was used. In each animal 6 identical microvascular fields were assessed using IVM and OPS imaging. Functional capillary density, defined as the length of red blood cell perfused capillaries per observation area [cm/cm^2], was analyzed by offline computer evaluation of the recorded images using the CapImage™ computer program.

- 76 -

Results and discussion: The typical honeycomb-like capillary network of the pancreas can be visualized with the CYTOSCAN™ A/R. The quantitative analysis of the OPS images showed a mean functional capillary density of 385.4 ±45 cm/cm² which is in agreement with previous studies using intravital microscopy. As it can be seen in the Bland-Altman analysis, these values are on average only 2.2 % (8.7 cm/cm²) less those obtained from IVM images.

In addition, just two data points are outside of the 95 % confidence interval and the regression line coincides with the mean. Thus, it becomes clear that there is a very good agreement between the two methods (IVM and OPS imaging) for the measurement of FCD in the rat pancreas under baseline conditions. The contrast and quality of the images obtained using IVM and the CYTOSCAN™ A/R are qualitatively the same, and therefore the time required for the analysis of images was comparable for both techniques.

Thus, OPS imaging is a suitable tool for quantitative analysis of pancreatic capillary perfusion during baseline conditions. The CYTOSCAN™ A/R would be a useful tool for the scientific and clinical evaluation of the microcirculation of the pancreas during surgery and transplantation in humans. Since pancreatic perfusion failure is an indication of the degree of postischemic damage to the organ (Hoffmann *et al., Res. Exp. Med. (Berl.) 195*:125-44 (1995); Hoffmann *et al., Microsc. Res. Tech. 37*:557-571 (1997)) the measurement of the FCD would be a useful diagnostic parameter for monitoring the condition of the pancreas.

Opthalmological Applications

In this embodiment of the present invention, a standard or high contrast OPS imaging probe is used *in vivo* in the field of opthalmology.

In each of the following aspects of this embodiment, one or more parameters, such as, capillary density, vessel (and microvessel) morphology, vessel density, vasospasm, red blood cell (RBC) velocity, cell morphology, vessel diameter, leukocyte-endothelial cell interactions, vascular dynamics (such as vasomotion), functional vessel density, functional capillary density, blood flow,

area-to-perimeter ratio, hemoglobin concentration, and hematocrit, may be quantitatively determined. Preferably, two or more parameters are determined.

In one aspect of this embodiment, a high contrast OPS imaging probe is used to visualize and characterize the microcirculation of the interior of the eye (especially the retinal microcirculation). In one embodiment, the OPS imaging probe can be utilized in a non-contact method. In this embodiment, the optics are set up so that the relaxed eye (focusing near infinity) focuses and images the OPS light onto the retina; alternatively, the imaging probe could be utilized in a direct contact manner, such as, by the use of a special diagnostic type of corneal contact lens. Such a visualization tool can be used for diagnostic purposes and treatment.

In a preferred embodiment, a fundus photographic unit, a laser delivering light of suitable wavelength to treat specific intraocular lesions, and the OPS imaging probe is functionally integrated. This type of instrument could be used for diagnostic purposes and treatment, as well as providing information regarding the effectiveness of various types of medications on the circulatory system in the area examined.

In order to be accurate, the exact area (spot) to be determined and treated or examined and re-examined in the eye must be easily found again. Therefore, a centering, tracking and grid device may be incorporated into the system. The tracking device is important to allow the area being evaluated and treated to always be in the same position relative to the instrumentation, even though there may be fine eye movements.

Also important in the optimization of such instrumentation is the incorporation of a recording device indicating the size of the vessels, lesions, etc., irrespective of magnification. At present, the field visualized by the instrument when used as a direct contact device externally is about 0.5mm. There will be some variation in the size of the intraocular field, depending upon the dioptic power of the eye being examined and the power of a corneal contact lens, if one is being used.

Image intensification can be incorporated so that minimal light of the desired wavelength is used to define the images. Ideally, the image will be in color

- 78 -

and in real time. The instrument will allow for immediate diagnosis of pathologic micro-circulatory problems. Real time video or photographs can be done for permanent records. Immediate laser or other types of treatment such as photodynamic therapy of the pathology can be performed in real time.

Optimization of this device will include some or all of the following features: a centering device; a method to visualize the same spot or area; a device to track eye movements and always be in the same position; a recording device indicating the size of vessels irrespective of magnification, i.e., calibration device; an image intensifying device; and a magnification means to expand the size of the image. Color images would be optional.

In another aspect of this embodiment, OPS imaging technology can be used to diagnose macular degeneration; retinal disorders (retinopathy), and glaucoma.

In another aspect of this embodiment, OPS imaging technology can be used to visualize the optic disk, retina, sclera, and changes in the vitreous humor.

In another aspect of this embodiment, OPS imaging technology can be used for early diagnosis and treatment of diabetes by looking at the ocular microcirculation, especially changes or differences in the sclera and/or aqueous humor of the eye.

In another aspect of this embodiment, OPS imaging was used to analyze the ocular microcirculation during operations on the internal cartoid artery (ICA). The aim of the following study was the intraoperative visualization and quantitative analysis of the microcirculation using OPS imaging in the flow area of the internal (ICA) and external (ECA) cartoid artery during reconstruction of stenosis of the cartoid artery.

Materials and Methods: Interoperatively, in 15 patients, the microvascular perfusion of the front part of the eye (sclera) was visualized and quantified using a CYTOSCAN™ A/R. The FCD, capillary diameter, and blood flow velocity were measured in the microvascular network of the ICA stenosis area in the ipsi and contralateral eye under control conditions (I); during ECA ischemia (II); during ICA ischemia (III); during shunt perfusion (IV); during shunt removal

(ischemia), selective after reperfusion of the ECA (V); and ICA (VI); 5 minutes after reperfusion (VII); and 20 minutes after reperfusion (VIII).

Results: The temporary ischemia during the implantation of the shunt caused a significant reduction in the nutritive ocular capillary perfusion of approximately 50% in comparison to the baseline values before ischemia. Furthermore, the short ischemia period was also associated with a significant decrease in the capillary diameter. The changes were even more pronounced following clamping of the ICA and the ECA when compared to a simple short ECA ischemia. In contrast, the post-ischemic shunt perfusion of the ICA was characterized by a significant increase ($p < 0.05$, paired t-test) of the FCD, the capillary diameter and the RBC velocity when compared to I and III. Renewed temporary ischemia during the shunt removal led to similar perfusion deficits like during shunt implantation. In contrast, the immediate post-ischemic reperfusion (VI) was associated with a significant increase ($P < 0.05$) in the FCD, the capillary diameter, and the RBC velocity. The increases in perfusion could also be observed both during shunt perfusion during the reperfusion phase and in the contralateral eye and 20 minutes post reperfusion less evidently.

Conclusions: OPS imaging makes it possible for the first time to directly visualize and quantify the ocular microcirculation. It allows immediate and reliable intraoperative monitoring of ischemia (perfusion deficit) and reperfusion caused changes in the cerebral microcirculation during reconstruction of the carotid artery. The ocular interruption of the microcirculation such as capillary stasis and constriction, as well as oscillating flow which occur immediately after even short ICA and ECA ischemia, indicate that there is a rapid manifestation of ischemia induced microvascular dysfunction. The maintenance of an adequate perfusion in the ICA perfusion area during the reconstruction leads to a significant improvement and protection of the ipsi and contralateral ocular microcirculation.

- 80 -

Applications During Pregnancy

In this embodiment of the present invention, the OPS imaging probe is used during normal or complicated pregnancy to monitor the woman's microvascular function.

In each of the following aspects of this embodiment, one or more parameters, such as, capillary density, vessel (and microvessel) morphology, vessel density, vasospasm, red blood cell (RBC) velocity, cell morphology, vessel diameter, leukocyte-endothelial cell interactions, vascular dynamics (such as vasomotion), functional vessel density, functional capillary density, blood flow, area-to-perimeter ratio, hemoglobin concentration, and hematocrit, may be quantitatively determined. Preferably, two or more parameters are determined.

In one aspect of this embodiment, a standard or high contrast OPS imaging probe is used to detect or monitor women whose pregnancy is complicated by preeclampsia (PE). As used herein, "preeclampsia" is a complication of a current or recent pregnancy, characterized by hypertension with proteinuria and/or edema. Preeclampsia is a systemic disease with an endothelial cell dysfunction. To investigate the way in which PE effects the microcirculation of the skin, microvascular function was studied with OPS imaging.

The aim of the following study was to investigate *in vivo* microcirculatory function in pregnancy and pregnancy complicated with preeclampsia.

Summary: In 10 preeclamptic and 10 normotensive pregnant women, the microcirculation of the skin was studied. The red blood cell velocity at rest (rCBV) and the local sympathetic veno-arteriolar reflex (VAR) during venous occlusion was studied in the nailfold using OPS imaging. Laser-Doppler fluxmetry was used to assess skin microcirculatory function during venous occlusion, arterial occlusion, and during rest.

Laser-Doppler fluxmetry showed no difference between the normotensive and the preeclamptic group. Although no differences were found in the absolute velocities during rest and during venous occlusion between the two groups as a whole, OPS imaging, showed a decrease in red blood cell velocity following

- 81 -

venous occlusion (58% (40-94) (median and range)) in the group with preeclampsia, compared to 84% (74-89) in the control group (P = 0.003).

This study shows that by using OPS imaging, there is an impaired local veno-arteriolar reflex in preeclampsia, not detectable by laser-Doppler fluxmetry measurements. OPS imaging may also permit the study of the effects of preeclampsia in other organ beds.

Introduction: The maternal cardiovascular system reacts to pregnancy with a decrease in peripheral vascular resistance and systemic blood pressure, accompanied by an increase in blood volume and cardiac output resulting in a normotensive condition (NT). These adaptations are necessary to meet the demands of normal pregnancy. This response, however, is impaired in pregnancies complicated with preeclampsia (PE). Pathophysiologic findings in PE are high blood pressure, proteinuria, decreased plasma volume, increased peripheral vascular resistance, vasoconstriction, and reduced organ perfusion (Roberts, J.M., and Redman, C.W.G., *Lancet 341*:1447-1451 (1993); Bosio, P.M., *et al.*, *Obstet. Gynacol. 94*:978-984 (1999)). The coagulation cascade is activated and there is an imbalance between prostacylin/thromboxane ratio causing platelet aggregation and a further increase in vasoconstriction (Walsh, S.W., *Am. J. Obstet. Gynocol. 152*:355-340 (1985)). Accumulating evidence suggests a generalized endothelial cell dysfunction in PE (Roberts, J.M., and Redman, C.W.G., *Lancet 341*:1447-1451 (1993)). The cause of the endothelial dysfunction is still elusive, but it is suggested that it is caused by blood borne products from a poorly perfused placenta (Roberts, J.M., and Redman, C.W.G., *Lancet 341*:1447-1451 (1993)).

In PE, a vascular dysfunction was found in isolated arteries from several organs (Aalkjaer, C., *et al.*, *Clin. Sci. 69*:477-482 (1985); McCarthy, A.L., *et al.*, *Am. J. Obstet. Gynacol. 168*:1323-1330 (1993); Vedernikov, Y., *et al.*, *Semin. Perinatol. 23*:34-44 (1999)). There is an impaired endothelium-dependent dilatation in PE compared to NT (McCarthy, A.L., *et al.*, *Am. J. Obstet. Gynacol. 168*:1323-1330 (1993); Knock, G.A., and Poston, L., *Am. J. Obstet. Gynacol. 175*:1668-1674 (1996)), and vascular smooth muscle cells of women with PE showed an increased sensitivity to vasopressors (Gant, N.F., *et al.*, *J. Clin. Invest.*

- 82 -

52:2682-2689 (1973)). Also, an increased sympathetic activity was found in blood vessels of skeletal muscle *in vivo* in PE (Schobel, H.P., *et al., N. Engl. J. Med. 335*:1480-1485 (1996)). These findings suggest that not only endothelial dysfunction is responsible for changes in vascular reactivity in PE.

However, most of these studies have been performed *in vitro* and assessment of vascular function *in vivo* has been done less frequently because of the difficulties in studying vascular function *in vivo*. An *in vivo* study with laser-Doppler fluxmetry (LDF), using ionophoresis of vascoactive agents, showed no altered vascular function in the microcirculation of the skin in women with PE (Eneroth-Grimfors, H., *et al., Brit. J. Obstet. Gynacol. 100*:469-471 (1993)). The reaction after arterial occlusion (the hyperemic reaction, an endothelial-dependent vasodilation) studied with LDF was increased in the skin of the hand in PE compared to NT, while in the skin of the arm no difference was seen (Beinder, E., and Lang, N., *Geburtsh u Frauenheilk 54*:268-272 (1994)). Vascular reactivity in local cooling, causing vasoconstriction, was significantly greater in both areas in PE (Beinder, E., and Lang, N., *Geburtsh u Frauenheilk 54*:268-272 (1994)). However, with capillaroscopy of the skin in the nailfold, no difference was found in the hyperemic reaction in women with PE (Rósen, L., *et al., Int. J. Microcirc. Clin. Exp. 8*:237-244 (1989)), while the brachial arteries of women with PE showed an altered hyperemic reaction studied with high-resolution ultrasonography and Doppler ultrasonography compared to NT (Yoshida, A., *et al., Hypertension 31*:1200 (1998); Veille, J.C., *et al., J. Soc. Gynacol. Invest. 5*:38-43 (1998)).

Microcirculatory dysfunction was demonstrated by Rosén, L., *et al., Int. J. Microcirc. Clin. Exp. 9*:257-266 (1990), who showed that the reaction to venous occlusion, causing a veno-arteriolar reflex (a local sympathetic reflex leading to an endothelium-independent vasoconstriction reaction), was depressed in the skin in PE studied with capillaroscopy. This study, however, was never repeated and the cause of an impaired veno-arteriolar reflex in combination with an increased sympathetic activity remains uncertain. That is the reason the present study was undertaken. Since the use of different methods and various vascular

- 83 -

beds resulted in contradictory results concerning vascular reaction to arterial occlusion in PE, the present study also studied the hyperemic reaction.

To observe vascular function of the cutaneous microcirculation in PE *in vivo* in a simple and non-invasive way, OPS imaging was used. Implanted in a small and hand-held device, this technique allows intravital observation not only of the microcirculation of the skin but also of internal human organs at bedside and during surgery (Groner, W., *et al., Nature in Medicine 5*:1209-1212 (1999). The technique has been validated by comparison to conventional capillaroscopy. To compare the results with another method that measures *in vivo* microvascular function also, laser-Doppler fluxmetry (LDF) was used. The control of vascular function by the sympathetic system was studied by assessment of the veno-arteriolar reflex (VAR) (Henriksen, O., *Acta Physiol. Scand. 143*:33-39 (1991)) using both devices. The control of endothelium-dependent vasodilation was studied with the hyperemic reaction (Östergren, J., and Fagrell, B., *Int. J. Clin. Microcirc. Clin. Exp. 5*:37-51 (1986)) with LDF.

Material and Methods:

(1) Subjects: Ten women with PE and 10 women with a normotensive pregnancy (control group) were enrolled after written informed consent. PE was defined as a diastolic blood pressur >90 mmHg developed after a gestational age of 20 weeks and proteinuria >300 mg/24 hours or dipstick ++/+++ (National High Blood Pressure Education Program Working Group Report on High Blood Pressure in Pregnancy, *Am. J. Obstet. Gynacol. 163*:1689-1712 (1990)). The Karotkoff V was used to determine diastolic blood pressure. Of the women with PE, six used medication of which three used infedipine (Adalat, 3-4 x 10 mg) and three methyldopa (Aldomet, 3 x 250 or 500 mg). Women from the control group were recruited by advertisements in the midwifery outpatient clinic of the hospital. None of them used medication. Women with diabetes mellitus, hypertension, and Raynaud's phenomenon diagnosed before pregnancy, or with fever, were not included in this study. The characteristics of the subjects are listed in Table 3.

(2) Methods: Laser Doppler Fluxmetry (LDF) (Perifleux 4001, PF 408 standard probe time constant 0.2 sec, Perimed, Sweden) was used to assess total

- 84 -

cutaneous blood flow (Stern, M.D., *et al., Am. J. Physiol.* 232:H441-H448 (1977)). Two probes were attached to the pulp of the finger using a probe holder (Perimed, Sweden) with double-sided adhesive tape. Laser light with a wavelength of 780 nm was conducted through optical fibers to the skin where it penetrated the skin to a depth of 1-1.5 mm and was partly reflected. The light, when backscattered by moving objects (erythrocytes), undergoes a frequency shift proportional to the velocity and number of moving objects and is expressed in arbitrary units (volts) and referred to as flux. The data were recorded and analyzed off-line (AcqKnowledge III and MP 100 WSW, Biopac System Inc., Santa Barbara, California).

The microcirculation of the nailfold was studied with OPS imaging (version E2, Cytometrics Inc., Philadelphia, PA). This technique makes use of green polarized light passed through a light guide and is placed above the organ bed to be measured. By cross-polarization of the reflected light all surface reflection is eliminated and remarkably sharp images can be recorded (FIG. 14). A 75 W halogen precision lamp was used as light source with light of a wavelength of 540 nm. A removable 5x objective was used with a final onscreen magnification of 325x for analysis. All images were recorded on a digital video recorder (Sony DSR-20P), off-line analyses of the images were accomplished with a software program (CapImage™, Dr. Zeintl Software engineering, Heidelberg, Germany) (Klyscz, T., *et al., Biomed Tech (Berl)* 42:168-175 (1997)).

(3) Measurements: With LDF, the mean flux at rest (RF) during 5 minutes, and the mean flux during 2 minutes of venous occlusion after 1 minute occlusion (VOF), to determine the VAR, were measured. Also, the highest flux after 1 minute of arterial occlusion (PF) and time until PF were measured. The decrease or increase in flux normalized to rest values was calculated as ((RF-VOF)/RF) and ((PF-RF)/RF), and expressed as percentages. During arterial occlusion, the residual LDF (biological zero) (Caspary, L., *et al., Int. J. Microcirc. Clin. Exp.* 7:367-371 (1988)) was determined, which was subsequently subtracted from all other measured LDF values. LDF measurements could be performed in

- 85 -

all but two women from the control group because of the unavailability of the laser-Doppler device on those occasions.

With OPS, the capillary blood cell velocity at rest (rCBV) was measured as the mean velocity during 30 seconds and the VAR was determined as the mean velocity during 30 seconds after 30 seconds of venous occlusion (roCBV). Both velocities were measured by use of the line-shift diagram method (Klyscz, T., et al., Biomed Tech (Berl) 42:168-175 (1997)). The decrease in red blood cell velocity during venous occlusion normalized to rest value was calculated and expressed in percentages ((rCBV-voCBV)/rCBV). From every subject, three capillaries were studied and mean values used for comparisons.

(4) Protocol: All subjects were asked to refrain from drinking caffeine-containing drinks from 2 hours before the investigation. The investigation took place in an air conditioned room with a temperature between 23 and 25°C after an acclimatization period of 15 minutes. The subjects lay down in lateral position on their dominating side, with their arm slightly bent at heart level on a pillow. A cuff was placed around their upper arm. At first, the capillaries of the 4th finger of the non-dominating hand were studied with OPS imaging, the device placed slightly above the surface of the nailfold. The fingers were imbedded in a mass of clay to stabilize the hand and a drop of paraffin oil on the nailfold was used to make the skin more transparent. Skin temperature was measured continuously with a digital thermometer (Keithley 871 A) taped on the skin proximal to the nailfold. From the capillaries of the nailfold, three well visualized capillaries were chosen for measurements. Each capillary was recorded for 2 minutes to measure rCBV, after which the cuff was inflated to 50 mmHg for 2 minutes to measure voCBV.

After these recordings, the measurements with LDF took place. The two probes were attached to the middle phalanx of the same finger, one at the palmer side and one at the dorsal side. After a period of rest for at least 5 minutes to determine RF, the cuff was inflated to 50 mmHg to measure VOF during 3 minutes. The cuff was then inflated to 200 mmHg for arterial occlusion to determine the biological zero, and deflated after 1 minute. For 2 more minutes the

- 86 -

flux was recorded for PF and time to peak. The blood pressure was measured at the end of the investigation.

(5) *Statistics*: Values were expressed as median with range unless stated otherwise and p-values were calculated with the Mann-Whitney U test and the Wilcoxon signal rank test. A p-value <0.05 was considered statistically significant.

Results: There were no differences in patient characteristics between both groups except for blood pressure (Table 3). The results of the laser-Doppler fluxmetry are presented in Table 4 and FIGs. 15A and 15B. There was no significant difference in flux or percentual change between patients with PE and the control group at rest, during venous occlusion or after arterial occlusion, at palmer and dorsal side of the finger. In the control group, there was even no significant change in flux during venous occlusion at dorsal side, while in the patient group, venous occlusion at palmer side did not provoke a significant reaction.

Analysis of capillary red blood cell kinetics obtained from OPS images revealed no difference between the rCBV and voCBV between the two groups. However, the percentual decrease in the blood cell velocity during venous occlusion in the women with PE, was significantly smaller than the decrease in the control group, 58% (40-94) vs. 84% (74-89) (P = 0.003, see FIG. 16).

Comment: The present study confirms an impaired VAR in PE identified using OPS imaging. This impaired reflex was also found by Rosén *et al.*, *supra*, with capillaroscopy. The VAR is one of the reflexes causing arteriolar constriction for maintaining arterial blood pressure in an upright position. It is a local sympathetic axon reflex (Henriksen, O., *Acta Physiol. Scand. 143*:33-39 (1991); Vissing, S.F., *et al., Acta Physiol. Scand. 159*:131-138 (1997)), the role of the endothelium in the VAR is still unknown (Henriksen, O., *Acta Physiol. Scand. 143*:33-39 (1991)). The VAR is elicited by venous distension causing arteriolar constriction resulting in a decrease in blood flow. Increasing transmural pressure of more than 25 mmHg by inflating a cuff around the arm causing venous occlusion can also provoke this reflex.

- 87 -

An impaired reflex could not be detected with LDF. This discrepancy may be explained by the fact that in LDF, not only the blood flow in the nutritive capillaries of the skin is measured like with OPS imaging, but also the flow in the subpapillary (thermoregulatory) plexus at a greater depth. It has been suggested that the VAR in these vessels is less obvious (Tooke, J.E., *et al., Int. J. Microcirc. Clin. Exp.* 2:277-284 (1983)). This could explain why no differences were found in the VAR with LDF in contrast to the results with OPS imaging.

Furthermore, we found no defect in hyperemia response following arterial occlusion between PE and NT. The hyperemic reaction is a largely endothelium-dependent vasodilation response to arterial occlusion. After the release of the cuff, the blood flow starts again and increases until it reaches a peak velocity after a few seconds and returns to rest value.

Previous investigators found an impaired hyperemic reaction of the brachial artery in women with PE compared to NT (Yoshida, A., *et al., Hypertension* 31:1200 (1998); Veille, J.C., *et al., J. Soc. Gynacol. Invest.* 5:38-43 (1998)). These results could not be confirmed in the cutaneous microcirculation using LDF. LDF is widely used, often to evaluate the microcirculation in vascular diseases and diabetes mellitus (Schabauer, A.M.A., nad Rooke, T.W., *Mayo Clin. Proc.* 69:564-574 (1994)). However, there is a great physiologic variability in flux, which causes poor reproducibility (Schabauer, A.M.A., nad Rooke, T.W., *Mayo Clin. Proc.* 69:564-574 (1994)). Several measures, like venous occlusion to provoke the VAR, and reactive hyperemia, by which the subjects are their own control, are used to reduce this variability.

In PE, a sympathetic overactivity has been found in the blood vessels of skeletal muscle. This could cause an increase in sympathetic vasoconstrictor activity and could play a role in the increase in peripheral vascular resistance (Schobel, H.P., *et al., N. Engl. J. Med.* 335:1480-1485 (1996)). Sympathetic overactivity may thus explain the impaired reaction to venous occlusion. An increased arteriolar constriction in PE would impair further vasoconstriction by sympathetic stimulation. Methyldopa, a centrally acting drug reducing sympathetic outflow, is first choice medication for long term blood pressure

- 88 -

control in PE, indeed suggesting involvement of the sympathetic nervous system. An alternative hypothesis could be that because of the sympathetic overactivity, the receptors of the smooth muscle cells are down-regulated, causing less vasoconstriction when stimulated. There is a down-regulation of the α_1- and α_2-adenoreceptors of the myocardium in heart failure, a condition associated with elevated sympathetic activity (Brodde, O.C., *Pharmacol. Rev. 43*:203-242 (1991)). It is not known what happens with receptors of the circulation of the skin during sympathetic overactivity. However, it cannot be excluded that the impaired VAR is a consequence of functional or structural changes of the microcirculation in PE, which are independent of the sympathetic nervous system and contribute to impaired vascular function.

In this study, the microcirculation of the skin with OPS imaging and LDF was investigated. In conclusion, OPS provided a more sensitive technique to evaluate vascular function in pregnancy than LDF. Using OPS imaging, an impaired veno-arteriolar reflex in women with PE was detected, that could not be detected with LDF. This result suggests impaired sympathetic vasoconstriction in the microcirculation of the skin. The ability to use OPS imaging for observation in other organ beds could help to clarify vascular dysfunction in PE.

Table 3:
Characteristics of Subjects

	Control (n=10)	Preeclampsia (n=10)
Age (year)	33.0 (22.5-33.6)	29.7 (22.8-32.4)
Gestational age (weeks)	31.3 (22.1-37.1)	32.9 (21.4-40.3)
Diastolic blood pressure (mmHg)	68 (50-78)	100* (75-112)
Systolic blood pressure (mmHg)	108 (90-110)	144* (120-172)
Hb (mmol/l)	7.5 (6.4-8.1)	7.9 (6.3-8.7)
Skin temperature (°C)	34.5 (32.9-35.6)	34.4 (31.9-35.5)

Results given as median and range. $P < 0.001$ for comparison with control group, Mann-Whitney U test.

- 89 -

Table 4:
Laser Doppler Fluxmetry Values in Volts

	Control (n=8)		Preeclampsia (n=10)	
	palmar	dorsal	palmar	dorsal
RF	1.40 (0.35-3.23)	0.39 (0.22-0.63)	0.71 (0.13-2.28)	0.31 (0.22-0.99)
VOF	0.62* (0.25-3.31)	0.29 (0.20-1.14)	0.47 (0.03-2.94)	0.25* (0.13-0.56)
PF	2.28* (0.78-5.44)	1.16* (1.00-1.83)	1.63* (0.53-3.58)	0.71* (1.39-2.60)
Time to peak (sec)	4.50 (3.4-7.1)	5.85 (3.7-8.3)	5.65 (3.1-7.9)	5.90 (2.8-8.7)

Results given as median and range.

* Values significantly different compared to the RF

In another aspect of this embodiment, a standard or high contrast OPS imaging probe is used to monitor intact placental microvasculature in preeclampsia/ fetal growth retardation.

It is well-known that fetal nutrition and oxygenation are dependent on well-developed and capillarised terminal villi of the placenta. In preeclampsia, fetal growth retardation is a common symptom. Using scanning electron microscopy, it has been shown that hypocapillarisation exists in the terminal villi (Habashi S. *et al, Placenta* 4:41-56 (1983)).

OPS imaging was used to examine, *ex vivo*, the surface of the maternal site of the placenta from 10 normotensive women with neonates appropriate for gestational age, and from 10 preeclamptic women with neonates small for gestational age. The aim of this study was to determine if images could be obtained of the microvasculature, and if the terminal villi of the latter group were hypocapillarised, compared with the first.

Within 10 minutes after delivery of the placenta, umbilical arteries and vein were cannulated and perfused with a mixture of 50 mL Ringers glucose, 5 mL Heparin and 50 mL Custodiol. Subsequently, the arteries were perfused with 5 mL Indian ink each and 10-13 mL synthetic baryta. It was clear that OPS images of

- 90 -

the capillaries in the terminal villi compare with images obtained by SEM showing microcirculatory units that are hypocapillarized, normo-capillarized, or hypercapillorized. OPS imaging thus adds a new and versatile facility for the postnatal study of the nature of fetal growth retardation (*i.e.*, due to genetics vs. due to placental deficiency, such as in pre-eclampsia).

Neonatology Monitoring

In this embodiment of the present invention, the OPS imaging probe is used in neonatology monitoring.

In each of the following aspects of this embodiment, one or more parameters, such as, capillary density, vessel (and microvessel) morphology, vessel density, vasospasm, red blood cell (RBC) velocity, cell morphology, vessel diameter, leukocyte-endothelial cell interactions, vascular dynamics (such as vasomotion), functional vessel density, functional capillary density, blood flow, area-to-perimeter ratio, hemoglobin concentration, and hematocrit, may be quantitatively determined. Preferably, two or more parameters are determined.

In one aspect of this embodiment, a standard or high contrast OPS imaging probe is used to quantitatively measure changes in the microcirculation of neonates during different disease states like sepsis and meningitis, and therefore be used for diagnosis of these conditions. Hemoglobin levels of the neonates can be monitored non-invasively.

In another aspect of this embodiment, a standard or high contrast OPS imaging probe is used to measure changes in the neonate microcirculation prior to, during, or following shock (hemorrhagic or septic).

The above applications would also be useful in monitoring premature infants.

- 91 -

High Altitude Studies/Space Physiology

In this embodiment of the present invention, the OPS imaging probe can be used in high altitude studies or to study space physiology.

One or more parameters, such as, capillary density, vessel (and microvessel) morphology, vessel density, vasospasm, red blood cell (RBC) velocity, cell morphology, vessel diameter, leukocyte-endothelial cell interactions, vascular dynamics (such as vasomotion), functional vessel density, functional capillary density, blood flow, area-to-perimeter ratio, hemoglobin concentration, and hematocrit, may be quantitatively determined. Preferably, two or more parameters are determined.

In one aspect of this embodiment, a standard or high contrast OPS imaging probe is used to observe and evaluate changes in the microcirculation at high altitudes to study, diagnose, and/or treat high altitude sickness. Changes in the microcirculation include an increase in the number of vessels, an increase in the number of WBCs that can be seen in those vessels, as well as an increase in leukocyte-endothelial cell interactions. Changes in Hb could also be determined as a result of high altitude.

Applications in Clinical Blood Rheology

In this embodiment of the present invention, the OPS imaging probe can be used to examine rheology of the blood.

One or more parameters, such as, capillary density, vessel (and microvessel) morphology, vessel density, vasospasm, red blood cell (RBC) velocity, cell morphology, vessel diameter, leukocyte-endothelial cell interactions, vascular dynamics (such as vasomotion), functional vessel density, functional capillary density, blood flow, area-to-perimeter ratio, hemoglobin concentration, and hematocrit, may be quantitatively determined. Preferably, two or more parameters are determined.

- 92 -

In one aspect of this embodiment, a standard or high contrast OPS imaging probe is used to observe and evaluate changes in a patient's blood rheology, that may be due to numerous clinical disorders, including, for example, sickle cell anemia, or excessive blood clotting that may occur in patients infected with malaria. This information could be used to study diseases which alter blood clotting, red blood cell aggregation, or alter blood rheology.

Applications in Critical Care or Intensive Care Medicine

In this embodiment of the present invention, the OPS imaging probe is used *in vivo* in critical care or intensive care medicine.

In one aspect of this embodiment, a standard or high contrast OPS imaging probe is used as a sublingual monitoring device on critically ill patients to diagnose, treat, or prevent sepsis and/or shock (hemorrhagic or septic). It has been found that in cases of sepsis and/or shock, there is either a drastic reduction of flow or no flow of the microcirculation. OPS imaging technology could be used to prevent the two conditions in critically ill patients or to try some therapies that would change the outcome. OPS imaging could also be used to monitor the efficacy of therapy.

In this patient population, one or more parameters, such as, capillary density, vessel (and microvessel) morphology, vessel density, vasospasm, red blood cell (RBC) velocity, cell morphology, vessel diameter, leukocyte-endothelial cell interactions, vascular dynamics (such as vasomotion), functional vessel density, functional capillary density, blood flow, area-to-perimeter ratio, hemoglobin concentration, and hematocrit, may be quantitatively determined using OPS imaging. Preferably, two or more parameters are determined.

In the following study, OPS imaging was used on intensive care patients.

Introduction: Whatever the cause, circulatory shock is one of the major challenges in intensive care medicine. Multiple organ failure often develops despite improvement in the profound cardiovascular alterations. Even when global hemodynamic alterations appear to be stabilized with fluids and vasoactive agents,

- 93 -

significant alterations in the microcirculation may persist and participate in the development of multiple organ failure (Garrison, R.N., *et al., Ann. Surg. 227*:851-860 (1998)).

The contribution of altered microvascular blood supply is quite straightforward in shock states associated with critical reductions in blood supply as in severe heart failure or hypovolemia. The alterations are more complex and also more controversial in septic shock. Using intravital microscopy in experimental conditions, various authors (Lam, C.J., *et al., J. Clin. Invest. 94*:2077-2083 (1994); Piper, R.D., *et al., Am. J. Respir. Crit. Care Med. 157*:129-134 (1998); Farquhar, I., *et al., J. Surg. Res. 61*:190-196 (1996); Wang, P., *Am. J. Physiol. 263*:G38-G43 (1992); Madorin, W.S., *et al., Crit Care Med 27*:394-400 (1999); Pannen, B.H.J., *et al., Am. J. Physiol. 272*:H2736-H2745 (1997)) observed that blood flow heterogeneity was increased after endotoxin administration. The number of transiently non perfused capillaries is increased in sepsis and this is probably due to the activation of various cellular elements with aggregation of leukocytes and platelets, and increased red blood cell stiffness (McCuskey, R.S., *et al., Cardiovasc. Res. 32*:752-763 (1996); Piper, R.D., *et al., Am. J. Respir. Crit. Care. Med. 154*:931-937 (1996)). Various authors have demonstrated the link between blood flow heterogeneity and decreased oxygen extraction capabilities in sepsis (Walley, K.R., *J. Appl. Physiol. 81*:885-894 (1996); Humer, M.F., *et al., J. Appl. Physiol. 81*:895-904 (1996); Drazenovic, R., *et al., J. Appl. Physiol. 72*:259-265 (1992)). Also transient flow may lead to focal ischemia / reperfusion injury in areas vascularized by these capillaries. In patients, the evidence for involvement of microcirculatory disturbances is still lacking. Access to the human microcirculation has for a long time been limited to the nailfold. Indeed, the size of intravital microscopes and the depth of the capillaries precluded their use in other sites. OPS imaging, which is based on reflection spectroscopy, in the clinical area recently allowed the investigation of mucosal sites. In critically ill patients, the usual sites available for non-invasive microcirculation visualization are the lip, the sublingual area, and sometimes the enterostomy site. Although technically feasible, the investigation of the rectal and

- 94 -

vaginal mucosa is more difficult. The OPS imaging technique had been incorporated in the CYTOSCAN™ A/R (Cytometrics, Philadelphia, PA). In this study, results using the CYTOSCAN™ A/R in the intensive care setting are reported.

PARA--Sublingual area: Although access to the sublingual area is very easy, an important question is whether this area is representative of microcirculatory alterations in circulatory failure. There is indeed some evidence to support an early involvement of the sublingual area in shock states. Weil and coworkers (Nakagawa Y, *et al.*, *Am J Respir Crit Care Med.157*(6 Pt 1):1838-1843 (1998)) recently reported that sublingual PCO_2 ($PslCO_2$), which represents the balance between oxygen supply and demand in this area, is markedly increased in shock states. Furthermore, $PslCO_2$ is inversely related to blood pressure and directly related to arterial lactate levels, a marker of tissue hypoxia. $PslCO_2$ was also very sensitive to therapeutic interventions.

Imaging the sublingual microcirculation is very promising. Contrary to animal preparations in which a quantitative measurement of the microcirculatory flow is easily available, the quantitative estimation is actually not feasible in critically ill patients because of the movements artifacts. Hence, a semi-quantitative analysis was developed in which the capillary index was calculated by the number of vessels crossing 3 vertical and 3 horizontal lines that were traced on the screen. These vessels were separated into large vessels (>20 μm, mainly venules) and small vessels (<20 μm, mainly capillaries). Blood flow velocity was estimated in a 20 second video sequence by eye, and classified into 4 groups: normal or high flow, low flow, intermittent flow, and no flow. In 3 healthy volunteers, sublingual vascularization consisted of large and small vessels in a ratio 40/60% (FIG.17). Almost all these vessels were well perfused (95%), although intermittent or absent flow could be observed in a very limited number of capillaries (5%).

In 21 patients with septic shock, a very different pattern was observed. The number of perfused vessels was markedly reduced (78%, p<0.05), and especially in the small vessels (39%, p<0.01). In these vessels, an increased number of

- 95 -

capillaries where flow was transient or absent was observed. A typical example is reported in FIG. 18. In 8 patients with low flow due to cardiogenic shock, capillary index was decreased and red blood cell conglomerates could be visualized in venules (FIG. 19). In these patients also, a decrease in the number of perfused vessels (75%, $p < 0.05$) was observed, especially in the small vessels.

These preliminary results suggest that severe alterations in the microcirculation can be observed in various shock states. It is likely that these alterations may be responsible for the increase in $PslCO_2$ that was reported by other groups (Nakagawa Y. *et al., supra*), but further studies are required to confirm this hypothesis.

Other sites of interest: The inner side of the mouth, including the lip and cheek can also be investigated. In many cases, microcirculation in the lip is better preserved, even in severe shock states. In 11 patients with septic shock and in cardiogenic shock, it was observed that 95% of the small vessels and all the large vessels were perfused in the lip area, while only 32% of the small vessels and all the large vessels were perfused in the sublingual area ($p < 0.05$). Hence, the study of the sublingual microcirculation is probably more relevant than lip microcirculation in shock states.

Probably more promising is the study of enterostomies, since the application of OPS imaging to the bowel mucosa allows direct visualization and characterization of gut mucosal blood flow. In FIG. 20, the OPS image of a patient with recurrent bowel necrosis is shown. In this patient, a very limited number of capillaries was observed in the gut mucosa and blood flow was almost completely stopped in these capillaries. This report supports the value of the use of OPS imaging in mesenteric ischemia and infarction. One use of OPS imaging is the early detection of ischemia, the quantification of the lesions, and the delineation of ischemic zones with some potential for recovery.

Conclusions: The introduction of OPS imaging through the CYTOSCAN™ A/R in the intensive care opens a new area of investigation with direct and non- invasive visualization of the microcirculation at the bedside.

- 96 -

Pharmaceutical Applications

In this embodiment of the present invention, the OPS imaging probe is used in the field of pharmaceutical development.

In one aspect of this embodiment, a standard or high contrast OPS imaging probe is used to study the effects of different pharmaceuticals on the microcirculation, such as tumor anti-angiogenesis drugs to determine if circulation to a tumor is cut off; cardiac angiogenesis drugs to determine if vessel growth and thus circulation (to the heart, for example) has improved; or anti-hypertension agents to determine the mechanisms of action of new treatments or hypertension etiology at the microvascular or cellular level. This could be measured under the tongue or directly on the tissue. Real time serial images and measurements could be obtained.

One or more parameters, such as, capillary density, vessel (and microvessel) morphology, vessel density, vasospasm, red blood cell (RBC) velocity, cell morphology, vessel diameter, leukocyte-endothelial cell interactions, vascular dynamics (such as vasomotion), functional vessel density, functional capillary density, blood flow, area-to-perimeter ratio, hemoglobin concentration, and hematocrit, may be quantitatively determined. Preferably, two or more parameters are determined.

Tumor angiogenesis plays a key role in tumor growth, formation of metastasis, detection and treatment of malignant tumors. Recent investigations provided increasing evidence that quantitative analysis of tumor angiogenesis is an indispensable prerequisite for developing novel treatment strategies such as antiangiogenic and antivascular treatment options. OPS imaging has been validated for non-invasive quantitative imaging of tumor angiogenesis *in vivo* and used to assess antiangiogenic tumor treatment *in vivo*.

Experiments were performed in amelanotic melanoma A-MEL 3 implanted in a transparent dorsal skinfold chamber of the hamster. Starting at day 0 after tumor cell implantation, animals were treated daily with the antiangiogenic compound SU5416 (25 mg/kg/bw) or vehicle (control) only. Functional vessel

- 97 -

density (fvd), diameter of microvessels (d) and red blood cell velocity (V_{RBC}) were visualized by both OPS imaging and fluorescence microscopy and analyzed using a digital image system.

The results were as follows: the morphological and functional properties of the tumor microvasculature could be clearly identified by OPS imaging. Data for fvd correlated excellently with data obtained by fluroescence microscopy (y = 0.99x + 0.48, r^2 = 0.97, R_S = 0.98, precision: 8.22 cm^{-1} and bias: –0.32 cm^{-1}). Correlation parameters d and V_{RBC} were similar (r^2 = 0.97, R_S = 0.99 and r^2 = 0.93, R_S = 0.94 for d and V_{RBC}, respectively). Treatment with SU5416 reduced tumor angiogenesis. At day 3 and 6 after tumor cell implantation, respectively, fvd was 4.8±2.1 cm^{-1} and 87.2±10.2 cm^{-1} compared to values of control animals of 66.6±10.1 cm^{-1} and 147.4±13.2 cm^{-1}. In addition to the inhibition of tumor angiogenesis, tumor growth and the development of metastasis was strongly reduced in SU5416 treated animals.

OPS imaging enabled noninvasive, repeated, and quantitative assessment of tumor angiogenesis and the effects of antiangiogenic treatment on tumor vasculature. Tumor angiogenesis can be used to more accurately classify and monitor tumor biologic characteristics and to explore aggressiveness of tumors *in vivo*.

In a related aspect of this embodiment, an OPS imaging probe is used to look at the effect of pharmaceuticals that are thought to improve perfusion. This includes, for example, the vasoactive class of drugs, which includes, *e.g.*, naftidrofuryl, pentoxifylline, and buflomedil. That is, pharmaceuticals used to combat perfusion problems can be tested in animal models or humans more accurately using OPS imaging, since the OPS imaging probe can be used to observe and quantify perfusion following administration of the drug. Further, OPS imaging could actually assist in determining the mechanism(s) by which these drugs exert their effects in humans.

In another aspect of this embodiment, a standard or high contrast OPS imaging probe is used to look at hemoglobin-based oxygen carriers (*i.e.*, DCL Hb, a synthetic hemoglobin) to determine their effects on the microcirculation, such

- 98 -

as, *e.g.*, whether there is an increased flow of RBC's as a result of using the product.

In another aspect of this embodiment, the OPS imaging probe can be used to study the effect of ultrasound enhancers (*i.e.*, injectable dyes) on the microcirculation.

In another aspect of this embodiment, the OPS imaging probe can be used to visualize and detect leakage of injectable dyes or other injectable contrast-generating agents, from the blood vessels into tissues.

Capillariscope Comparison

In this embodiment of the present invention, a standard or high contrast OPS imaging probe is used to visualize and characterize capillary beds in the nailfold, as has been done before using standard capillaroscopy.

In one aspect of this embodiment, a standard or high contrast OPS imaging probe is used to study, diagnose, and evaluate patients with circulation disturbances, such as, for example, Raynaud's phenomenon, osteoarthritis, or systemic sclerosis.

The OPS imaging probe produces better results than the standard capillariscope used to visualize and characterize capillaries in the skin. Comparisons have show that the method is comparable (and in most cases better) when looking at healthy and disease state individuals. The site of the OPS imaging probe is on the nailfold. The measurements obtained were RBC velocity and diameter. Other parameters, such as capillary density, vessel (and microvessel) morphology, cell morphology, vessel density, vasospasm, vessel diameter, leukocyte-endothelial cell interactions, vascular dynamics (such as vasomotion), functional vessel density, functional capillary density, area-to-perimeter ratio, blood flow, hemoglobin concentration, and hematocrit, may be quantitatively determined. Preferably, two or more parameters are determined. I n   t h e following study, OPS imaging was validated with conventional capillaroscopy. To this end, capillaroscopy (CAP) was compared to OPS imaging in the

- 99 -

microcirculation of the nailfold. Three capillaries of 10 healthy male volunteers, age 23.5 ± 0.8 years (mean $\pm$ SD), were visualized with CAP and OPS and stored on videotape for offline analyses. The red blood cell velocity at rest (rCBV) was measured with CapImage™. To assess the respective quality of the images a contrast ratio was calculated for both devices. The rCBV was not significantly different between OPS and CAP, P=0.32, Wilcoxon matched pairs test. The rCBV measured by OPS was 0.737 ± 0.237 mm/sec and with CAP 0.782 ± 0.196 mm/sec, mean difference between the single measurements: 0.071 ± 0.130 mm/sec. A significant higher contrast ratio was found for the images of OPS (OPS 0.34 ± 0.08, CAP 0.17 ± 0.06 P= 0.0039). It can be concluded that OPS imaging provides recordings of the microcirculation of the nailfold with the same, if not better, accuracy and resolution as CAP. Additionally, advantages of OPS imaging include its ease of use and being applicable in many other organ beds.

Anesthesiology

In this embodiment of the present invention, the OPS imaging probe is used in the area of anesthesiology.

In each of the following aspects of this embodiment, one or more parameters, such as, capillary density, vessel (and microvessel) morphology, vessel density, vasospasm, red blood cell (RBC) velocity, cell morphology, vessel diameter, leukocyte-endothelial cell interactions, vascular dynamics (such as vasomotion), functional vessel density, functional capillary density, blood flow, area-to-perimeter ratio, hemoglobin concentration, and hematocrit, may be quantitatively determined. Preferably, two or more parameters are determined.

In one aspect of this embodiment, a standard or high contrast OPS imaging probe is used to monitor blood loss during surgery. For example, an OPS imaging probe can be used to non-invasively and continuously monitor the hemodynamic parameters of an anesthetized patient, such as, *e.g.*, hemoglobin concentration and hematocrit.

In another aspect of this embodiment, a standard or high contrast OPS

imaging probe is used on an anesthetized patient to monitor the clumping of red blood cells, and the early formation of microemboli during a surgical procedure.

A high contrast OPS imaging probe is used to monitor and detect air or fat bubbles in the blood that may arise due to any number of clinical situations, including, for example, the use of bubble oxygenators during cardiac bypass surgery, the introduction of air from a dialysis circuit, or decompression during laparoscopy. The ability to directly detect bubbles in the blood may foster the early discovery of a lung or brain embolism, that would prove fatal if not treated.

OPS imaging has been used to study ventilation with Positive End-Expiratory Pressure (PEEP), which reduces splanchnic blood flow and could thereby contribute to gut-derived sepsis. PEEP effects on the capillary level are largely unknown. Research into this issue in a murine model could provide insight into molecular mechanisms in PEEP as genetically modified mice and murine antibody-markers are widely available. Therefore, a murine model was established using OPS-imaging to visualize the intestinal microcirculation. Anesthetized mice (n=14, c57bl6, male) were mechanically ventilated. After laparotomy, the distal 2cm of the ileum was exposed and continuously superfused with Tyrode solution. An OPS-probe was positioned over the exposed intestinal serosa. Mice were randomly assigned to PEEP or control groups. In the latter, recordings were made at three stages (steady state); at baseline, at PEEP of 3 mmHg and at PEEP of 7mmHg. In controls, PEEP was not applied and recordings were made at corresponding times. Functional Capillary Density (FCD) was measured as the number of visible capillaries per area (CapImage™-software). In the PEEP-group, FCD decreased significantly ($p < 0.05$ vs. baseline and controls) to $56 \pm 18\%$ (PEEP3 mmHg, mean $\pm$ SD in % of baseline) and again significantly ($p < 0.05$ vs. PEEP3 and controls) to $39 \pm 14\%$ (PEEP=7 mmHg), whereas controls remained stable ($96 \pm 23\%$ and $80 \pm 23\%$). This study demonstrated that PEEP reduces intestinal capillary perfusion. Furthermore, a murine model for studying the effects of mechanical ventilation was successfully established.

Disseminated Intravascular Coagulation (DIC)

As used herein,"DIC" is the generation of fibrin in the blood and the consumption of procoagulants and platelets occurring in complications of obstetrics, (*e.g.*, abruptio placenta), infection (especially gram-negative),
5   malignancy and other severe illnesses. Some other causes of DIC include intravascular hemolysis, vascular disorders, thrombosis, snake bite, massive tissue injury, trauma (especially head trauma in children), hypoxia, liver disease, infant and adult respiratory distress syndrome (RDS), Purpura fulminans, and thermal injury.

10   The most serious clinical form of DIC is shown in extensive consumption of coagulation proteins, significant deposition of fibrin, and bleeding. In mild forms of DIC, there are endogenous markers of thrombin generation with little or no obvious coagulation problems.

In this embodiment of the present invention, a standard or high contrast
15   OPS imaging probe is used to visualize, characterize, identify, and/or monitor DIC in a patient.

In each of the following aspects of this embodiment, one or more parameters, such as, capillary density, vessel (and microvessel) morphology, vessel density, vasospasm, red blood cell (RBC) velocity, cell morphology, vessel
20   diameter, leukocyte-endothelial cell interactions, vascular dynamics (such as vasomotion), functional vessel density, functional capillary density, blood flow, area-to-perimeter ratio, hemoglobin concentration, and hematocrit, may be quantitatively determined. Preferably, two or more parameters are determined.

In one aspect of this embodiment, a standard or high contrast OPS imaging
25   probe is used to visualize, identify, and/or monitor DIC, due to infection, and more particularly due to meningitis.

- 102 -

Leukocyte Kinetics/Leukocyte-Endothelial Cell Interactions

In another embodiment of the present invention, a standard or high contrast OPS imaging probe is used to visualize, characterize, and monitor changes in leukocyte kinetics, such as occurs during inflammation and infection, or any other disease or therapy that effects leukocytes. This may assist the medical practitioner in determining the source of "fever of unknown origin." Leukocyte-endothelial cell interactions (such as, for example, leukocyte adhesion or leukocyte rolling) could also be visualized, characterized, and monitored.

As used herein, the term "leukocyte adhesion" means a type of leukocyte-endothelial cell interaction whereby the leukocytes are sticking in one place for a period of time.

As used herein, the term "leukocyte rolling" means a type of leukocyte-endothelial cell interaction whereby the leukocytes are rolling along the wall of the vessel at a rate slower than the RBC velocity.

The effects of TNF-α on leukocyte rolling in iNOS Deficient Mice were studied using OPS Imaging.

Nitric oxide (NO) is an important endogenous modulator of leukocyte-endothelial cell interactions. The aim of this study was to determine the manner in which NO affects TNF-α induced leukocyte rolling and adhesion. Postcapillary venules were examined with OPS imaging under baseline conditions with tyrode superfusion including 96% N_2 and 5% CO_2 and following TNF-α (100ng/ml) superfusion for 3 hours on the hind leg muscle of iNOS knockout mice and their wild-types. Leukocyte rolling and adhesion were quantified off-line from the video recordings at 30 minute intervals.

No difference was found in leukocyte rolling or adherence both in iNOS deficient and wild type mice between baseline and 3 hours tyrode superfusion. When TNF-α was included in the superfusate, the total number of leukocytes increased in both groups. The number of rolling leukocytes however was less in iNOS deficient compared to wild-type mice, due to the increased number of adhering leukocytes in the iNOS knockout mice. In some venules of the iNOS

- 103 -

knockout mice, leukocyte accumulation was so abundant, that plugging of the vessels occurred. In the wild-type mice, adherence was less and more leukocytes exhibited rolling behavior. This *in vivo* study was supported by post-mortem histologic analyses.

Basic and Clinical Research Applications

In this embodiment of the present invention, the OPS imaging probe is used for *in vitro* or *in vivo* basic or clinical research in any or all of the areas mentioned above (*i.e.*, cardiology, cardiac surgery, wound care, diabetes, hypertension, opthalmology, neurosurgery, plastic/reconstructive surgery, transplantation, anesthesiology, and pharmacology, especially for evaluating agents that inhibit or promote angiogenesis, or anti-hypertension agents).

Experimental animal models of numerous diseases with microvascular pathologies (*i.e.*, diabetes, hypertension, Raynaud's) could be developed and OPS imaging technology used to study disease etiology, improved or earlier methods of diagnosis, disease progession, and new therapies.

Teaching Tool

In a final embodiment of the present invention, the OPS imaging probe can be used as a teaching tool for medical students, and/or science students studying, for example, physiology, anatomy, pharmacology, the microcirculation, and disease states affecting the microcirculation.

While various embodiments of the present invention have been described above, it should be understood that they have been presented by way of example only, and not limitation. The illumination techniques of the present invention can be used in any analytical, *in vivo*, or *in vitro* medical application (clinical or research) that requires optically measuring or visually observing characteristics of an object. The spectral absorption and scattering features of the object can also be measured with OPS imaging. Thus, the breadth and scope of the present

invention should not be limited by any of the above-described exemplary embodiments, but is intended to cover all changes and modifications that are within the spirit and scope of the invention as defined by the following claims and their equivalents.

5   All publications and patents mentioned in this specification are indicative of the level of skill of those skilled in the art to which this invention pertains. All publications and patents are herein incorporated by reference to the same extent as if each individual publication or patent application were specifically and individually indicated to be incorporated by reference.

What Is Claimed Is:

1. A method of detecting a circulation disturbance comprising:

(a) obtaining a single captured image or a sequence of images of the microcirculation of an individual afflicted with, or suspected of being afflicted with a circulation disturbance, using an orthogonal polarization spectral ("OPS") imaging probe, comprising the steps of:

(i) illuminating a tissue in the microcirculatory system of said individual with light polarized in a first plane of polarization, and

(ii) capturing at least one image or a sequence of images reflected from said tissue, wherein said reflected image(s) are passed through an analyzer having a plane of polarization substantially orthogonal to said first plane of polarization to produce a raw reflected image(s), thereby obtaining the captured image(s); and

(b) analyzing said captured image(s) to identify characteristics of the microcirculation, thereby detecting said circulation disturbance.

2. The method of claim 1, wherein said OPS imaging probe is a high-contrast OPS imaging probe.

3. The method of claim 1, further comprising visualizing and characterizing blood cell components.

4. The method of claim 3, wherein said blood cell components are red blood cells, white blood cells, or platelets.

5. The method of claim 4, wherein said blood cell components are red blood cells

6. The method of claim 1, further comprising visualizing extravascular red blood cells.

7. The method of claim 6, wherein said extravascular red blood cells are caused by a hemorrhage.

8. The method of claim 1, further comprising analyzing one or more characteristics selected from the group consisting of: hemoglobin concentration, hematocrit, vessel morphology, area-to-perimeter ratio, vessel density, capillary density, vessel diameter, functional vessel density, vasospasm, functional capillary density, red blood cell velocity, cell morphology, blood flow, leukocyte-endothelial cell interactions, and vascular dynamics.

9. The method of claim 8, wherein two or more of said characteristics are analyzed.

10. The method of claim 1, wherein said image is a single captured image.

11. The method of claim 10, wherein said characteristics of the microcirculation are vessel diameter, vessel morphology, cell morphology, capillary density, vessel density, area-to-perimeter ratio, or vasospasm.

12. The method of claim 1, wherein said images are a sequence of images.

13. The method of claim 12, wherein said characteristics of the microcirculation are red blood cell velocity, functional capillary density, functional vessel density, blood flow, leukocyte-endothelial cell interactions, or vascular dynamics.

- 107 -

14. A method of monitoring the microcirculation of an individual before, during, or after a medical procedure comprising:

(a) obtaining a single captured image or a sequence of images of the microcirculation of an individual before, during, or after a medical procedure, using an OPS imaging probe, comprising the steps of:

(i) illuminating a tissue in the microcirculatory system of said individual with light polarized in a first plane of polarization, and

(ii) capturing at least one image or a sequence of images reflected from said tissue, wherein said reflected image(s) are passed through an analyzer having a plane of polarization substantially orthogonal to said first plane of polarization to produce a raw reflected image(s), thereby obtaining the captured image(s); and

(b) analyzing said captured image(s) to monitor the microcirculation of said individual before, during, or after a medical procedure.

15. The method of claim 14, wherein said OPS imaging probe is a high-contrast OPS imaging probe.

16. The method of claim 14, wherein said medical procedure is surgery.

17. The method of claim 14, further comprising analyzing one or more characteristics selected from the group consisting of: hemoglobin concentration, hematocrit, vessel morphology, cell morphology, vessel density, capillary density, vessel diameter, functional vessel density, vasospasm, functional capillary density, red blood cell velocity, cell morphology, blood flow, leukocyte-endothelial cell interactions, area-to-perimeter ratio, and vascular dynamics.

18. The method of claim 17, wherein two or more of said characteristics are analyzed.

- 108 -

19.   The method of claim 14, wherein said image is a single captured image.

20.   The method of claim 19, wherein said characteristics of the microcirculation are vessel diameter, vessel morphology, cell morphology, capillary density, vessel density, area-to-perimeter ratio, or vasospasm.

21.   The method of claim 14, wherein said images are a sequence of images.

22.   The method of claim 21, wherein said characteristics of the microcirculation are red blood cell velocity, functional capillary density, functional vessel density, blood flow, leukocyte-endothelial cell interactions, or vascular dynamics.

23.   A method of diagnosing an epithelial or intraepithelial lesion comprising:

(a) obtaining a captured image of epithelial or intraepithelial cells within a tissue by use of an OPS imaging probe, comprising the steps of:

(i) illuminating said tissue with light polarized in a first plane of polarization, and

(ii) capturing a reflected image reflected from said tissue, wherein said reflected image is passed through an analyzer having a plane of polarization substantially orthogonal to said first plane of polarization to produce a raw reflected image, thereby obtaining the captured image; and

(b) analyzing said captured image to diagnose said epithelial or intraepithelial lesion.

24.   The method of claim 23, wherein said OPS imaging probe is a high-contrast OPS imaging probe.

25. The method of claim 23, wherein said epithelial or intraepithelial lesion is a pre-malignant epithelial or intraepithelial neoplasm.

26. The method of claim 23, wherein said epithelial or intraepithelial lesion is a malignant epithelial or intraepithelial neoplasm.

5

27.   The method of claim 25, wherein said epithelial or intraepithelial lesion is from the cervix.

28.   The method of claim 26, wherein said epithelial or intraepithelial lesion is from the cervix.
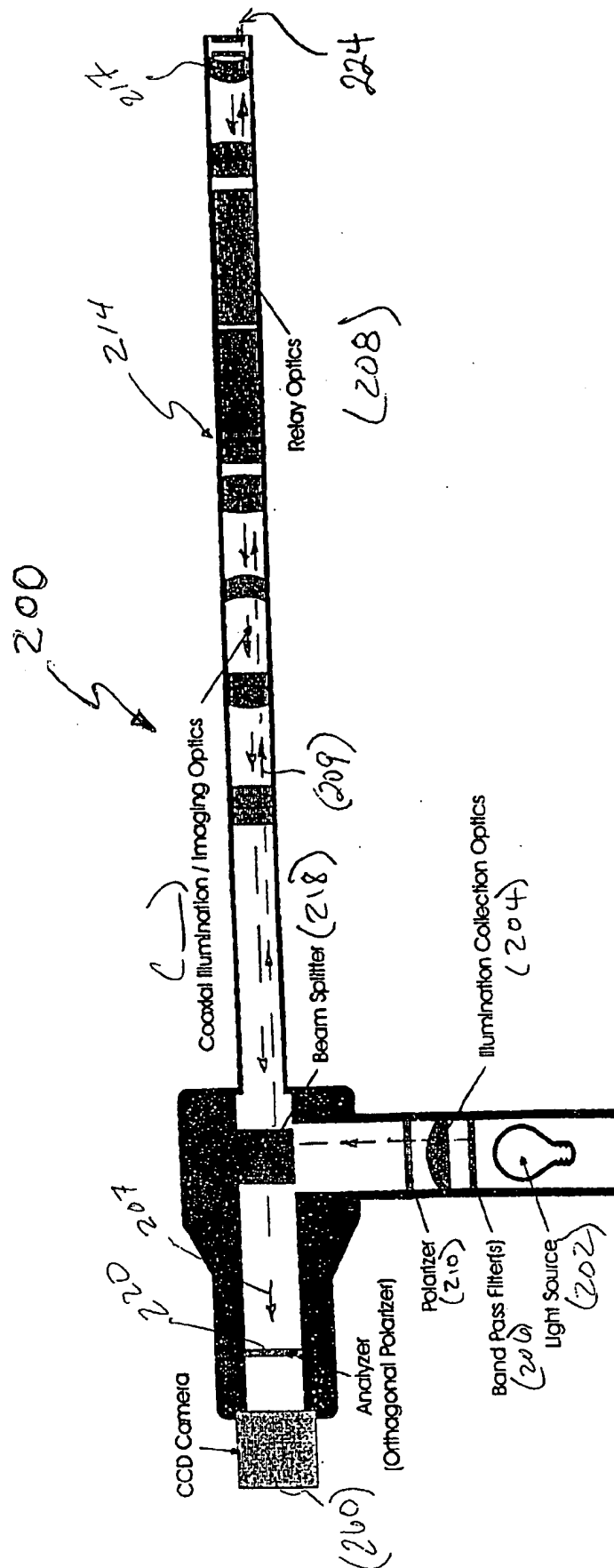
Figure 1
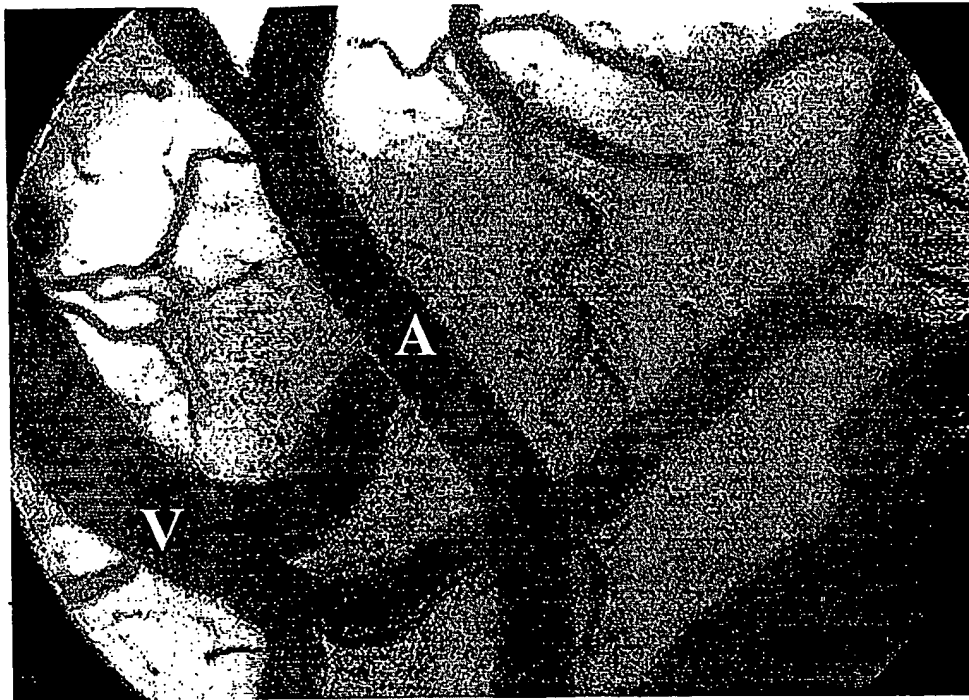
Figure 2
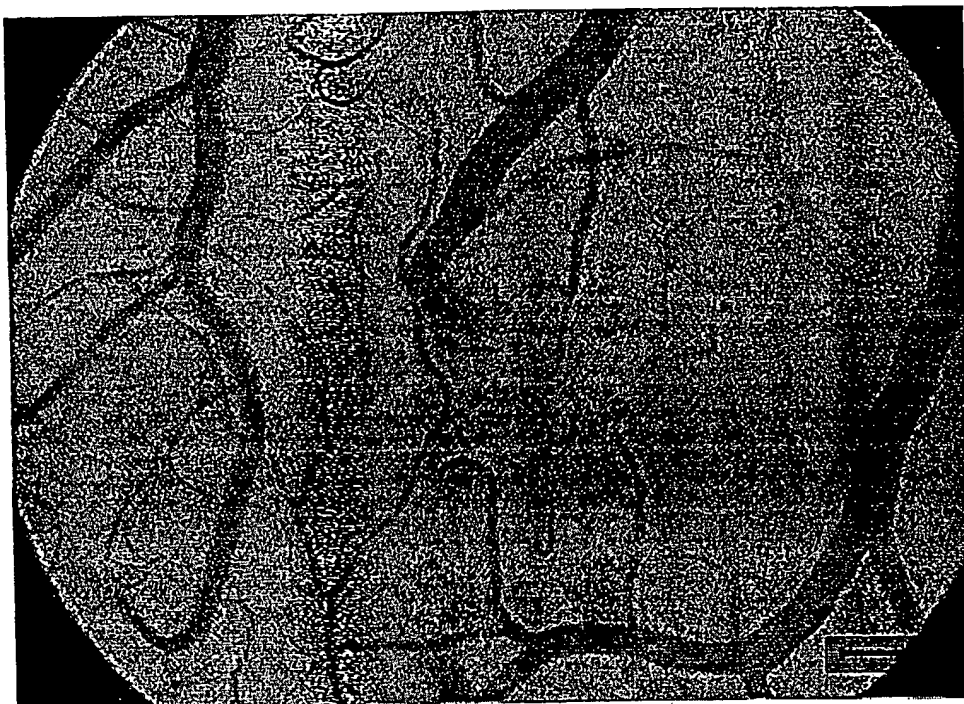
Figure 3
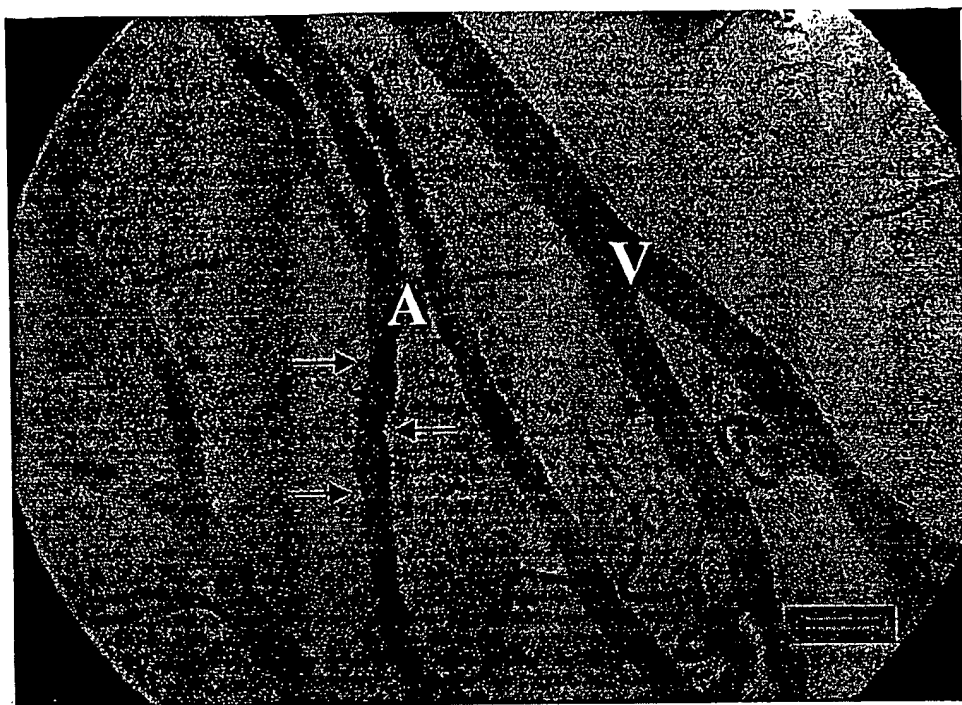
Figure 4

Figure 5
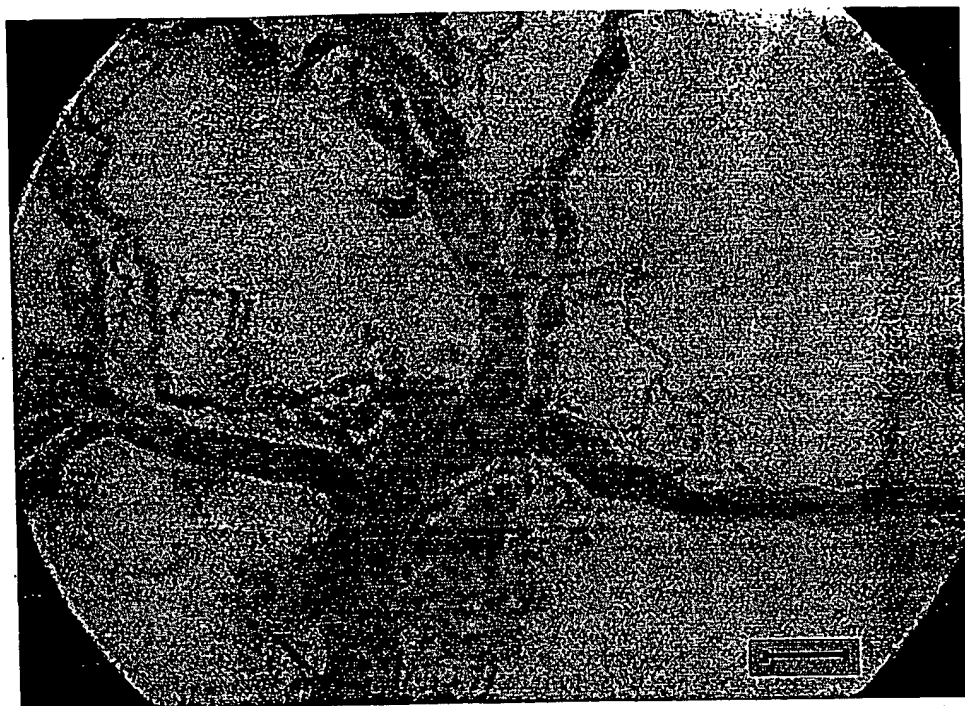
Figure 6
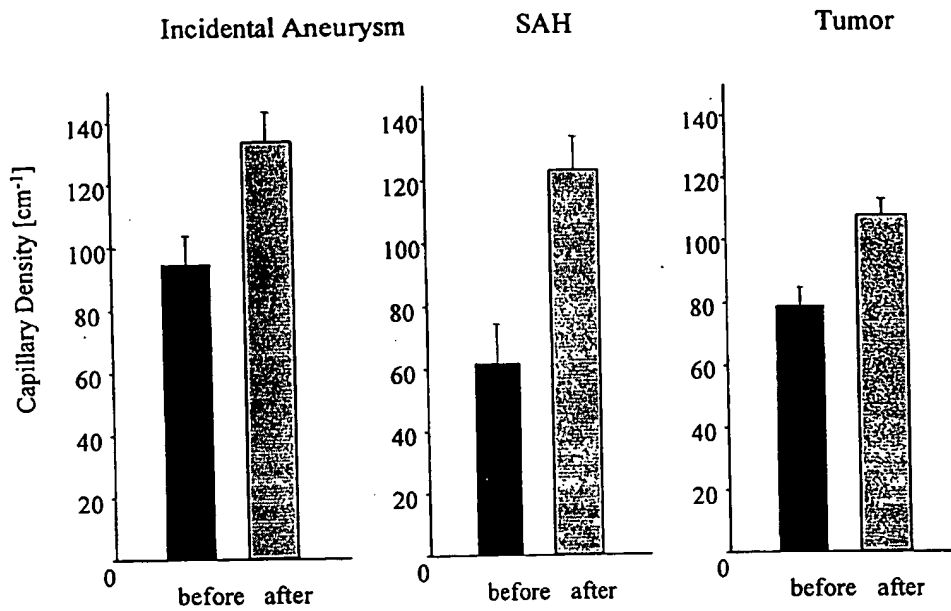
Figure 7

Figure 8

Incidental Aneurysm

SAH
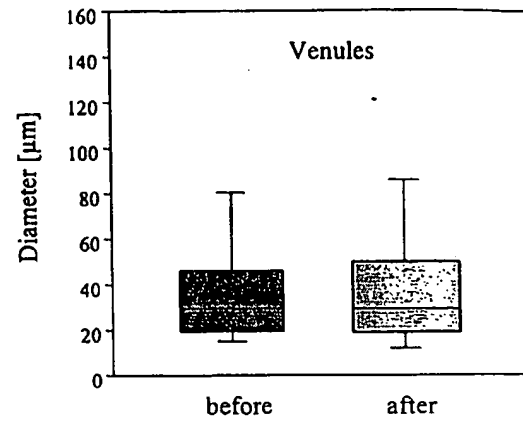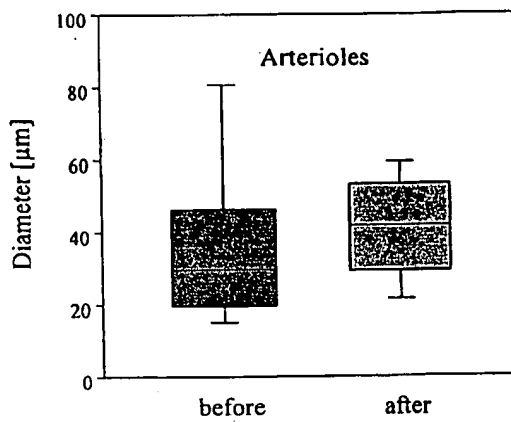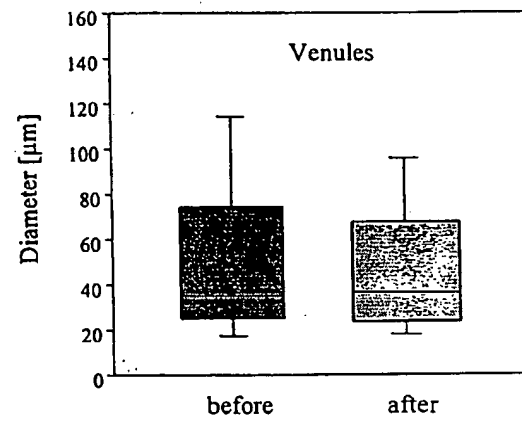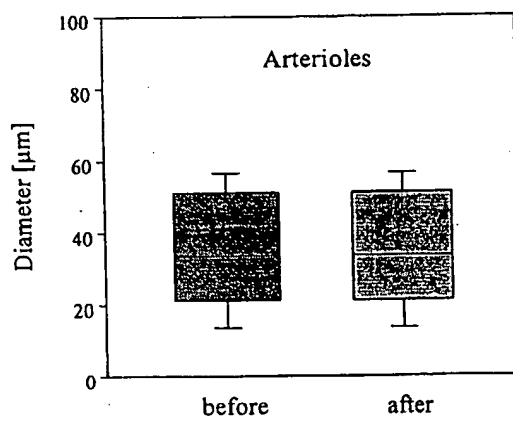
Tumor
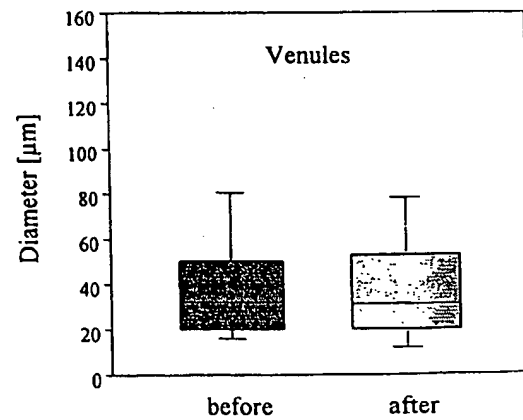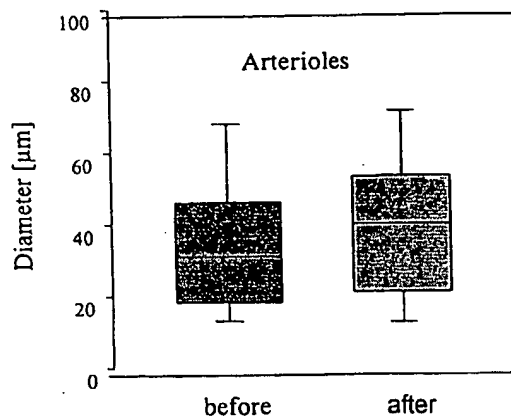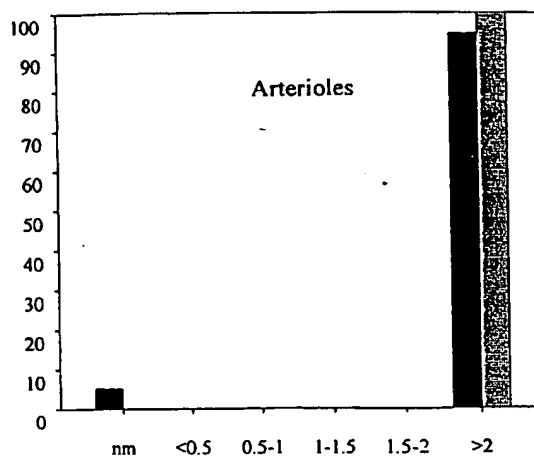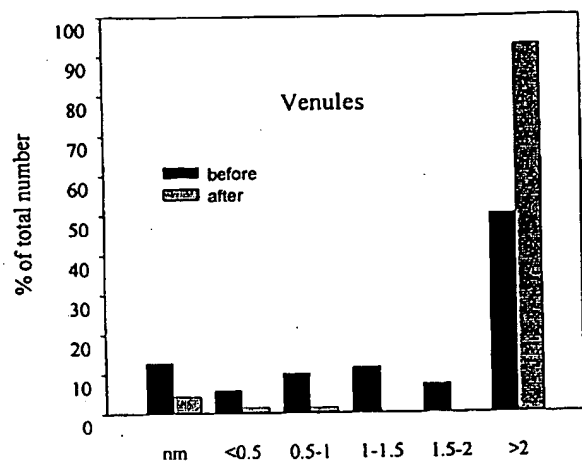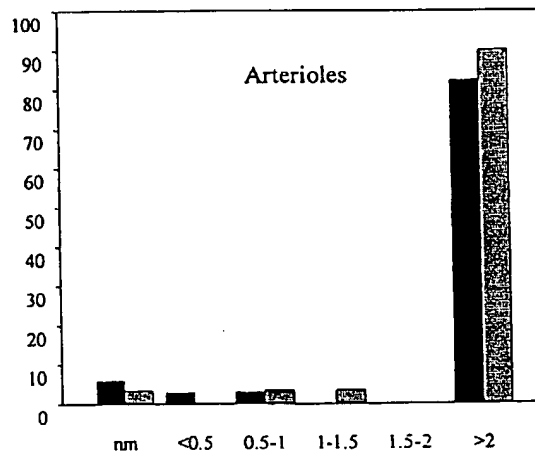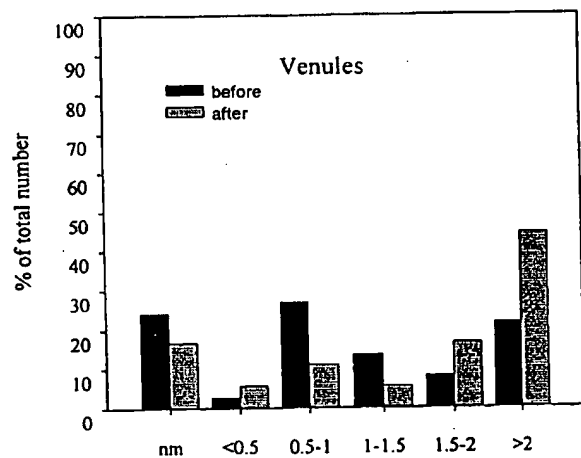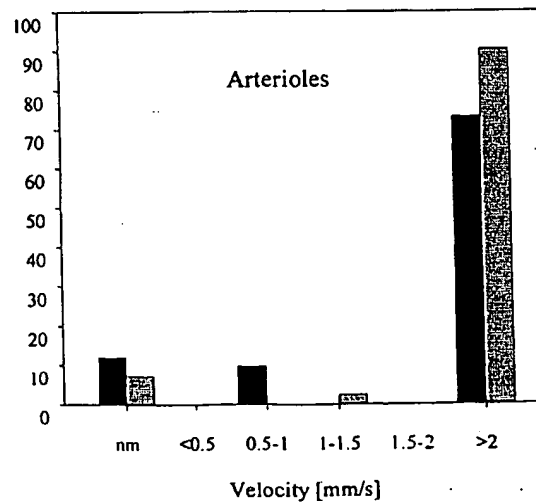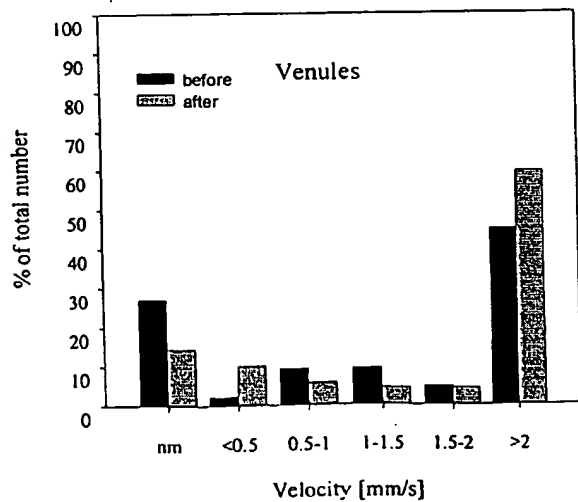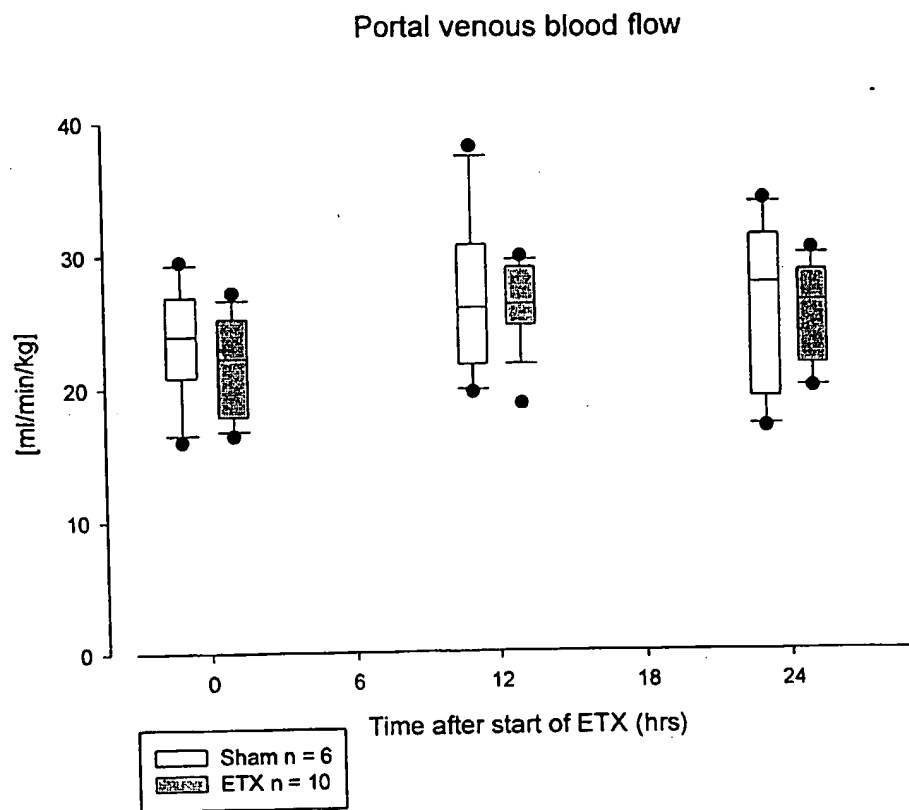
Figure 9

Figure 10

Arterial-ileal mucosal pCO$_2$ gap
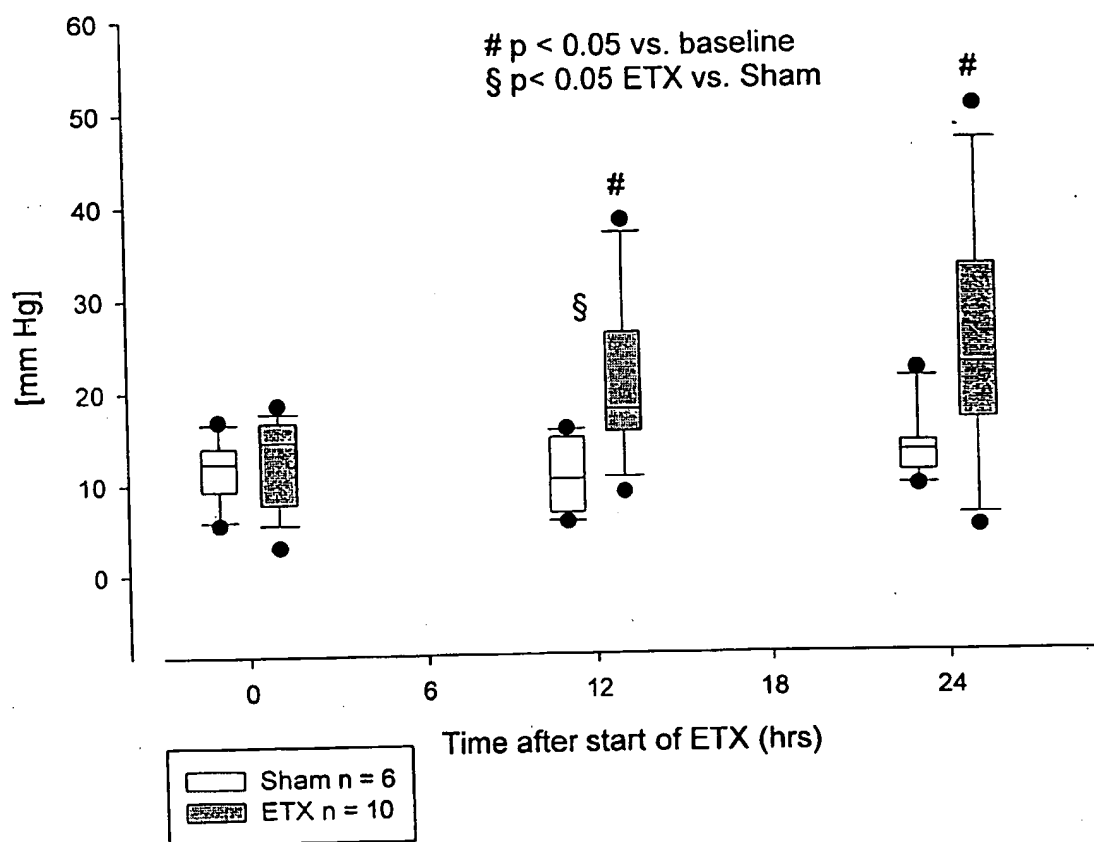
Figure 11
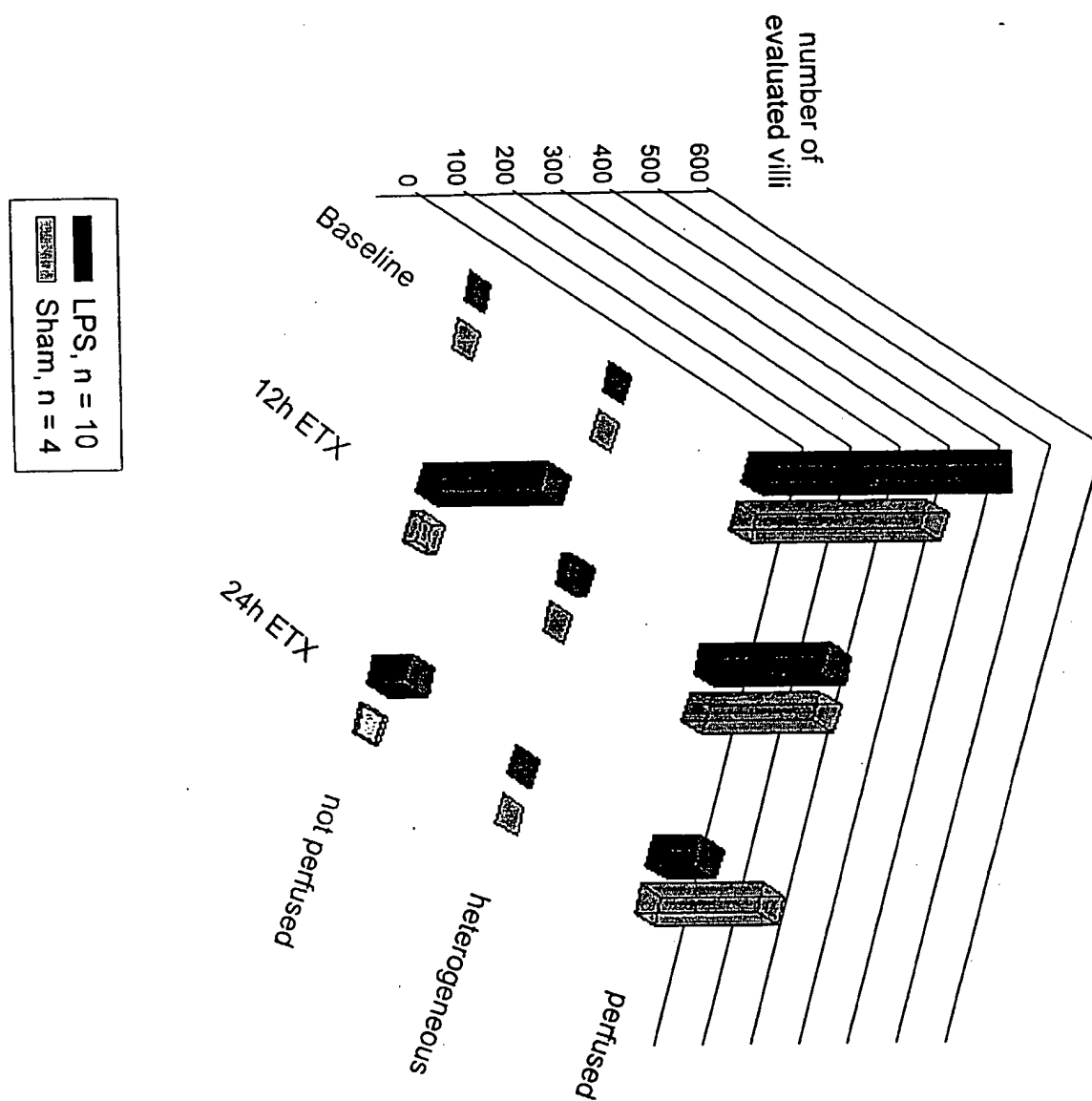
Figure 12

Figure 13

3 cm
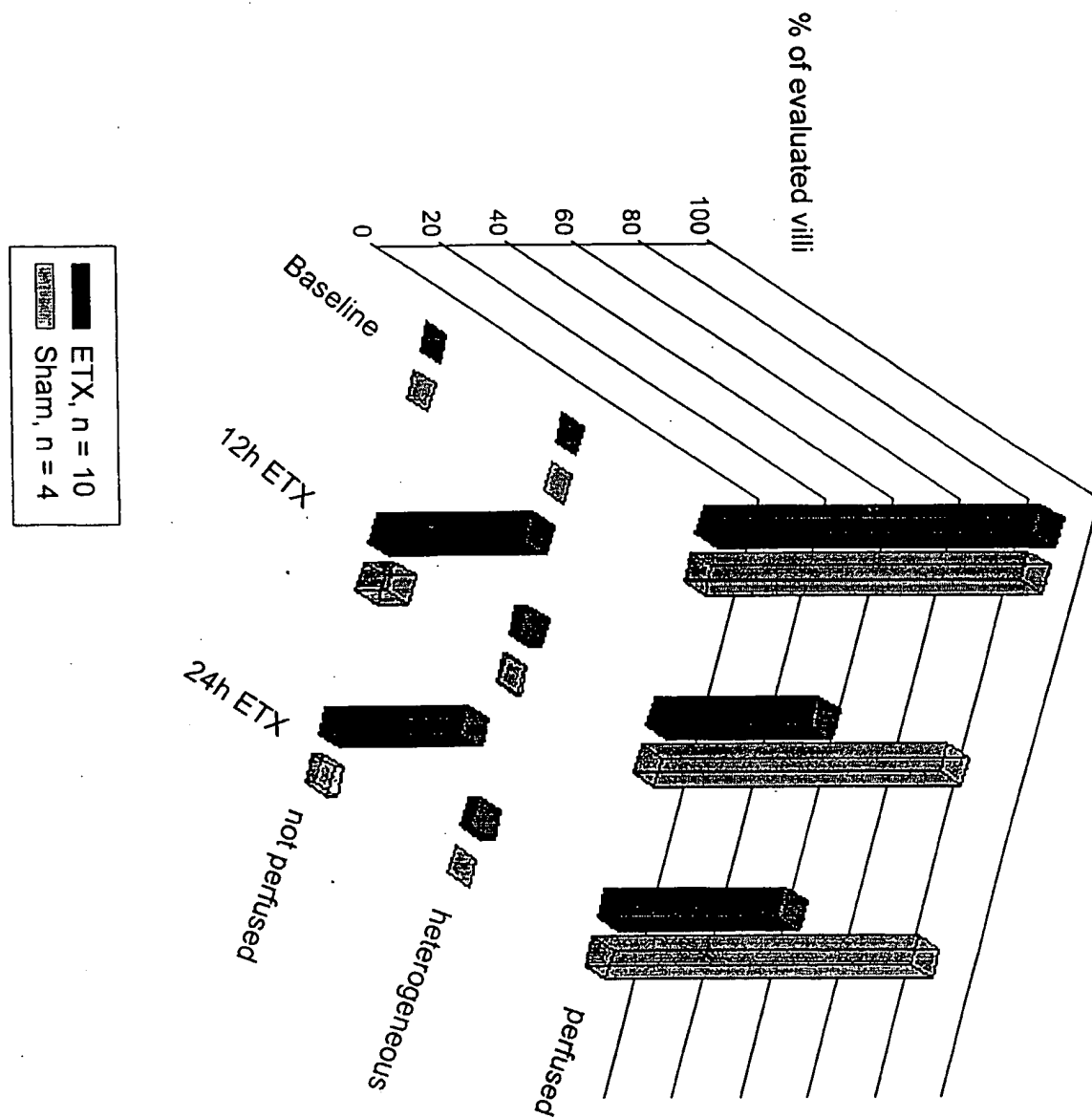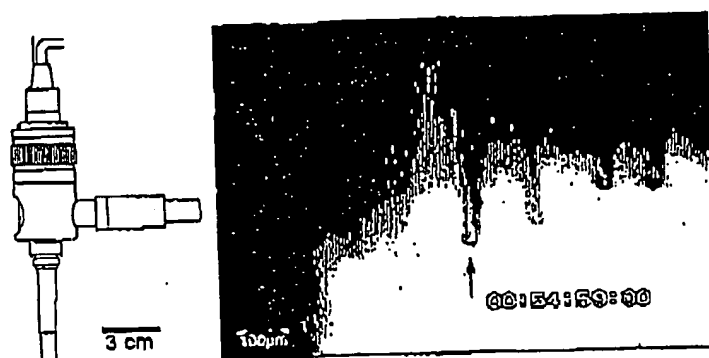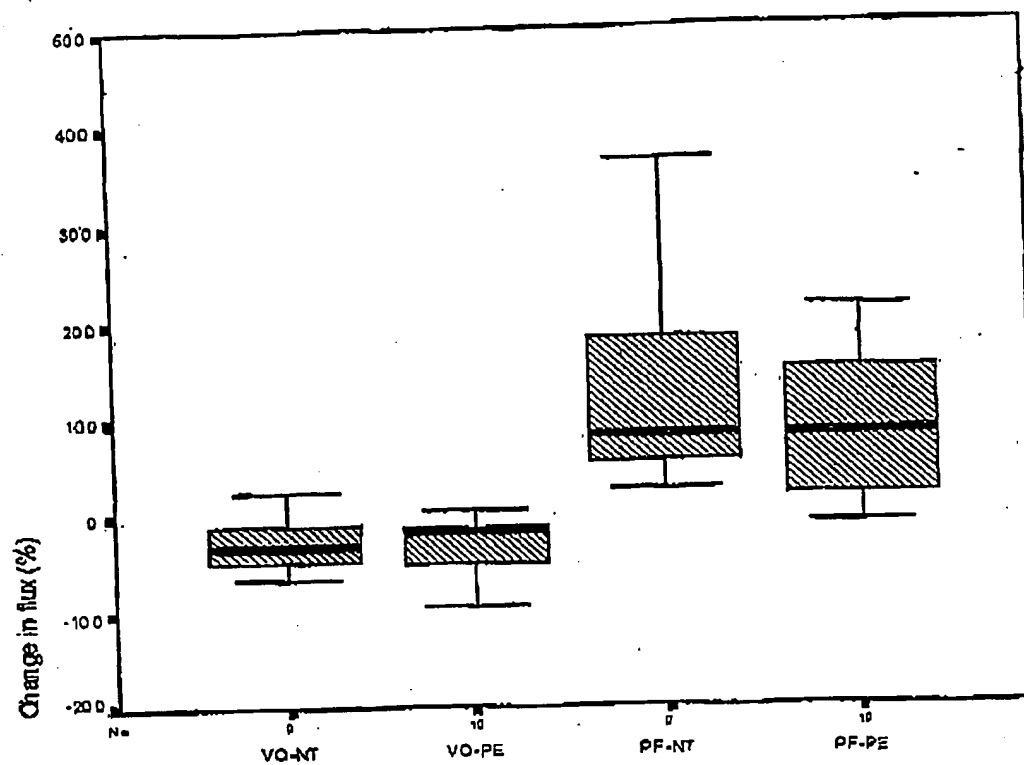
Figure 14

Figure 15A
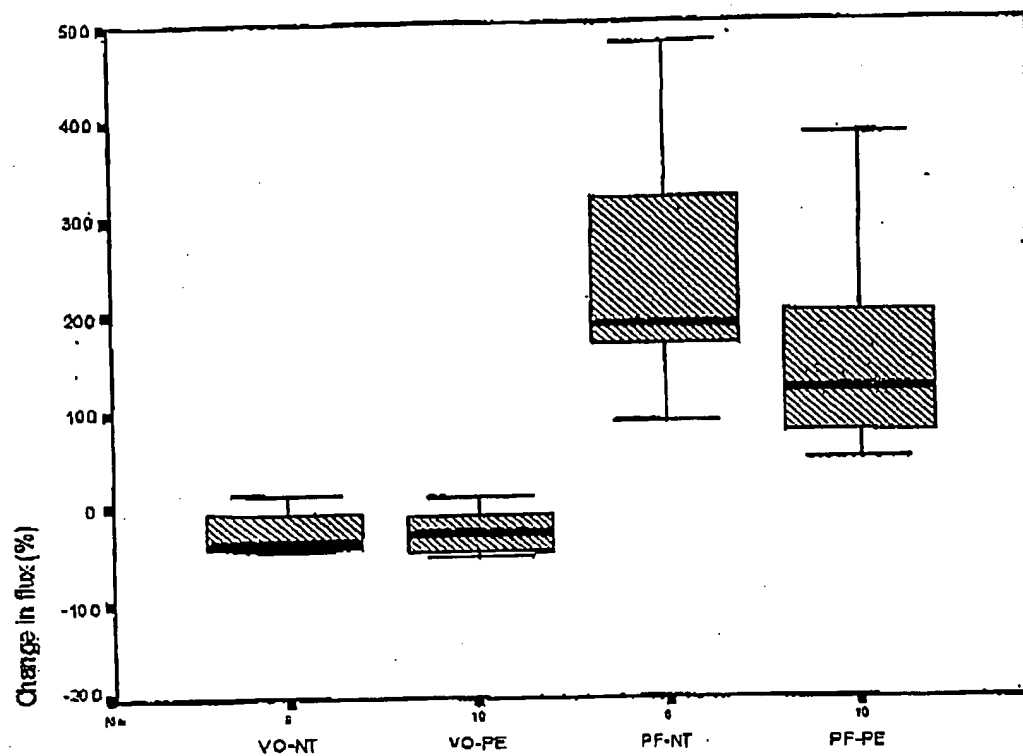
Figure 15B
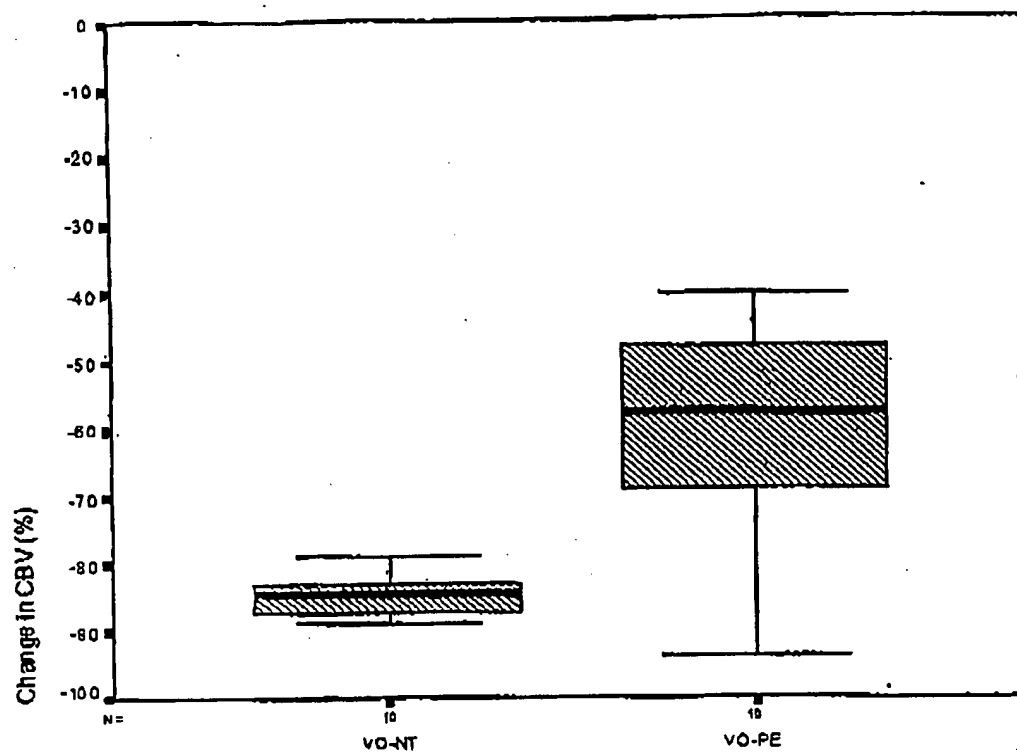
Figure 16

Figure 17
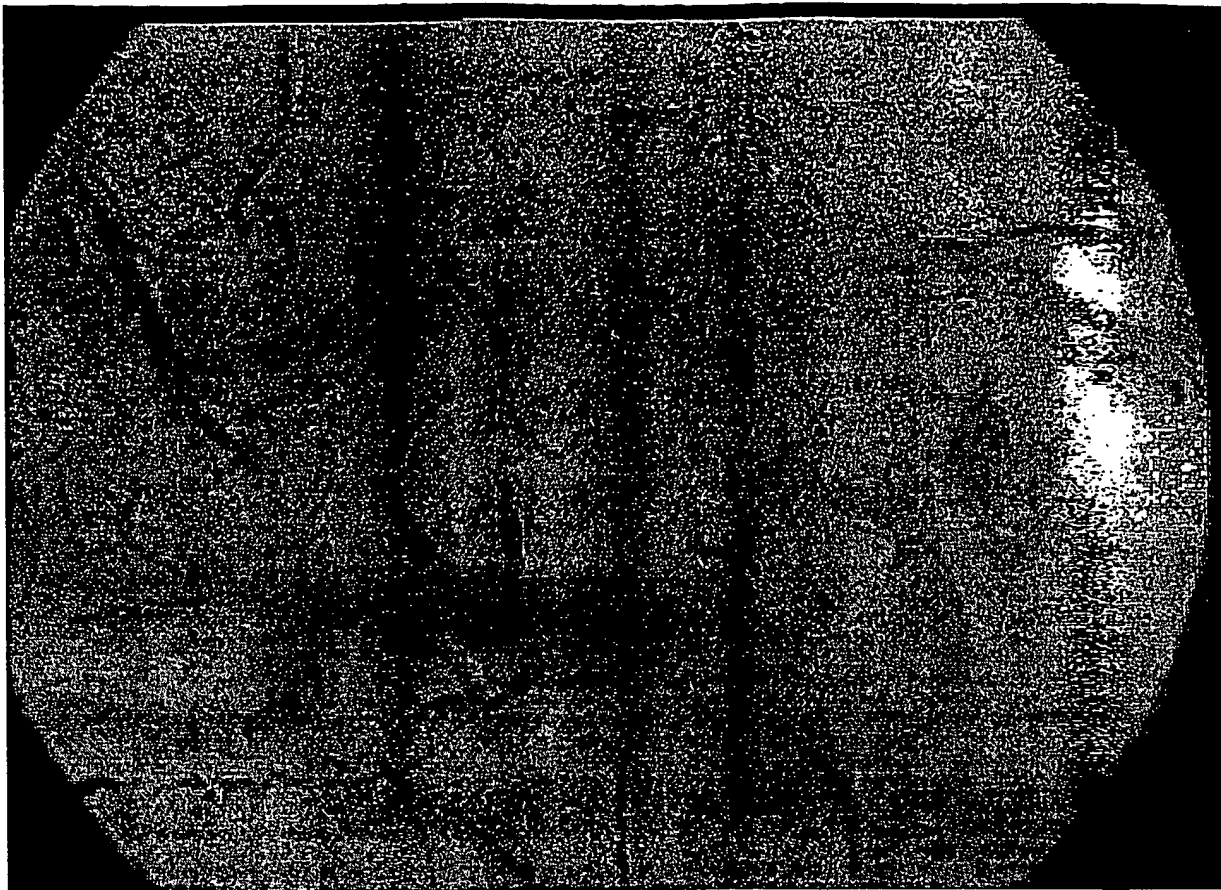
Figure 18
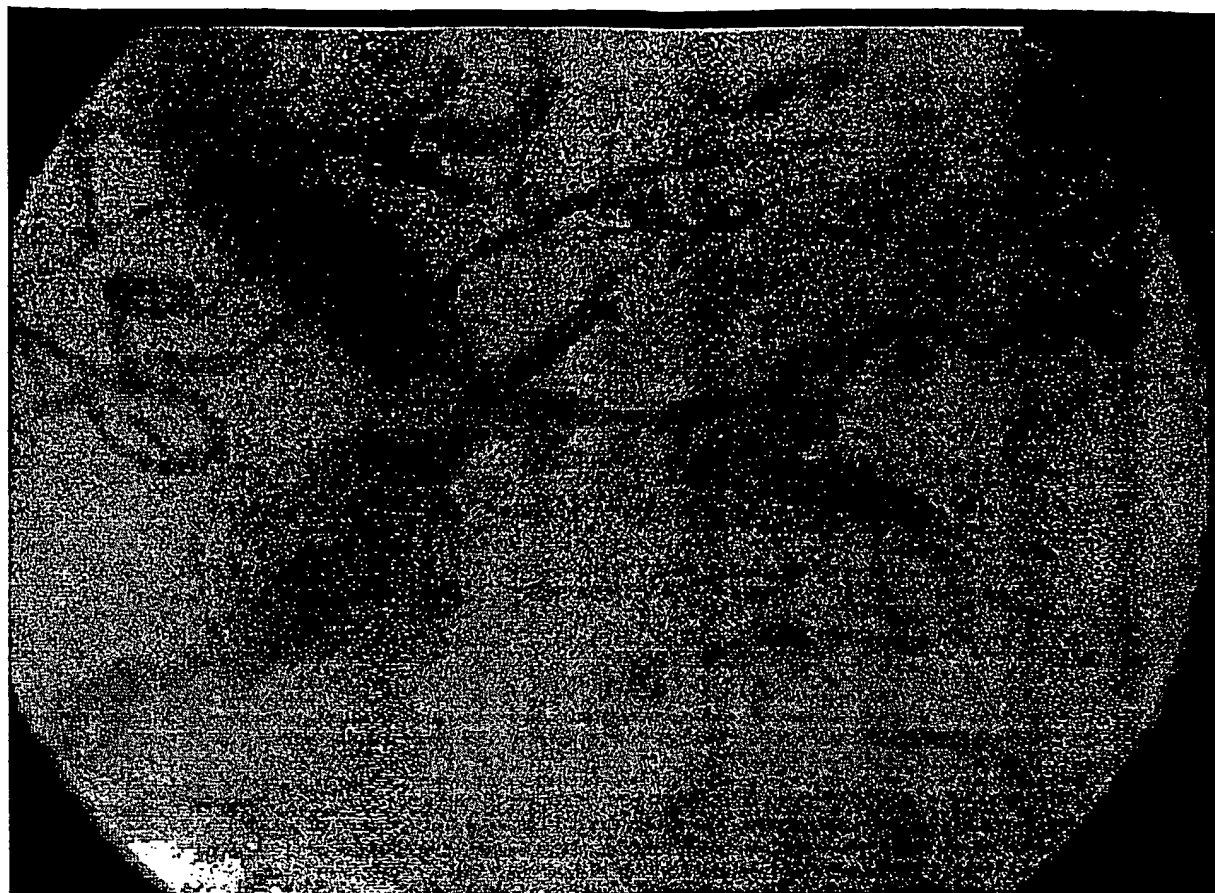
Figure 19
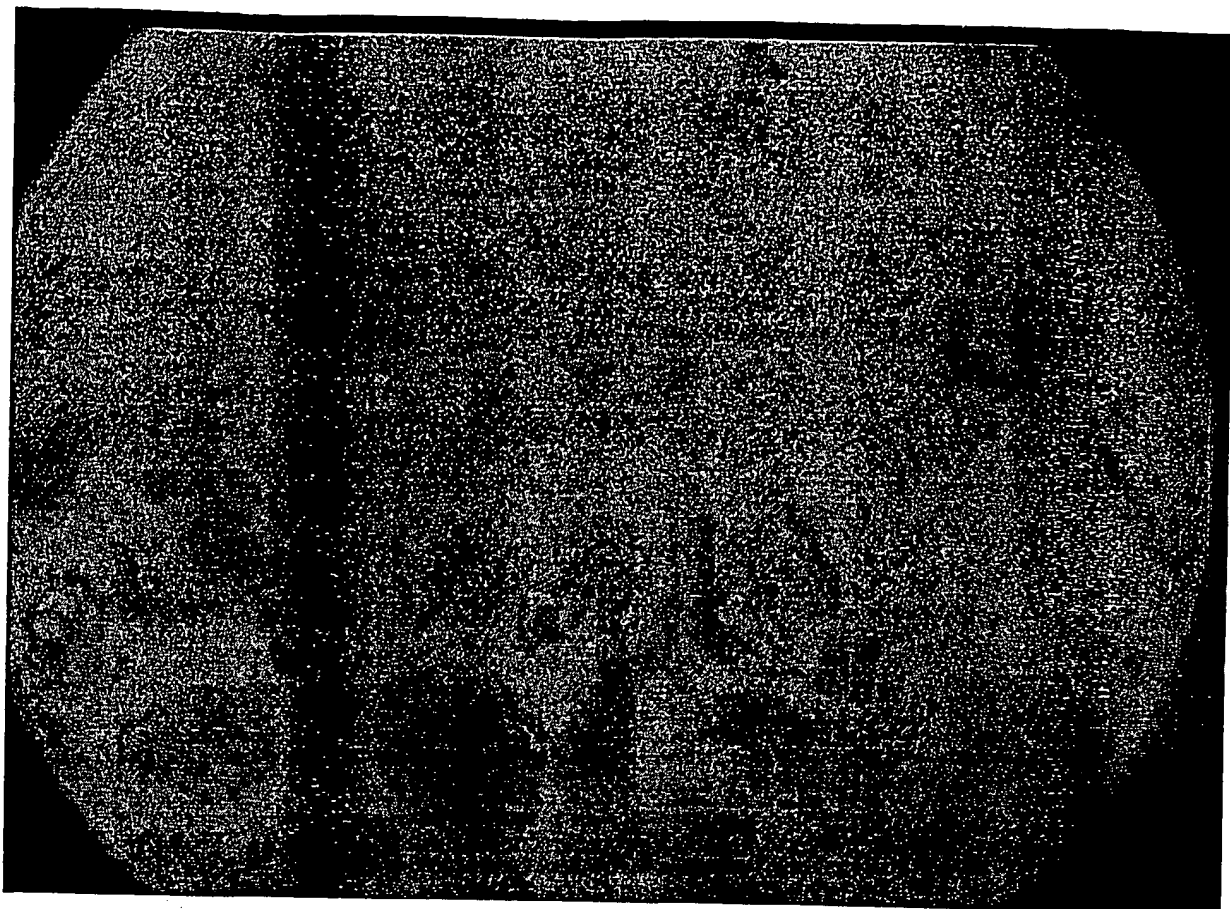
Figure 20

(51) International Patent Classification⁷: A61B 5/00

(21) International Application Number: PCT/US00/26106

(22) International Filing Date:
22 September 2000 (22.09.2000)

(25) Filing Language: English

(26) Publication Language: English

(30) Priority Data:
60/155,487   23 September 1999 (23.09.1999)   US
60/209,529   5 June 2000 (05.06.2000)   US

(71) Applicants and
(72) Inventors: NADEAU, Richard, G. [US/US]; 364 Walnut Lane, North East, MD 21901 (US). WINKELMAN, James, W. [US/US]; 62 Rangeley Road, Chestnut Hill, MA 02167 (US).

(74) Agents: KESSLER, Edward, J. et al.; Sterne, Kessler, Goldstein & Fox P.L.L.C., Suite 600, 1100 New York Avenue, N.W., Washington, DC 20005-3934 (US).

(81) Designated States (national): AE, AG, AL, AM, AT, AU, AZ, BA, BB, BG, BR, BY, BZ, CA, CH, CN, CR, CU, CZ, DE, DK, DM, DZ, EE, ES, FI, GB, GD, GE, GH, GM, HR, HU, ID, IL, IN, IS, JP, KE, KG, KP, KR, KZ, LC, LK, LR, LS, LT, LU, LV, MA, MD, MG, MK, MN, MW, MX, MZ, NO, NZ, PL, PT, RO, RU, SD, SE, SG, SI, SK, SL, TJ, TM, TR, TT, TZ, UA, UG, US, UZ, VN, YU, ZA, ZW.

(84) Designated States (regional): ARIPO patent (GH, GM, KE, LS, MW, MZ, SD, SL, SZ, TZ, UG, ZW), Eurasian patent (AM, AZ, BY, KG, KZ, MD, RU, TJ, TM), European patent (AT, BE, CH, CY, DE, DK, ES, FI, FR, GB, GR, IE, IT, LU, MC, NL, PT, SE), OAPI patent (BF, BJ, CF, CG, CI, CM, GA, GN, GW, ML, MR, NE, SN, TD, TG).

Published:
— with international search report

(88) Date of publication of the international search report:
4 October 2001

For two-letter codes and other abbreviations, refer to the "Guidance Notes on Codes and Abbreviations" appearing at the beginning of each regular issue of the PCT Gazette.

(54) Title: MEDICAL APPLICATIONS OF ORTHOGONAL POLARIZATION SPECTRAL IMAGING

(57) Abstract: Medical applications of orthogonal polarization spectral (OPS) imaging technology are provided. This technology provides for a high contrast image of sub-surface phenomena such as blood vessel structure, blood flow within vessels, gland structure, etc., as well as a high resolution image of the surface of solid organs. Numerous clinical (diagnostic and therapeutic), as well as research applications of this technology, in the medical and pharmaceutical fields, are discussed.

A. CLASSIFICATION OF SUBJECT MATTER

IPC(7) :A61B 5/00
US CL :600/310, 476

According to International Patent Classification (IPC) or to both national classification and IPC

B. FIELDS SEARCHED

Minimum documentation searched (classification system followed by classification symbols)

U.S. : 600/310, 476, 322, 473, 479; 356/39-42, 364, 369, 445; 382/128, 130, 133, 134

Documentation searched other than minimum documentation to the extent that such documents are included in the fields searched

Electronic data base consulted during the international search (name of data base and, where practicable, search terms used)

C. DOCUMENTS CONSIDERED TO BE RELEVANT

Category*	Citation of document, with indication, where appropriate, of the relevant passages	Relevant to claim No.
X,P	US 5,983,120 A (GRONER et al) 09 November 1999, see the entire document.	1-5, 8-11, 14 - 20
A	US 5,598,842 A (ISHIHARA et al) 04 February 1997, see the entire document.	1-28

☐ Further documents are listed in the continuation of Box C.   ☐ See patent family annex.

	Special categories of cited documents:	"T"	later document published after the international filing date or priority date and not in conflict with the application but cited to understand the principle or theory underlying the invention
"A"	document defining the general state of the art which is not considered to be of particular relevance		
"E"	earlier document published on or after the international filing date	"X"	document of particular relevance; the claimed invention cannot be considered novel or cannot be considered to involve an inventive step when the document is taken alone
"L"	document which may throw doubts on priority claim(s) or which is cited to establish the publication date of another citation or other special reason (as specified)	"Y"	document of particular relevance; the claimed invention cannot be considered to involve an inventive step when the document is combined with one or more other such documents, such combination being obvious to a person skilled in the art
"O"	document referring to an oral disclosure, use, exhibition or other means		
"P"	document published prior to the international filing date but later than the priority date claimed	"&"	document member of the same patent family

Date of the actual completion of the international search	Date of mailing of the international search report
11 APRIL 2001	30 APR 2001
Name and mailing address of the ISA/US Commissioner of Patents and Trademarks Box PCT Washington, D.C. 20231	Authorized officer ERIC WINAKUR
Facsimile No. (703) 305-3230	Telephone No. (703) 308-3940

Form PCT/ISA/210 (second sheet) (July 1998)*